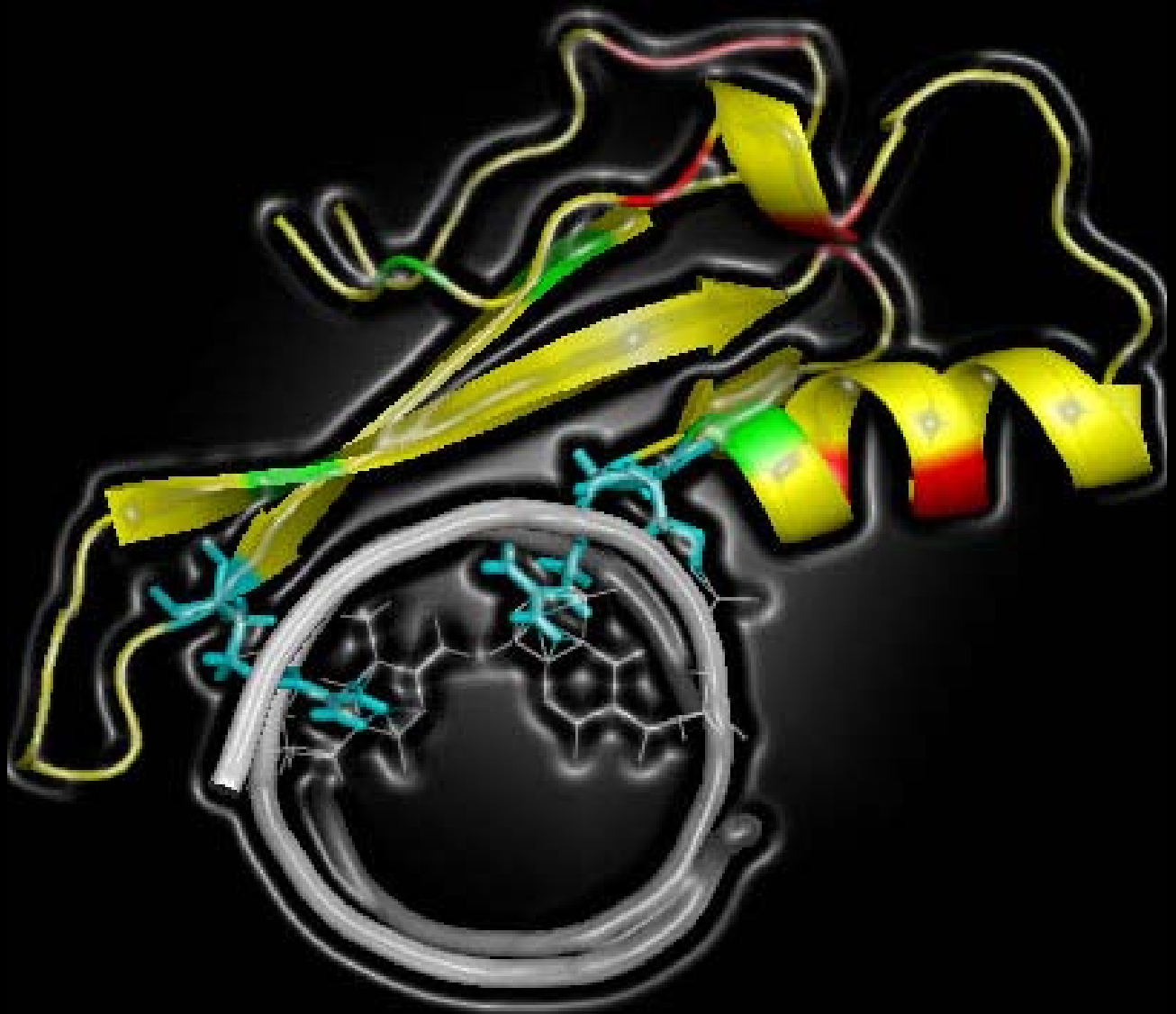

Role of MeCP2 in heterochromatin organization during differentiation and disease

Noopur Agarwal



Role of MeCP2 in heterochromatin organization during differentiation and disease

Noopur Agarwal



München 2008

**Role of MeCP2 in heterochromatin organization during
differentiation and disease**
Noopur Agarwal

Dissertation
an der Fakultät für Biologie
der Ludwig-Maximilians-Universität
München

Vorgelegt von
Noopur Agarwal
aus
Bareilly, India

München, den 03. September 2008

Erstgutachter: Prof. Dr. Heinrich Leonhardt

Zweitgutachter: Prof. Dr. Angelika Böttger

Tag der mündlichen Prüfung: 16.03.2009

SUMMARY	I
ZUSAMMENFASSUNG	III
1. INTRODUCTION	1
1.1. Chromatin organization and assembly	1
1.2. Epigenetic modifications of chromatin	3
1.3. Molecules that read epigenetic information	7
1.4. Cellular differentiation and MeCP2	17
1.5. Rett syndrome and MeCP2	17
2. AIMS OF THE WORK	23
3. RESULTS	25
3.1. MeCP2 interacts with HP1 and modulates its heterochromatin association during myogenic differentiation	25
3.2. MeCP2 Rett mutations affect large scale chromatin organization	39
4. DISCUSSION	75
4.1. Chromatin clustering is induced by MeCP2 and not HP1 during differentiation	75
4.2. Chromatin clustering is affected by mutations in MeCP2	76
4.3. Modes of MeCP2 binding that lead to higher order chromatin structures	78
5. OUTLOOK	82
6. REFERENCES	83
7. ANNEX	99
7.1. Abbreviations	99
7.2. Acknowledgements	102
7.3. Anchor side chains of short peptide fragments trigger ligand-exchange of Class II MHC molecules	104
7.4. Contributions	116
7.5. Curriculum Vitae	118

FIGURES

Figure 1. Schematic model of the levels of chromatin organization.	2
Figure 2. Epigenetic modifications and higher order chromatin organization in the cell	3
Figure 3. Scheme and alignment of different isomers of human heterochromatin protein1	8
Figure 4. Summary of HP1 protein interactions	9
Figure 5. Scheme of different members of methyl CpG binding family and alignment of their MBD domain	12
Figure 6. Interaction of MeCP2 with other proteins	14
Figure 7. Alignment of MeCP2 from different species	16
Figure 8. Localization of MECP2 gene, functional domains of the corresponding gene product and structure of the MBD domain	19
Figure 9. Model depicting different modes of MeCP2 binding and MeCP2 induced higher order chromatin structure	79

TABLES

Table 1. Summary of HP1 protein interactions	10
Table 2. Studies of Rett syndrome using mouse models	21

SUMMARY

The organization of the genome in a eukaryotic cell is quite complex and dynamic. Chromatin is compacted at various levels inside the cell nucleus and these correlate with specific epigenetic modifications like DNA and histone modifications and the presence of proteins that recognize these modifications. All these processes can affect DNA accessibility and, consequently, the establishment and maintenance of tissue specific gene expression patterns.

During cellular differentiation, lineage specific genes become transcriptionally activated and, concomitantly, the remaining of the genome is silenced and stably kept in a heterochromatic state. Two major families of factors recognize the typical heterochromatic modifications: the MBD family consisting of MBD1, MBD2, MBD3, MBD4 and MeCP2; and the HP1 family comprising HP1 α , HP1 β and HP1 γ .

I investigated initially whether there is potential cross talk between these two families of epigenetic factors (MeCP2 and HP1) and how they work in synergy and affect each other during differentiation. I found that, in contrast to MeCP2, the level of expression of the three HP1s remained constant during myogenic differentiation, though HP1 γ relocalized to heterochromatin. The latter was correlated with the presence of MeCP2. In agreement with this, I could show that MeCP2 directly interacted via its N terminal domain with the chromoshadow domain of HP1.

Our group has recently shown that MeCP2 level increased dramatically during differentiation, and that MeCP2, via its methyl-cytosine binding domain, induced heterochromatin clustering *in vivo*. Hence, I next tested the role of MeCP2 in large-scale heterochromatin organization by analyzing whether this MeCP2 function is disrupted in disease. In 1999, MECP2 gene was found to be mutated in a neurological disease called Rett syndrome. Little is known about how MeCP2 causes Rett syndrome. Most studies so far have focused on finding MeCP2 target genes. I have concentrated my efforts on testing whether MeCP2 Rett mutations have an effect on its ability to bind and reorganize chromatin. I found that several methyl-cytosine binding domain mutations significantly disrupted MeCP2's ability either to bind or to cluster heterochromatin. These mutations segregated onto two distinct surfaces of the methyl-cytosine binding domain. These data assigns now novel functions to this domain, which is the most frequently mutated in Rett patients.

From this work, I conclude that MeCP2 plays an important function in regulating chromatin organization, and that disrupting this ability of MeCP2 may lead to disease

ZUSAMMENFASSUNG

Die Organisation des Genoms in einer eukaryotischen Zelle ist komplex und dynamisch. Chromatin wird auf mehreren Ebenen im Inneren des Zellkerns kondensiert, und diese Ebenen korrelieren mit den spezifischen epigenetischen Modifikationen wie DNA- und Histonmodifikationen sowie mit dem Vorhandensein der Proteine, die diese Modifikationen erkennen. All diese Prozesse können die Verfügbarkeit der DNA und infolgedessen die Etablierung und Erhaltung gewebsspezifischer Genexpressionsmuster beeinflussen.

Während der Zelldifferenzierung werden linienspezifische Gene durch Transkription aktiviert. Gleichzeitig wird das restliche Genom vorübergehend inaktiviert und stabil in einem heterochromatischen Stadium gehalten. Die Faktoren, die typische Heterochromatin-Modifikationen erkennen, werden in zwei Familien eingeteilt: Die MBD-Familie besteht aus MBD1, MBD2, MBD3, MBD4 und MeCP2; die HP1-Familie beinhaltet HP1 α , HP1 β und HP1 γ .

Anfänglich habe ich untersucht, ob es zwischen den zwei Familien epigenetischer Faktoren (MeCP2 und HP1) möglicherweise zu Interdependenzen kommt, wie sie zusammenwirken und sich während der Differenzierung gegenseitig beeinflussen. Wir fanden heraus, dass im Gegensatz zu MeCP2 die Expression der drei HP1s während der myogenen Differenzierung konstant blieb. Allerdings konnten wir eine Umverteilung von HP1 γ zum Heterochromatin beobachten, die mit dem Vorhandensein von MeCP2 korreliert. Damit übereinstimmend konnten wir zeigen, dass MeCP2 über seine terminale N-Domäne direkt mit der Chromoshadow-Domäne von HP1 interagiert.

Unsere Arbeitsgruppe hat vor kurzem gezeigt, dass der MeCP2-Spiegel während der Differenzierung dramatisch ansteigt und MeCP2 über seine Methyl-Cytosin-bindende Domäne in vivo die Heterochromatin-Clusterbildung induziert. Demzufolge habe ich als nächstes die Rolle von MeCP2 in der übergeordneten Heterochromatin-Organisation untersucht und getestet, ob diese Funktion von MeCP2 bei einer Krankheit gestört ist. Seit 1999 ist bekannt, dass das MeCP2-Gen beim Rett-Syndrom, einer neurologischen Erkrankung, mutiert ist. Es ist wenig darüber bekannt, wie MeCP2 das Rett-Syndrom auslöst. Die meisten Untersuchungen haben sich darauf konzentriert, MeCP2-Zielgene zu finden. Wir wollten herausfinden, ob Rett-MeCP2-Mutationen sich auf die Fähigkeit zur Bindung und Reorganisation von Chromatin auswirken. Es zeigte sich, dass mehrere Mutationen der Methyl-Cytosin-bindenden Domäne die Fähigkeit von MeCP2

zur Bindung oder Clusterbildung von Heterochromatin stören. Diese Mutationen zeigten sich auf zwei genau umschriebenen Oberflächen der Methyl-Cytosin-bindenden Domäne. Die gewonnenen Daten weisen dieser Domäne, die bei Rett-Patienten am häufigsten mutiert, neue Funktionen zu. Wir schließen daraus, dass MeCP2 eine wichtige Rolle bei der Regulation der Chromatinorganisation spielt, und dass die Störung dieser Funktion von MeCP2 zu einer Erkrankung führen kann.

1. INTRODUCTION

The expression and stability of the genome within the eukaryotic nucleus is controlled by chromatin organization. Misregulation of chromatin structure can lead to incorrect gene activation or improper gene silencing. In the past years, a lot of effort has concentrated in the identification of factors that contribute to the organization of chromatin within the cell nucleus. These studies have provided insight into many aspects of chromatin organization, but it is still unclear how epigenetic modifications determine chromatin higher-order organization. In this dissertation, I will describe my work addressing the question of how chromatin organization is controlled by epigenetic factors and how this organization plays a role during the process of cellular differentiation during development and disease etiology. More specifically, I have focused on the role of MeCP2, an epigenetic factor in chromatin organization.

In the first section of this introductory chapter, I provide a brief summary of what is currently known about chromatin organization. In the second section I briefly describe what are the epigenetic modifications of chromatin. In the third section I introduce the molecules that read this epigenetic information. In section four, I describe the role MeCP2 plays during differentiation. Finally I give an overview of the involvement of MeCP2 in causing a neurological disease called Rett syndrome.

1.1. Chromatin organization and assembly

In the nucleus of eukaryotic cells, DNA is compacted, folded and organized within chromatin. The term “chromatin” (from the Greek word color), was first used to describe nuclear structures, which were observed by staining cells with aniline dyes (Flemming, 1882). Chromatin was subdivided further into “heterochromatin” and “euchromatin”. The term heterochromatin was used to describe chromosome portions which remained in a mitotic, condensed state in the interphase nucleus as revealed by light microscopy of moss thallus cells stained with carmine acetic acid (Heitz, 1928).

The fundamental basic structure of chromatin is called nucleosome (**Figure 1**). It consists of an octamer made from a double tetramer of the four core histones, H2A, H2B, H3 and H4. 146 bp long DNA is coiled around these core histones (reviewed in (Olins and Olins, 2003)). Nucleosomes complexed with linker histone H1 are called chromatosome. Chromatosomes are connected by 20-60 bp of DNA and form the 11nm

fiber. This is known as “beads-on-a-string” structure. (Olins and Olins, 1974) and is the 1st higher order chromatin conformation. The “beads-on-a-string” structure coils into a 30nm diameter possibly helical structure, which is known as 30nm fiber or “solenoid structure” (reviewed in (Horn and Peterson, 2002)) (**Figure 1**). Further higher order conformations such as “loop domain model” have also been proposed (discussed by (Cook, 2001)) (**Figure 1**).

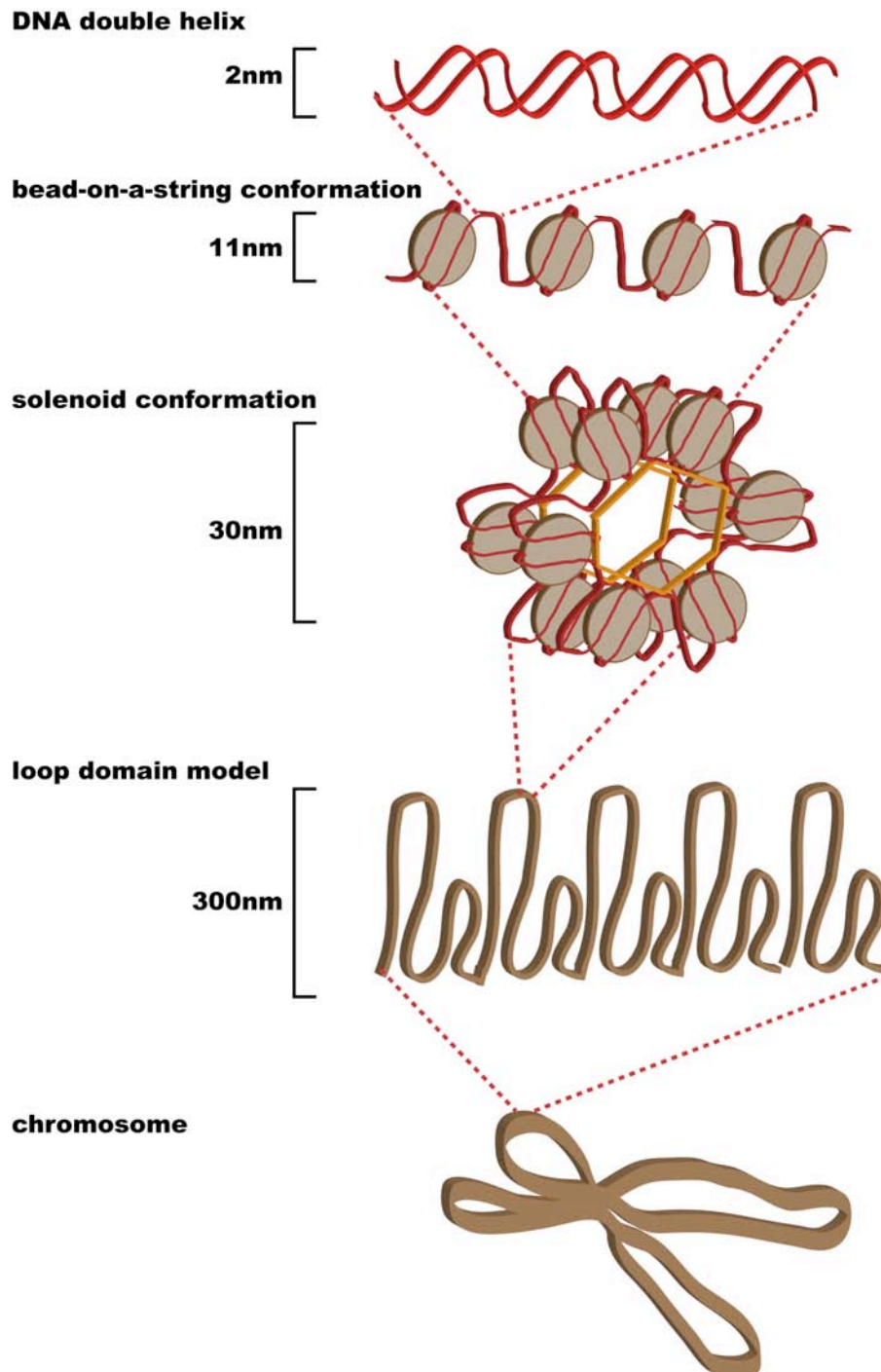


Figure 1. Schematic model of the levels of chromatin organization.

Chromatin organization is not only important for compaction of DNA into the nucleus, but is also important for controlling several genomic functions like DNA transcription, replication, repair and recombination. Modifications of chromatin proteins and DNA are referred to as epigenetic modifications.

1.2. Epigenetic modifications of chromatin

Epigenetics are a set of mechanisms and phenomenon that affect the phenotype of an organism or cell without changing the genotype. It refers to features such as chromatin and DNA modifications that are stable over multiple rounds of cell division but do not involve changes in the underlying DNA sequence of the organism (Wu and Morris, 2001). Epigenetic modifications regulate gene expression which in turn is important for differentiation. Thus while most of these features are considered dynamic over the course of development in multicellular organisms, some epigenetic features show transgenerational inheritance and are passed from one generation to the next.

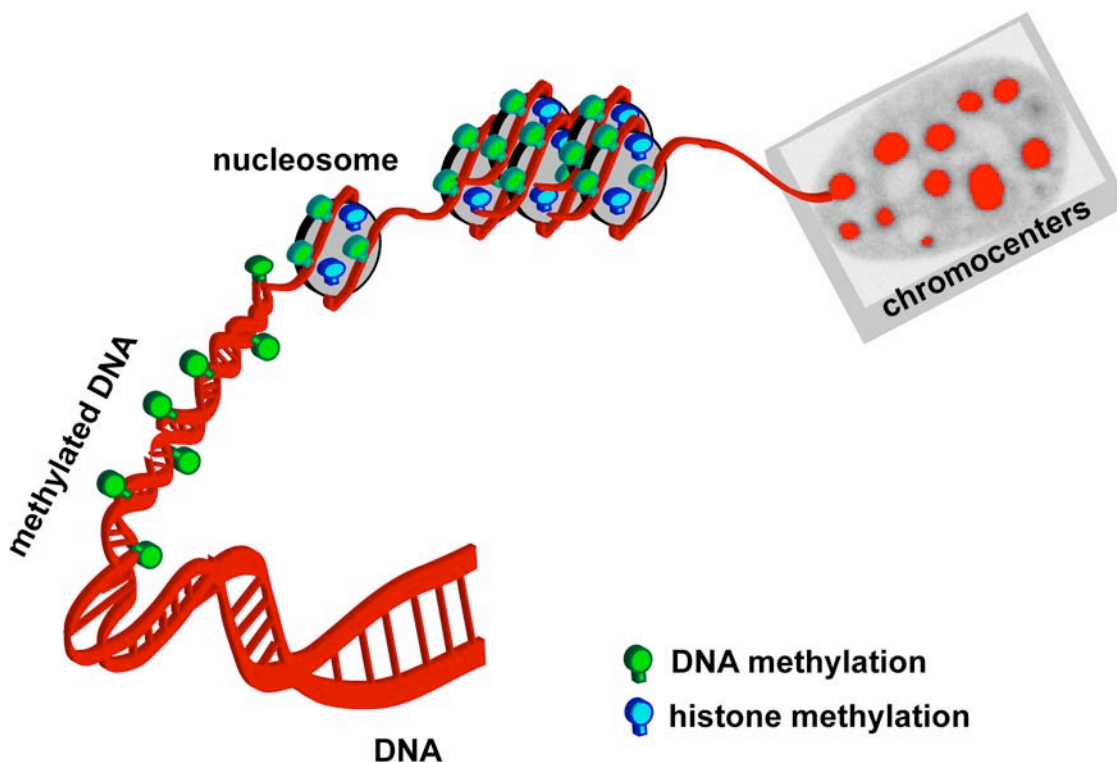


Figure 2. Epigenetic modifications and higher order chromatin organization in the cell.

Epigenetic processes include genomic imprinting, gene silencing, X chromosome inactivation, position effect variegation, reprogramming, maternal effects, regulation of histone modifications and heterochromatin. The molecular basis of epigenetics involves modifications to DNA and chromatin proteins e.g. histones (**Figure 2**).

1.2.1. Histone modifications

Histones constitute the basic components of nucleosomes and as such are a prime candidate for epigenetic modification (reviewed in (Bhaumik et al., 2007)). The N-terminal “tails” are very rich in positively charged amino acids like lysine and arginine, which interact with the DNA backbone as well as with core regions of nucleosomes, and lead to chromatin compaction. The net charge of the histone tails is changed when these residues are covalently modified, leading to a change in their capacity to interact with DNA. Multiple modifications of histones like acetylation, methylation, phosphorylation, ubiquitination, sumoylation, poly(ADP-ribosyl)ation have been described. Here, I will briefly summarize acetylation and methylation.

The acetylation and deacetylation of histones H3 and H4 is catalyzed by enzymes termed histone acetyl-transferases (HATs) or histone deacetylases (HDACs) respectively. Histone tails are normally positively charged due to amine groups present on their lysine and arginine amino acids. These positive charges help the histone tails to interact with and bind to the negatively charged phosphate groups on the DNA backbone. Acetylation, which occurs normally in a cell, neutralizes the positive charges on the histone by changing amines into amides and decreases the ability of the histones to bind to DNA. Histone deacetylases removes those acetyl groups, restoring positive charges to the histone tails and encouraging high-affinity binding between the histones and DNA backbone. Histone acetyl transferases (HAT) acetylate conserved lysine amino acids on histone proteins by transferring an acetyl group from acetyl CoA to lysine to form ϵ -N-acetyl lysine. Histone acetylation is generally linked to transcriptional activation and is associated with euchromatin. Initially, it was thought that acetylation of lysine neutralizes the positive charge normally present, thus reducing affinity between histone and (negatively charged) DNA which renders DNA more accessible to transcription factors. More recently, it has emerged that lysine acetylation and other posttranslational modifications of histones generate binding sites for specific protein-

protein interaction domains, such as the acetyl-lysine binding bromodomain. In contrast, histone deacetylases (HDAC) remove acetyl groups from ϵ -N-acetyl lysine amino acids on histones, causing the DNA to wrap more tightly around the histones. This change interferes with gene transcription by blocking access by transcription factors. The overall result of histone deacetylation is a global (non specific) reduction in gene expression.

Histone methylation (**Figure 2**) involves the addition of methyl groups to N-terminal lysines (Lachner et al., 2003) and arginines (Stallcup, 2001) of histone H3 and H4. This modification does not have an affect on the charge of the modified histones (Strahl and Allis, 2000) and has been found to be associated with both transcriptional activation and silencing. Methylation at K4 and K36 of histone H3 as well as arginine is associated with transcriptional activity, whereas methylation at K9 and K27 of H3 and K20 of H4 are associated with silencing (Peters et al., 2003). Different enzymes are associated with methylation marks in eu- and heterochromatin. Histone methyl transferases (HMT), histone-lysine N-methyl transferases and histone-arginine N-methyl transferases, are enzymes which catalyze the transfer of one to three methyl groups from the cofactor S-Adenosyl methionine to lysine and arginine residues of histone proteins. G9a is shown to be involved in di-methylation of H3K9 in euchromatin (Tachibana et al., 2001), while Suv39h1/2 is thought to be responsible for tri-methylation of H3K9 in heterochromatin (Peters et al., 2003).

1.2.2. DNA modifications

The direct modification of DNA, specifically DNA methylation, is another important aspect of epigenetics (**Figure 2**) that has been shown to influence gene expression, by changing chromatin structure. This process is evolutionarily conserved and has been observed in many organisms from bacteria to mammals. Methyl groups are added on either cytosines or adenines, at the C5 or N6 position, resulting in the formation of either 5-methyl cytosines (5mC) or N6-methyladenine (N6mA). Methylation in prokaryotes is associated with a protective mechanism that prevents the host DNA from restriction endonucleases, which are used to digest the foreign DNA (Srinivasan and Borek, 1964). Eukaryotic DNA is primarily methylated at cytosine residues. In humans, it is estimated that approximately one percent of the DNA bases are methylated at 5-methyl cytosines (Kriaucionis and Bird, 2003)

DNA methylation is essential for embryonic development, since mice lacking DNMTs do not survive (Li et al., 1992; Okano et al., 1999). DNA methylation is also important for X chromosome inactivation (XCI) in females. Furthermore, DNA methylation is important for direct transcriptional silencing and suppression of recombination. In humans, several DNMTs (DNA methyl transferases) have been found (reviewed in (Cheng and Blumenthal, 2008). Out of these DNA methyl transferases 1, 3a, and 3b (DNMT1, DNMT3a, DNMT3b) are associated with the process of DNA methylation. It is thought that DNMT3a and DNMT3b are the de novo methyl transferases that set up DNA methylation patterns early in development, while DNMT1 maintains these patterns, copying them to the daughter strands during DNA replication. In both cases, SAM (S-adenosyl-L-methionine) serves as a methyl-group donor. DNMT3L is a protein that is homologous to DNMT3a and 3b but has no catalytic activity. Instead, it assists the de novo methyl transferases by increasing their ability to bind to DNA and stimulates their activity. Finally, DNMT2 has been identified as an "enigmatic" DNA methyl transferase homolog, containing all 10-sequence motifs common to all DNA methyl transferases; however, DNMT2 does not methylate DNA (Okano et al., 1998) but instead methylates cytosine 38 in the anticodon loop of tRNA (Goll et al., 2006; Rai et al., 2007).

Resetting of methylation marks during mammalian embryonic development is necessary. Reprogramming refers to erasure and remodeling of epigenetic marks, such as DNA methylation, during mammalian development (Reik and Walter, 2001). While many genes are highly methylated in sperm DNA (Groudine and Conkin, 1985; Rai et al., 2007) genes are often less methylated in oocytes (Monk et al., 1987; Sanford et al., 1987). After fertilization the paternal and maternal genomes are once again demethylated and remethylated (except for differentially methylated regions associated with imprinted genes). This reprogramming is likely required for totipotency of the newly formed embryo and erasure of acquired epigenetic changes (Huppke et al., 2000; Kafri et al., 1992; Sanford et al., 1987). After implantation, the DNA of the extra embryonal membranes (yolk sac and placenta) becomes dramatically demethylated, while the DNA of the fetal tissues is subjected to a de novo methylation process (Monk et al., 1987; Razin and Szyf, 1984; Sanford et al., 1987). During the process of gametogenesis the primordial germ cells must have their original biparental DNA methylation patterns erased and re-established based on the sex of the transmitting parent (Chaillet et al., 1991; Gomperts et al., 1994; Kafri et al., 1992). In vitro manipulation of pre-implantation

embryos has been shown to disrupt methylation patterns at imprinted loci (Mann et al., 2003).

1.3. Molecules that read epigenetic information

Epigenetic information in the form of DNA and histone modifications needs to be interpreted into gene expression/repression programs. Methylated histone H3 and methylated cytosines are associated with gene silencing and are recognized by the members of heterochromatin protein 1 (HP1) family and the methyl CpG binding protein family (MBD), respectively. Both these families of chromatin associated factors have been connected with transcriptional repression.

1.3.1. Heterochromatin Protein 1

Heterochromatin protein 1, a major component of heterochromatin was first identified in *Drosophila melanogaster* (James and Elgin, 1986) where it acts as a dominant suppressor of position effect variegation (PEV). HP1 belongs to a highly conserved family of chromatin proteins, with homologues that are found from fission yeast (Swi6, Chp2 and Chp1) to humans (HP1 α , HP1 β and HP1 γ) (Huisinga et al., 2006). The CBX (chromobox) class of genes encodes the HP1 family of protein. In humans, HP1 α , HP1 β and HP1 γ are encoded by chromobox homolog (CBX5), 1(CBX1) and 3(CBX3) respectively.

Three functional domains have been characterized in HP1. First, is the chromodomain (CD) at the N terminus. This domain is highly conserved and binds to di and trimethylated K9 at histone H3 (Aasland and Stewart, 1995). Second, is the chromoshadow domain (CSD) at the carboxy terminus. It is associated with homo and/or heterodimerization and interaction with other proteins. Third, is the variable linker or hinge region. It is present in between chromodomain and chromoshadow domain. It contains a nuclear localization signal (**Figure 3**).

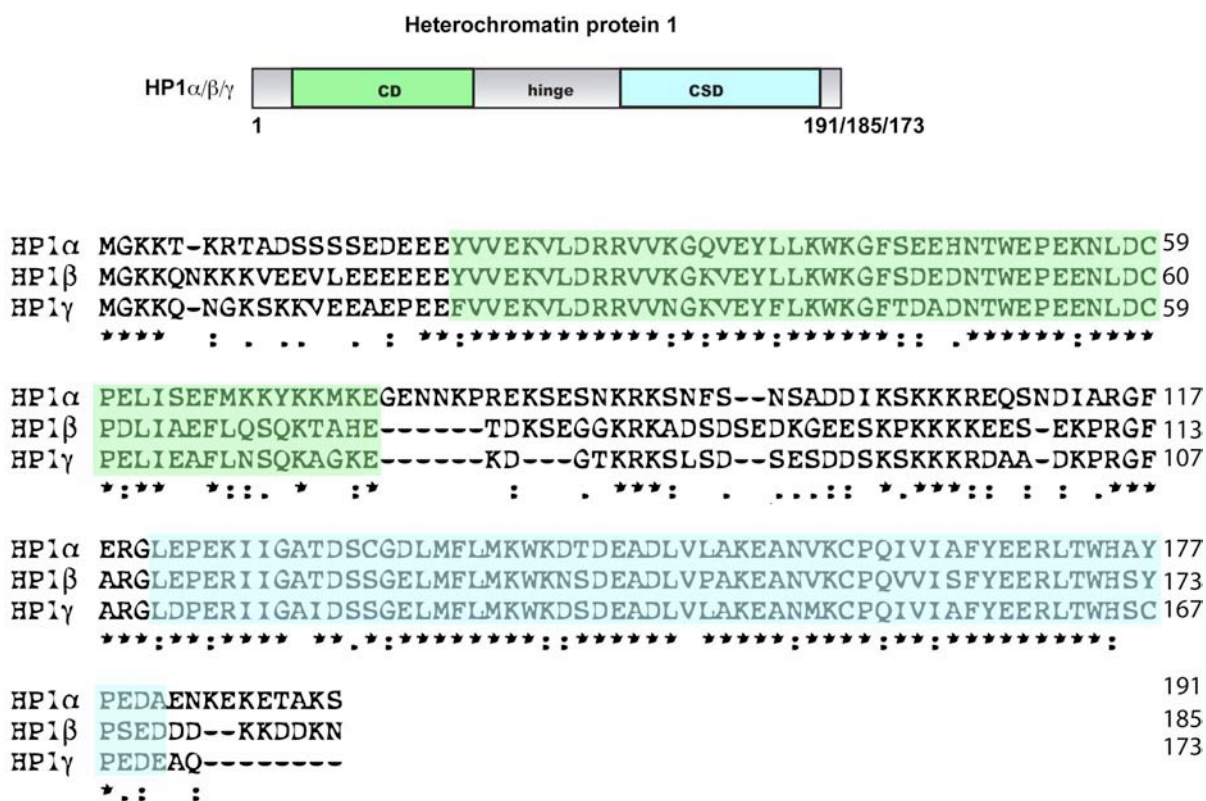


Figure 3. Scheme and alignment of different isomers of human heterochromatin protein1. ‘*’ indicates positions which have a single fully conserved residue. ‘:’ indicates that either of the strong groups (STA, NEQK, NHQK, NDEQ, QHRK, MILV, MILF, HY, FYW) is conserved. ‘.’ Indicates either of the weak groups (CSA, ATV, SAG, STNK, STPA, SGND, SNDEQK, NDEQHK, NEQHRK, FVLIM, HFY) is conserved. These are all the positively scoring groups that occur in the Gonnet Pam250 matrix. The strong and weak groups are defined as strong score >0.5 and weak score =<0.5 respectively.

Purified chromodomain is found as a monomer, whereas chromoshadow domain can form dimers in solution (Brasher et al., 2000). Localization studies of the protein have suggested that HP1 is not only localized to heterochromatin but also to euchromatin regions (Horsley et al., 1996; Minc et al., 1999). Studies in mammalian cells have shown that HP1 α and HP1 β are mainly distributed at pericentric heterochromatin domains whereas HP1 γ is localized in discrete euchromatin sites (Minc et al., 1999). In addition to its binding to methylated K9 of histone H3, HP1 has been shown to interact with several other histone and non-histone proteins.

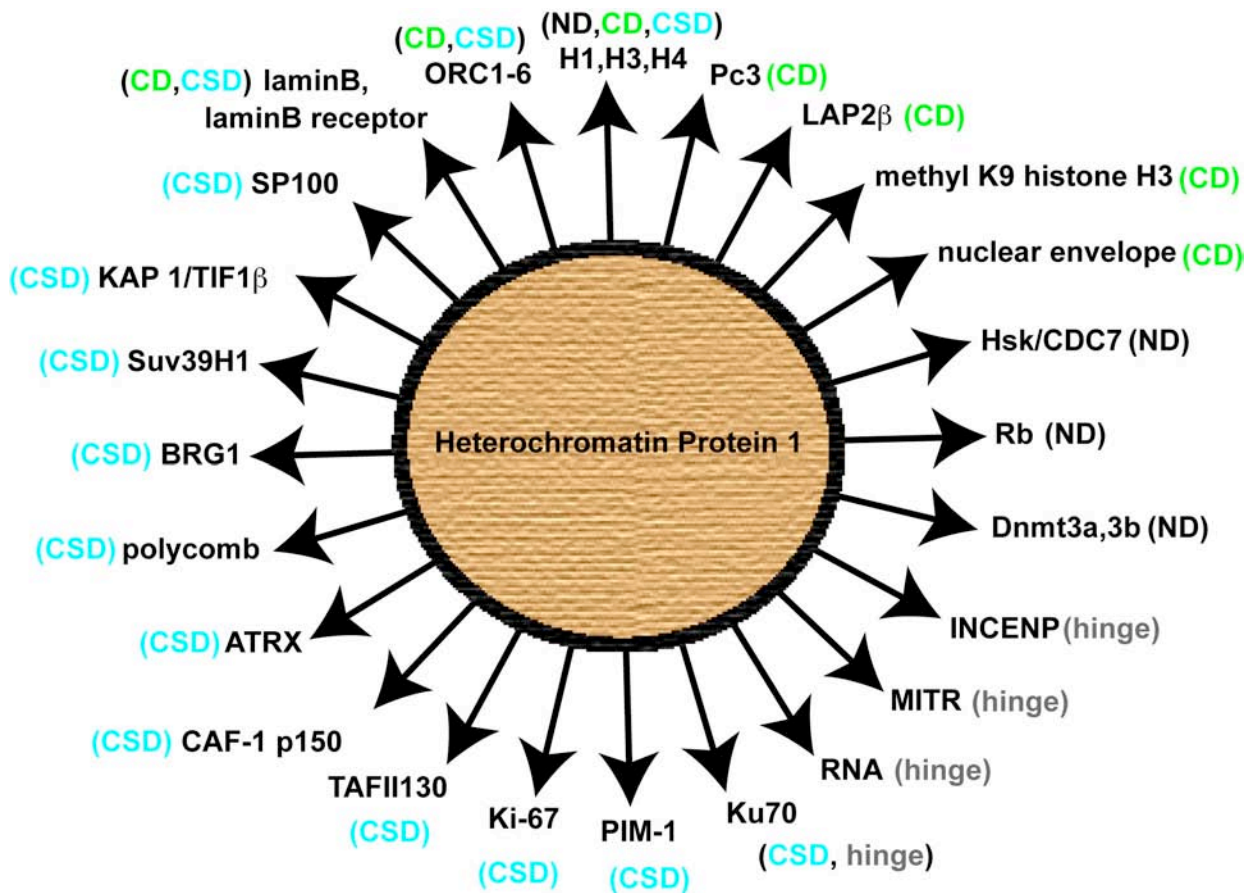


Figure 4. Summary of HP1 protein interactions. In parenthesis, is indicated the domain involved in interaction. CD (chromodomain), CSD (chromoshadow domain) and ND (not determined).

Table 1. Summary of HP1 protein interactions.

Interacting partners	Interaction domain	Reference
Kap-1/Tif1 β (Kruppel box associated protein)	CSD	(Nielsen et al., 1999)
CAF-1 p150 (chromatin assembly factor 1 p150 subunit)	CSD	(Murzina et al., 1999)
TAF_{II}130 (TATA-binding protein associated factor p130)	CSD	(Vassallo and Tanese, 2002)
SP100 (nuclear auto antigen Speckled 100 kD)	CSD	(Seeler et al., 1998)
Suv39H1	CSD	(Melcher et al., 2000)
Pc (polycomb)	CSD	(Yamamoto et al., 2004)
ATRX (SWI2/SNF2 DNA helicase/ATPase)	CSD	(McDowell et al., 1999)
Histone H4	CSD	(Zhao et al., 2000) (Polioudaki et al., 2001)
PIM-1 (proviral integration site 1)	CSD	(Koike et al., 2000)
Ki-67 (cell proliferation antigen of monoclonal antibody Ki-67)	CSD	(Scholzen et al., 2002)
LBR (lamin B receptor)	CSD	(Ye et al., 1997)
BRG1 (SWI/SNF related transcriptional activation)	CSD	(Nielsen et al., 2002)
Ku70 (K 70 auto antigen)	CSD, hinge	(Song et al., 2001)
MITR (myocyte enhancer factor 2 (MEF2)-interacting transcription repressor)	hinge	(Zhang et al., 2002)
INCENP (inner centromere protein)	hinge	(Ainsztein et al., 1998)
ORCI-6 (origin recognition complex 1-6)	CD, CSD	(Pak et al., 1997)
Pc3 (cohesion subunit Pc3)	CD	(Nonaka et al., 2002)
H3K9Me3 (trimethyl K9 histone H3)	CD	(Bannister et al., 2001)
Histone H3	CD	(Nielsen et al., 2001) (Polioudaki et al., 2001)
LAP2β (lamin associated polypeptide 2 β)	CD	(Kourmouli et al., 2001)
lamin B	CD	(Kourmouli et al., 2001)
Hsk I/CDC7 (<i>S. pombe</i> homolog of CDC7/ cell division cycle 7)	ND	(Baillis et al., 2003)
RNA	ND	(Muchardt et al., 2002)
Histone H1	ND	(Nielsen et al., 2001)
Rb (retinoblastoma)	ND	(Nielsen et al., 2001)
Dnmt 3a, 3b (DNA methyl transferase 3a, 3b)	ND	(Bachman et al., 2001)

The data above show that HP1 forms a web of protein interactions via multiple domains (**Figure 4, Table 1**).

Furthermore, fluorescence photobleaching recovery experiments (FRAP) (Cheutin et al., 2003) showed that HP1 binding to pericentric heterochromatin is not stable, but rather

highly dynamic. This allows for modifications to occur while maintaining a stable chromatin state.

1.3.2. Methyl CpG binding proteins

For quite sometime DNA methylation has been correlated with transcription repression. In the most direct way, methylation of cytosines (5mC) prevents the binding of basal transcriptional factors that require contact with cytosines in the major groove of the DNA double helix. A second indirect way methylation of cytosines can induce transcription repression is via methyl-CpG binding proteins.

The methyl-CpG-binding protein family comprises MeCP2, MBD1, MBD2, MBD3 and MBD4, which share the conserved methyl-CpG-binding domain (Hendrich and Bird, 1998) (**Figure 5**).

MBD1 is the largest member of the family, around 50-70kDa and contains a sequence motif, the CXXC motif, shared with Dnmt1 (Cross et al., 1997). There are at least five splicing variants of the mRNA of human MBD1 (Fujita et al., 1999; Ng et al., 2000) and three variants in mice (Jorgensen et al., 2004). The major difference between them is the presence of either two or three CXXC cysteine rich regions. Unlike MeCP2, MBD1 can repress transcription of methylated and unmethylated templates (Cross et al., 1997; Fujita et al., 1999). The solution structure of the MBD domain of MBD1 has been solved (Ohki et al., 1999). The structure of this domain is very similar to that of MeCP2. Though, in MeCP2, three solvent exposed hydrophobic residues have been predicted to directly contact the methyl groups in the major groove (Wakefield et al., 1999). In MBD1 however, only one position out of these three contain a hydrophobic residue, the tyrosine 34.

MBD2 is a 44-kDa protein with 414 amino acids. It binds to methylated DNA with its MBD domain, and it has also been shown to possess transcription repression activity. Out of these roughly amino acids 140-400 including the MBD are highly similar to MBD3 (Hendrich and Bird, 1998). The N-terminal part of the protein consists largely of lysine and arginine repeats. MBD2b, lacking this amino terminal 140 amino acids has been reported to show a demethylase activity (Bhattacharya et al., 1999) although these results have not been confirmed. MBD2 interacts with the NuRD complex generating

the MeCP1 complex. This was the first methyl CpG binding activity, which was isolated in mammals (Meehan et al., 1989).

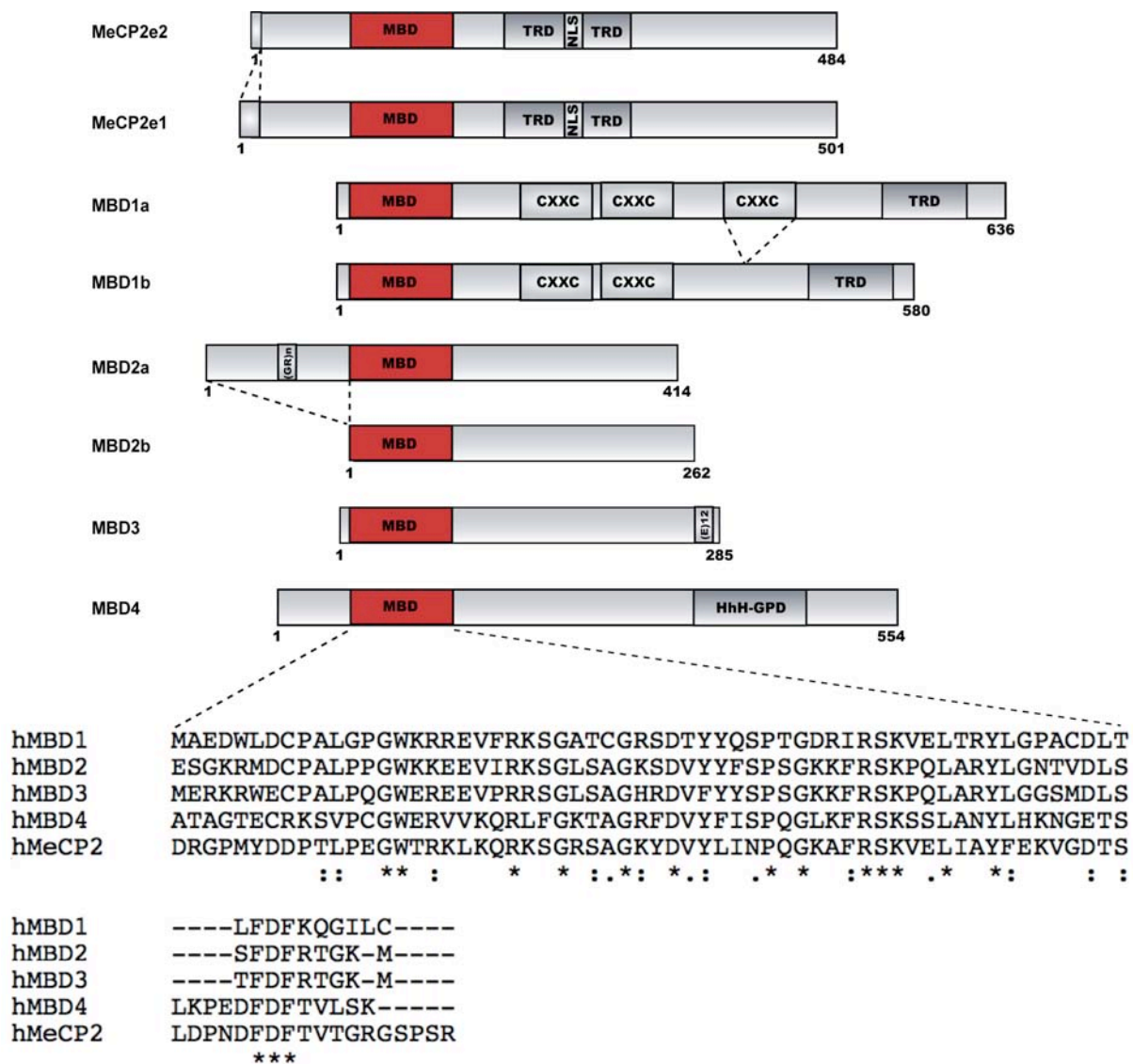


Figure 5. Scheme of different members of methyl CpG binding family and alignment of their MBD. Symbols are as indicated in Figure 3.

MBD3 is the smallest member of the family, around 30 kDa. It is the only member of the MBD family, which does not bind to methylated CpGs due to two amino acid substitutions within the MBD domain of MBD3 (Saito and Ishikawa, 2002). Some other vertebrates like *Xenopus*, Zebrafish have two MBD3 forms, one of which can bind to the methylated CpGs (Wade et al., 1999). The global demethylation event, characteristic of early mammalian development is absent in both Zebrafish (Macleod et al., 1999) and

Xenopus (Stancheva and Meehan, 2000). MBD3 is also a member of the NuRD co-repressor complex, which plays an important role in transcription silencing via histone deacetylation. MBD3 has been shown to be important during embryonic development (Hendrich et al., 2001).

MBD4 is a 63-kDa protein that is not associated with histone deacetylase activity or transcription regulation. Its carboxyl terminal has homology to bacterial repair enzymes (Hendrich and Bird, 1998). MBD4 plays a major role in preventing the mutational risk, by transition of 5mC→T by deamination. The MBD domain of MBD4 binds to methylated CpG dinucleotides, but has preference for 5mC paired with TpG (Hendrich et al., 1999). The C-terminal glycosylase moiety present in MBD4 specifically removes Ts from G-T mismatches (Hendrich and Tweedie, 2003). It has been shown that MBD4^{-/-} cells show a 3.3 fold increased C→T transition, compared to wild type (Millar et al., 2002; Wong et al., 2002).

MeCP2 is the founding member of the MBD (methyl CpG protein binding) family (Lewis et al., 1992). MeCP2 is quite conserved among different family members (**Figure 7**). The crystal structure of MeCP2-MBD in complex with DNA (Ho et al., 2008) has been shown to be similar to the unliganded structure (Wakefield et al., 1999). The MBD has a wedge shaped structure, with one face of the wedge composed of a beta sheet and the other face consisting of the alpha helix and hairpin loop. Two main functional domains have been defined for MeCP2. The MBD domain, which is capable of binding to one or more symmetrically methylated CpGs (Nan et al., 1993). Recently, it has been shown that high affinity binding of MeCP2 to DNA requires AT rich sequences adjacent to CpG sites on DNA (Klose et al., 2005). The second well-characterized domain of MeCP2 is the transcriptional repression domain or TRD (Nan et al., 1997), which is required for large distance (2kb mRNA) transcriptional repression *in vitro* and *in vivo*. MeCP2 after binding specifically to methylated DNA recruits Sin3A and HDAC, which further deacetylates the tails of H3 and H4 histones. This deacetylation leads to compaction of chromatin and thus the chromatin becomes inaccessible to transcription factors. Silencing can be relieved by inhibition of histone deacetylases (Jones et al., 1998). MeCP2 interacts with several other proteins as summarized in (**Figure 6**).

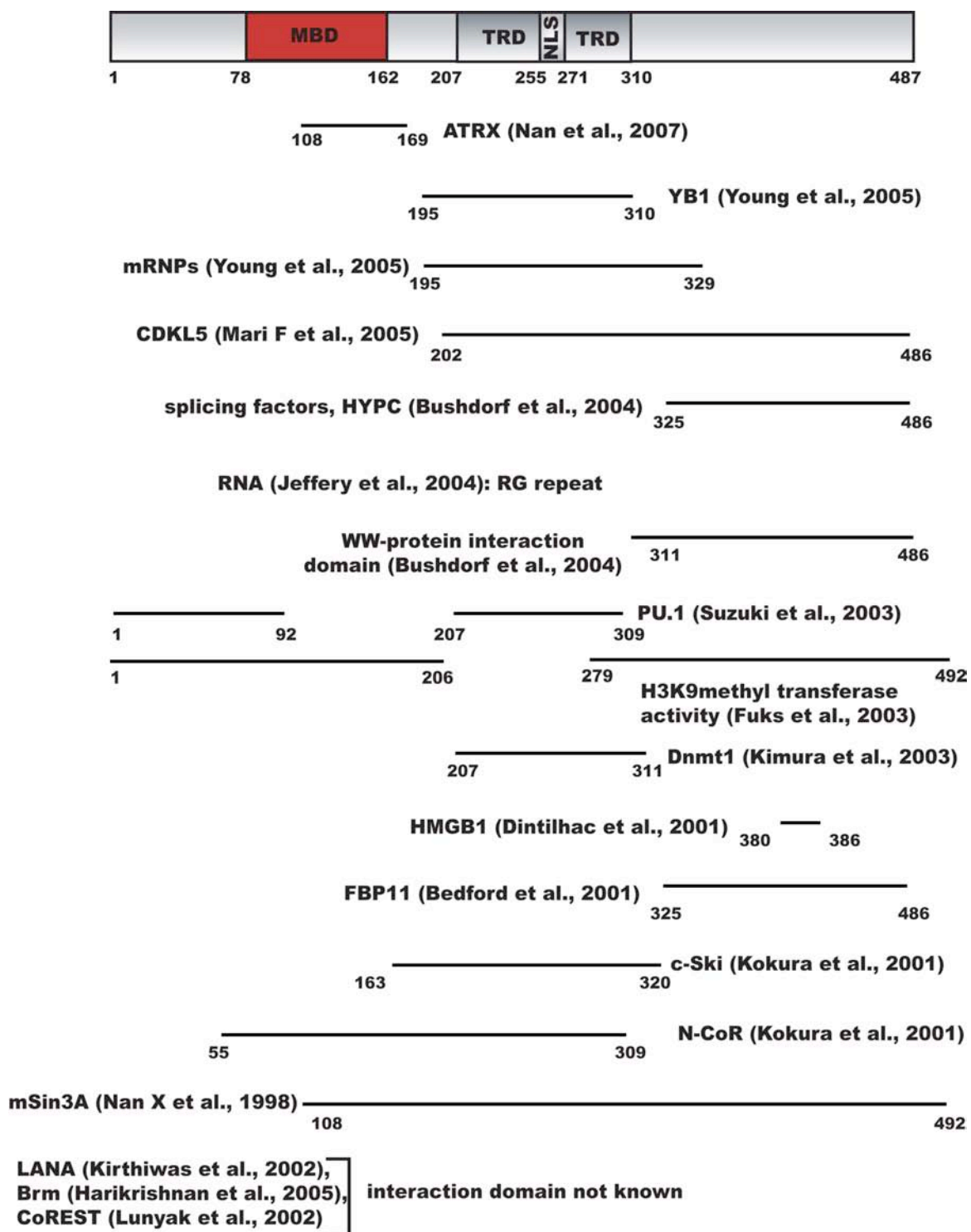


Figure 6. Interaction of MeCP2 with other proteins.

MeCP2 is known to lower transcriptional noise, rather than acting as a global repressor. Further, recently it has been shown that the C-terminal domain of MeCP2 can also interact with unmethylated DNA (Nikitina et al., 2007a).

MECP2 is expressed in different tissues as shown by Northern blot analysis (Coy et al., 1999; D'Esposito et al., 1996; Reichwald et al., 2000; Shahbazian et al., 2002). The gene consists of 4 exons (Reichwald et al., 2000). *In vivo* MeCP2 exists in two alternatively spliced isoforms. MeCP2A/MeCP2e2 (Nan et al., 1993) and MeCP2B/MeCP2e1 (Mnatzakanian et al., 2004). MeCP2B/MeCP2e1 utilizes exon 1 of MeCP2, skips exon2, and uses full-length exons 3 and 4 and is the longer form of MeCP2. The larger transcript, which is found mostly in the brain (Kriaucionis and Bird, 2003) is 10kb long, is composed of 1.5kb coding region and 8.5kb untranslated 3' UTR region (Coy et al., 1999; Reichwald et al., 2000). MeCP2A/MeCP2e2 utilizes exon 2,3 and 4 of MeCP2 gene. This shorter and more predominant form migrates as a 1.9 kb band. This form is mostly expressed in heart, kidney and skeletal muscle.

To understand the function of MeCP2 in development, it is important to know in detail its changes during differentiation.

```

Homo sapiens MVAGMLGLREEKSEDQDLQGLKDKPLKFKVKKDKKEEKEGKHEPVQPSAHHSAEPAEAG
Macaca fascicularis MVAGMLGLREEKSEDQDLQGLKDKPLKFKVKKDKKEDKEGKHEPVQPSAHHSAEPAEAG
Rattus norvegicus MVAGMLGLRKEKSEDQDLQGLKDKPLKFKVKKDKKEDKEGKHEPLQPSAHHSAEPAEAG
Mus musculus MVAGMLGLREEKSEDQDLQGLRDKPLKFKKAKDKKEDKEGKHEPLQPSAHHSAEPAEAG
*****;*****;*****;*****;*****;*****;*****;*****

Homo sapiens KAETSESGSAPAVPEASASPQRRIIRDRGPMYDDPTLPEGWTRKLKQRKSGRSAGKY
Macaca fascicularis KAETSESGSAPAVPEASASPQRRIIRDRGPMYDDPTLPEGWTRKLKQRKSGRSAGKY
Rattus norvegicus KAETSESSGSAPAVPEASASPQRRIIRDRGPMYDDPTLPEGWTRKLKQRKSGRSAGKY
Mus musculus KAETSESSGSAPAVPEASASPQRRIIRDRGPMYDDPTLPEGWTRKLKQRKSGRSAGKY
*****;*****;*****;*****;*****;*****;*****;*****

Homo sapiens DVYLINPQGKAFRSKVELIAYFEKVGDTSLDPNDFDFTVTGRGSPSRREQKPPKKPKSPK
Macaca fascicularis DVYLINPQGKAFRSKVELIAYFEKVGDTSLDPNDFDFTVTGRGSPSRREQKPPKKPKSPK
Rattus norvegicus DVYLINPQGKAFRSKVELIAYFEKVGDTSLDPNDFDFTVTGRGSPSRREQKPPKKPKSPK
Mus musculus DVYLINPQGKAFRSKVELIAYFEKVGDTSLDPNDFDFTVTGRGSPSRREQKPPKKPKSPK
*****;*****;*****;*****;*****;*****;*****;*****

Homo sapiens APGTGRGRGRPKGSGTTRPKAATSEGVQVQRVLEKSPGKLLVKMPFQTSPGGKAEGGGAT
Macaca fascicularis APGTGRGRGRPKGSGTTRPKAATSEGVQVQRVLEKSPGKLLVKMPFQTSPGGKAEGGGAT
Rattus norvegicus APGTGRGRGRPKGSGTTRPKAATSEGVQVQRVLEKSPGKLLVKMPFQASPGGKGEKGGAT
Mus musculus APGTGRGRGRPKGSGTTRPKAATSEGVQVQRVLEKSPGKLLVKMPFQASPGGKGEKGGAT
*****;*****;*****;*****;*****;*****;*****;*****

Homo sapiens TSTQVMVIKRPGRKRKA EADPQAI PKKRGRKPGSVVAAAAEAKKKAVKESSIRSVQETV
Macaca fascicularis TSTQVMVIKRPGRKRKA EADPQAI PKKRGRKPGSVVAAAAEAKKKAVKESSIRSVQETV
Rattus norvegicus TSAQVMVIKRPGRKRKA EADPQAI PKKRGRKPGSVVAAAAEAKKKAVKESSIRSVQETV
Mus musculus TSAQVMVIKRPGRKRKA EADPQAI PKKRGRKPGSVVAAAAEAKKKAVKESSIRSVHETV
**;*****;*****;*****;*****;*****;*****;*****

Homo sapiens LPIKKRKTRETVSIEVKEVVKPLLVS TLGEKSGKGLKTCKSPGRKS KESSPKGRSSSASS
Macaca fascicularis LPIKKRKTRETVSIEVKEVVKPLLVS TLGEKSGKGLKTCKSPGRKS KESSPKGRSSSASS
Rattus norvegicus LPIKKRKTRETVSIEVKEVVKPLLVS TLGEKSGKGLKTCKSPGRKS KESSPKGRSSSASS
Mus musculus LPIKKRKTRETVSIEVKEVVKPLLVS TLGEKSGKGLKTCKSPGRKS KESSPKGRSSSASS
*****;*****;*****;*****;*****;*****;*****;*****

Homo sapiens PPKKEHHHHHHHSESPKAPVLLPLP PPPPEPESSE DPTSPPEPQDLSSSVCKEEKMPR
Macaca fascicularis PPKKEHHHHHHHSESPKAPVLLPLP PPPPEPESSE DPTSPPEPQDLSSSVCKEEKMPR
Rattus norvegicus PPKKEHHHHHHHAESP KAPMPLL-- P PPPPEPQSS EDPI SPPEPQDLSSSICKEEKMPR
Mus musculus PPKKEHHHHHHHSEST KAPMPLL-- S PPPPEPESSE DPI SPPEPQDLSSSICKEEKMPR
*****;*****;*****;*****;*****;*****;*****;*****

Homo sapiens GGSLESDGCPKEPAKTQ PAVATAA-----TAAE KYKHRGEGERKDIVSSSMRPNRE
Macaca fascicularis GGSLESDGCPKEPAKTQ PAVATAA-----TAAE KYKHRGEGERKDIVSSSMRPNRE
Rattus norvegicus AGSLESDGCPKEPAKTQ PMVAAAATT TTTTPTVAE KYKHRGEGERKDIVSSSMRPNRE
Mus musculus GGSLESDGCPKEPAKTQ PMVATTT-----TVAE KYKHRGEGERKDIVSSSMRPNRE
.*****;*****;*****;*****;*****;*****;*****;*****

Homo sapiens EPVDSRTPVTERVS
Macaca fascicularis EPVDSRTPVTERVS
Rattus norvegicus EPVDSRTPVTERVS
Mus musculus EPVDSRTPVTERVS
*****;*****;*****;*****;*****;*****;*****;*****

```

Figure 7. Alignment of MeCP2 from different species. Symbols are as indicated in figure 3.

1.4. Cellular differentiation and MeCP2

In developmental biology the term differentiation is used to describe the diversification of pathways, wherein a less specified cell becomes a more specialized cell type. A cell that is able to differentiate into many cell types is known as pluripotent, while the cell that is able to differentiate into all cell types is called totipotent. Differentiation occurs numerous times during the development of a multicellular organism as the organism develops from a single zygote to a complex system of tissues and cell types. Differentiation is a common process in adults as well: adult stem cells divide and create fully differentiated daughter cells during tissue repair and during normal cell turnover. When a cell differentiates its size, shape, polarity, metabolic activity, and responsiveness to signals may change dramatically. These changes are largely due to highly controlled modifications in gene expression. With few exceptions, cellular differentiation does not involve a change in the DNA sequence itself. Thus, different cells can have very different physical characteristics despite having the same genome. Differentiation is driven by the activity of nuclear proteins that regulate transcription. During differentiation, proliferating cells eventually get committed, migrate, withdraw from cell cycle, and form neurons, myofibrils etc.

Further it has been shown that MeCP2 is involved in the differentiation of neuronal cells, in particular in the development and maintenance of dendritic spines, rather than in cell fate decision (Armstrong et al., 1995; Armstrong et al., 1998; Kishi and Macklis, 2004). Our studies in muscle differentiation, also point in a similar direction. Wherein, the level of expression of MeCP2 increases dramatically from myoblasts to myotubes (Brero et al., 2005). Though neurogenesis has been intensively studied *in vivo*, a reproducible *in vitro* differentiation system is still lacking. Moreover most of the existing cell lines are tumor derived. Therefore, we chose to use a well-established *in vitro* myogenic differentiation system to perform our studies.

1.5. Rett syndrome and MeCP2

Rett syndrome (RTT, OMIM: 321750) is a neurological disorder, first reported by Dr. Andreas Rett in 1966. It is the second most common mental retardation disease in females after Down's syndrome with an incidence of one in every 10,000 to 15,000

females born. The females develop normally until 6 to 8 months of age and then show a progressive stop in development accompanied by regression of acquired skills.

1.5.1. Clinical features of Rett syndrome patients

Clinical features include deceleration of head growth, loss of purposeful hand movement, ataxia, acoustic features, seizures, stereotypic hand movements “hand wriggling” and respiratory dysfunction. 80% of RTT cases have been reported to be sporadic (Amir et al., 1999; Bienvenu et al., 2000; Buyse et al., 2000; Cheadle et al., 2000; Huppke et al., 2000; Xiang et al., 2000). It is further characterized by loss of acquired motor and language skills, autistic features and stereotypical hand movements.

1.5.2. Genetics behind Rett syndrome

Familial occurrences suggested that RTT is an X-linked dominant disorder (**Figure 8**), with possible male lethality. Genetic mapping of such familial cases have identified chromosome X position q28 (Xq28) (Ellison et al., 1992; Sirianni et al., 1998). The mutation was mapped on the gene MECP2 (Amir et al., 1999). Due to X chromosome inactivation (XCI), each cell of the female body expresses only one of the X chromosome alleles. XCI is a random process. The severity of the disease in females depends on which cells the X chromosome having the wild-type gene was inactivated.

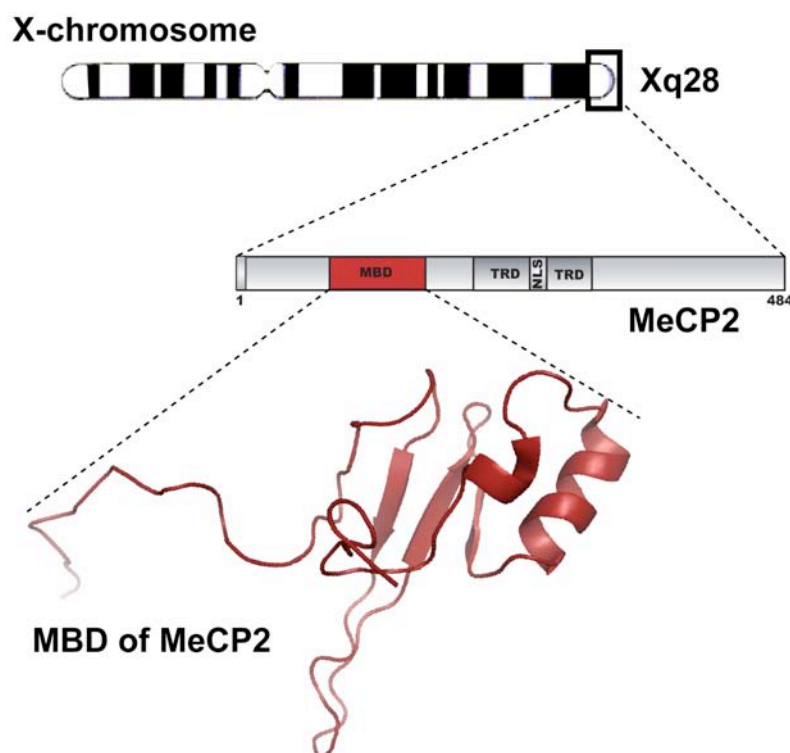


Figure 8. Localization of MECP2 gene, functional domains of the corresponding gene product and structure of the MBD domain.

The majority of Rett mutations found on MECP2 are due to direct C→T conversions in CpG dinucleotides (Dragich et al., 2000). Sperm DNA is more highly methylated than same sequences in oocytes, because of the need for greater compaction. Also, methylated cytosines become converted to uracil, which is not easily identified by the repair machinery. Due to these reasons sperm DNA is liable to more mutations in a highly CG-rich gene such as MeCP2 (Thomas, 1996), and therefore females are more susceptible to RTT than males, as they get one of their X chromosomes from the paternal side.

1.5.3. Genotype-phenotype correlations

The studies done on genotype-phenotype correlations have yielded inconsistent results. Some groups showed that truncation mutations led to more severe symptoms as compared to missense mutations (Cheadle et al., 2000; Monros et al., 2001), however

others groups could not find such a correlation (Amir et al., 1999; Bienvenu et al., 2000; Huppke et al., 2000). This could be explained by the fact that in females there is random X chromosome inactivation, and the severity of the symptoms depends upon the number and types of cells having the mutated form of MeCP2 in the active X chromosome. Since in males, there is no XCI, the genotype-phenotype correlation could be clearer. Unfortunately, much less cases of RTT males have been reported.

1.5.4. Mouse models for Rett syndrome

The brain size of RTT patients and MeCP2 null mice is smaller than normal individuals (Armstrong, 1997; Chen et al., 2001). In the MeCP2 null mice, the hippocampus CA2 neurons are quite smaller than the wild type. Also, the nuclei of the neurons throughout the CNS were noticeably smaller (Chen et al., 2001). In addition, in heterozygous female RTT brains, neurons in layer III and V of the frontal, motor and inferior temporal cortex were smaller, with shorter apical and basilar dendritic branches (Armstrong et al., 1995; Armstrong et al., 1998).

There has been substantial effort in the development of mouse models for Rett syndrome. These models have focused on firstly mimicking the clinical phenotypes seen in Rett patients. More recently, efforts have been made to rescue MeCP2 gene expression and restoration of MeCP2 function. The latter have the major drawback that induction of wild type MeCP2 in the context of a null genotype would rather not reflect the disease problem where a mutated gene product is present throughout. The different mouse genetic models and ensuing studies are summarized in Table 2.

Table 2. Studies of Rett syndrome using mouse models.

Mouse model	Short summary of the mouse model	Reference
Null	MeCP2 lacking male ES cells could not support development. (embryonic lethality).	(Tate et al., 1996)
Null	MeCP2 null mice were produced using Cre-LoxP recombination system to delete exon 3 of MeCP2 gene; mimics Rett syndrome; MeCP2 plays a role in mature neurons and its role is not restricted to immature neurons	(Chen et al., 2001)
Null	MeCP2 null mice were produced by Cre-LoxP recombination system to delete exon 3 and 4 of MeCP2 in ES cells; mimics Rett syndrome; MeCP2 is required for a stable brain function, rather than in brain development.	(Guy et al., 2001)
Truncated	Mouse with a stop codon after codon 308, they called the mutated allele as MeCP2308; MeCP2 was localized to heterochromatin domain <i>in vivo</i> , but histone H3 was hyperacetylated.	(Shahbazian and Zoghbi, 2002)
Truncated	MeCP2 308/X; X-chromosome inactivation (XCI) patterns were unbalanced in more than 60% of the animals, favoring expression of the wild type allele.	(Young and Zoghbi, 2004)
Null	MeCP2 null mouse model produced by Cre-LoxP recombination system to delete exon 3 of MeCP2; looked on the olfactory system and found that posttranslational protein modifications play an important role and concluded that not only transcription should be considered but also the brain region and the age of the mouse and the posttranslational modifications should be considered.	(Matarazzo and Ronnett, 2004)
Heterozygous	MeCP2 +/- female mice; showed that MeCP2 mutant neurons affect the development of nearby neurons and environment affects the level of MeCP2 expression in wild type cells.	(Braunschweig et al., 2004)
Transgenic	Mouse model that transgenically expressed MeCP2, under control of an endogenous human promoter, by using a large insert of genomic clone from PAC, which contained a MeCP2 locus. Even mild overexpression of protein can lead to symptoms like Rett syndrome. Thus the authors could show that MeCP2 levels are tightly regulated.	(Collins et al., 2004)
Truncated	MeCP2 308/Y; studied social behavior in mice and found that MeCP2 might regulate expression/ function of genes involved in social behavior.	(Moretti et al., 2005)

Truncated	Male mouse with truncated MeCP2; displayed increased anxiety-like behavior and an abnormal stress response, similar to patients with RTT. The changes were associated with increased serum corticosterone levels. The results show that MeCP2 regulates Crh expression.	(McGill et al., 2006)
Conditional tissue specific rescue	MeCP2 gene is silenced by insertion of a <i>lox-stop</i> cassette in intron 2, which could be conditionally activated by Tamoxifen; mouse showed restoration of neuronal function by late expression of MeCP2 suggesting that Rett syndrome symptoms can be reversed.	(Guy et al., 2007)
Transgenic	Mouse model that transgenically expressed MeCP2, HA-MeCP2 transgene is downstream of an inducible promoter in the transgenic mice. The transgenic mice were further crossed with <i>Mecp2^{-/+}</i> females. Authors show that Rett-like behavior could be improved in <i>Mecp2^{-/+}</i> females by targeted gene re-introduction.	(Jugloff et al., 2008)

2. AIMS OF THE WORK

Recently, our group and others have shown that large-scale heterochromatin organization takes place during terminal differentiation. In this work, I focused on two major non-histone markers of heterochromatin, MeCP2 and HP1 and their role during this process.

Using an *in vitro* myogenic differentiation system, as the model system for the study, I investigated their expression levels, their interaction and their localization during differentiation. Furthermore, I tested whether HP1 plays a role in chromatin organization during cellular differentiation. Based on the outcome that MBD family members and not HP1 family members are involved in large-scale chromatin organization, I tested whether these pathways are redundant or synergistic.

Furthermore, I have investigated the relevance of MeCP2 *in vivo* by testing the affect of a large series of MeCP2 mutations found in Rett syndrome. I have analyzed whether or not these MeCP2 mutations affect its capacity to bind to chromatin, the dynamics of its binding and its ability to cluster chromatin *in vivo*.

3. RESULTS

3.1. MeCP2 interacts with HP1 and modulates its heterochromatin association during myogenic differentiation

MeCP2 interacts with HP1 and modulates its heterochromatin association during myogenic differentiation

Noopur Agarwal¹, Tanja Hardt¹, Alessandro Brero¹, Danny Nowak¹,
Ulrich Rothbauer², Annette Becker¹, Heinrich Leonhardt² and M. Cristina Cardoso^{1,*}

¹Max Delbrück Center for Molecular Medicine, 13125 Berlin and ²Ludwig Maximilians University Munich, Biocenter, Department of Biology, 82152 Planegg-Martinsried, Germany

Received March 7, 2007; Revised and Accepted July 20, 2007

ABSTRACT

There is increasing evidence of crosstalk between epigenetic modifications such as histone and DNA methylation, recognized by HP1 and methyl CpG-binding proteins, respectively. We have previously shown that the level of methyl CpG-binding proteins increased dramatically during myogenesis leading to large-scale heterochromatin reorganization. In this work, we show that the level of HP1 isoforms did not change significantly throughout myogenic differentiation but their localization did. In particular, HP1 γ relocalization to heterochromatin correlated with MeCP2 presence. Using co-immunoprecipitation assays, we found that these heterochromatic factors interact *in vivo* via the chromo shadow domain of HP1 and the first 55 amino acids of MeCP2. We propose that this dynamic interaction of HP1 and MeCP2 increases their concentration at heterochromatin linking two major gene silencing pathways to stabilize transcriptional repression during differentiation.

INTRODUCTION

Post-translational modifications of chromatin such as histone and DNA methylation are recognized by epigenetic regulators HP1 (heterochromatin protein 1) and MeCP2 (methyl CpG-binding protein 2) respectively and play an important role in transcriptional regulation. These non-histone chromatin factors read the epigenetic marks and translate them into inactive chromatin states.

MeCP2 is a member of a family of proteins, which share a conserved methyl cytosine-binding domain (MBD) that recognizes methylated CpG dinucleotides (1).

Moreover, MeCP2 contains a nuclear localization signal [NLS; (2)] and a transcriptional repression domain (TRD), which binds a corepressor complex containing mSin3a and histone deacetylases [HDACs; (3)].

HP1 proteins are conserved from yeast to humans (4) and recognize histone H3 trimethylated at the lysine 9 position [H3K9Me3; (5,6)]. In mammals, three isoforms viz α , β , γ have been identified (7,8). Functionally, three domains have been defined in HP1(s). The chromodomain [CD; (9)] and the chromo shadow domain [CSD; (10)] are highly conserved and are linked by the poorly conserved hinge domain. The CD has been shown to be important for binding methylated histones, while the CSD is known to interact with several proteins (11) as well as mediate homo (12) and heterodimerization of HP1 isoforms (13). The hinge domain interacts with DNA (14) and RNA (15).

In mouse cells, both HP1 and MeCP2 accumulate at pericentric regions of chromosomes organized into chromocenters, which play an important role in epigenetic gene regulation possibly by creating silencing compartments within the nucleus. Recently, we have shown that the level of MeCP2 as well as of MBD proteins starkly increased during myogenic differentiation concomitant with large-scale chromatin reorganization (16). To investigate a potential crosstalk between both epigenetic regulators, we analyzed the amount and localization of HP1 with respect to MBD proteins during cellular differentiation. We found that although the level of HP1 proteins does not change dramatically, there is spatial relocalization of HP1 (especially HP1 γ) during myogenesis from a more diffused distribution to a focal enrichment at pericentric heterochromatin. Furthermore, this redistribution to heterochromatin correlates with MeCP2 and MBD1 protein presence. We also demonstrate that HP1 and MeCP2 interact physically with each other,

*To whom Correspondence should be addressed: Tel: +49 30 94062109; Fax: +49 30 94063343; Email: cardoso@mdc-berlin.de
Present address:

Tanja Hardt, Medical Proteomics Center, Ruhr University, 44801, Germany
Alessandro Brero, Ludwig Maximilians University, Gene Center, 81377 Munich, Germany

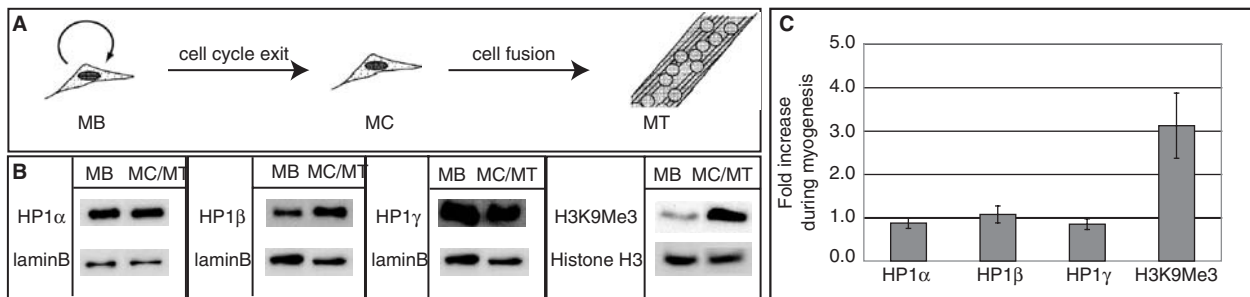


Figure 1. Level of HP1 proteins during differentiation. (A) Schematic representation of myogenesis. (B) Western blot analysis of the level of HP1 isoforms and of HP1-binding site on chromatin (H3K9Me3) in MB versus MC/MT. Lamin B and histone H3 are taken as controls for equal nuclear protein amounts and for total histone H3, respectively. (C) Quantitative analysis of western blots. Error bars indicate SDs.

strengthening the argument that they cooperate in the formation of repressive subnuclear compartments involved in epigenetic gene silencing.

MATERIALS AND METHODS

Expression plasmids

The following HP1 plasmids were used: GFP-tagged full-length human HP1 α /HP1 β /HP1 γ (17); YFP-tagged deletion mutants of human HP1 α /HP1 β /HP1 γ and full-length human HP1 α /HP1 β tagged with DsRed2 (18). To construct a DsRed2 fusion of HP1 γ , the BamHI–HindIII fragment of GFP-HP1 γ containing HP1 γ was subcloned into BglII–HindIII site of pDsRed2-C1 (Clontech). MeCP2 constructs used were GFP/YFP/mRFP1-tagged full-length and deletion mutants of rat MeCP2 (16). MeCP2Y.6 and MeCP2G.7 were constructed by subcloning XhoI–HindIII and XhoI–PstI fragments of MeCP2 from MeCP2Y into pEYFP-N1 and pEGFP-N1 (Clontech) cut with the same restriction enzymes, respectively. pEGFP-N1 (Clontech) was used as a control.

Cell culture and transfection

Pmi28 mouse myoblast cells (MB) were cultured as described in (19), transfected using Transfectin (Biorad) and differentiated as described before (16). Differentiated cultures include syncytial myotubes (MT) and unfused myocytes (MC).

HEK293-EBNA human cells (Invitrogen) were maintained in Dulbecco's modified Eagle's medium (DMEM) supplemented with 10% fetal bovine serum at 37°C with 5% CO₂. 4×10^5 HEK293-EBNA cells plated onto 100 mm diameter culture dishes were transfected using PEI (poly-ethyleneimine 25 kDa from Polysciences 1 mg/ml in ddH₂O, neutralized with HCl). For transfection 500 μ l of DMEM without serum, 12 μ g of DNA and 50 μ l of PEI were mixed well, incubated for 10 min at room temperature, vortexed and added to the cells dropwise. The culture was incubated at 37°C overnight, next day cells were washed in PBS, pelleted and used for co-immunoprecipitation assays.

Immunofluorescence analysis and microscopy

Proliferating and differentiated Pmi28 cultures were fixed in 3.7% formaldehyde/PBS and permeabilized with 0.5% TritonX-100/1XPBS and immunostained as described in (20). Primary antibodies used were: mouse monoclonal anti-HP1 isoform-specific antibodies (Chemicon), rabbit polyclonal anti-MeCP2 (Upstate) and anti-MBD1 (Santa Cruz) antibodies. Secondary antibodies used were: anti-mouse IgG-Cy5, anti-rabbit IgG-FITC (Jackson Immuno Research). Samples were counterstained with DAPI and examined on a Zeiss Axiovert 200 using 40 \times and 63 \times objectives. Images were acquired with a PCO Sensicam QE cooled CCD camera using Zeiss Axiovision V.3 software and processed with Adobe Photoshop. To quantify the correlation between HP1 γ localization at chromocenters and presence of MeCP2 or MBD1, we analyzed 375 MB cells; 71 cells with positive staining for MeCP2; 99 cells with positive staining for MBD1; 125 cells transfected with MeCP2-GFP and 345 MT nuclei from two independent experiments done in triplicate. The mean and SDs were plotted using Microsoft Excel software (Figure 2).

Immunoprecipitation and western blot analysis

Differentiated and non-differentiated Pmi28 cells were grown on p100 culture dishes, boiled in Laemmli sample buffer and analyzed on western blots (Figure 1). Immunoprecipitations (Figures 3 and 4) were done as described before (21). The following primary antibodies were used: rabbit polyclonal anti-lamin B [kind gift of R.Bastos; (22)], rabbit polyclonal anti-H3K9Me3 (Upstate), rabbit polyclonal anti-MeCP2 (Upstate), chromatographically purified rabbit IgG (Organon Teknika), mouse monoclonal anti-HP1 α /HP1 β /HP1 γ (Chemicon), rabbit polyclonal anti-histone H3 (Upstate), mouse monoclonal anti-GFP (Roche), GFP binder (23), anti-mRFP1 rabbit polyclonal antiserum. Secondary antibodies used were: anti-mouse IgG HRP (Amersham) and anti-rabbit IgG HRP (Sigma). Immunoreactive signals were visualized using an ECL plus Detection kit (Amersham) and recorded using a luminescence imager (Luminescent Image Analyzer LAS-1000, Fuji). To compare the amounts of the different proteins in proliferating and differentiated myogenic cultures,

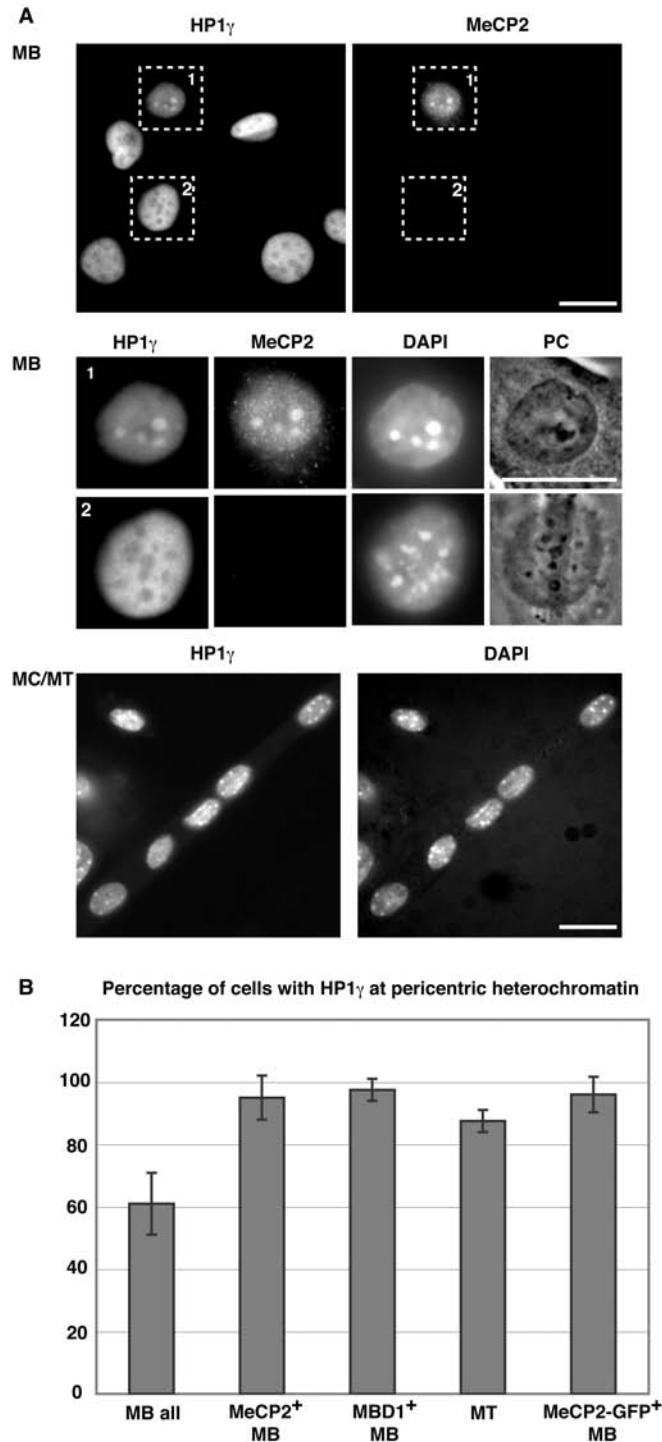


Figure 2. Pericentric heterochromatin association of HP1 γ increases during differentiation and correlates with the presence of MeCP2 and MBD1 proteins. (A) Cells were stained with HP1 γ and MeCP2-specific antibodies and DNA counterstained with DAPI, highlighting the chromocenters. In the upper panels, overview images and below them representative magnified MB cells are shown, of which only the MeCP2 positive cell has HP1 γ accumulated at chromocenters. The lower panels show an overview of a differentiated culture, with most nuclei having HP1 γ at chromocenters. Scale bar: 20 μ m. (B) Percentage of cells with HP1 γ at pericentric heterochromatin and correlation with MeCP2 and MBD1 proteins. Error bars indicate SD.

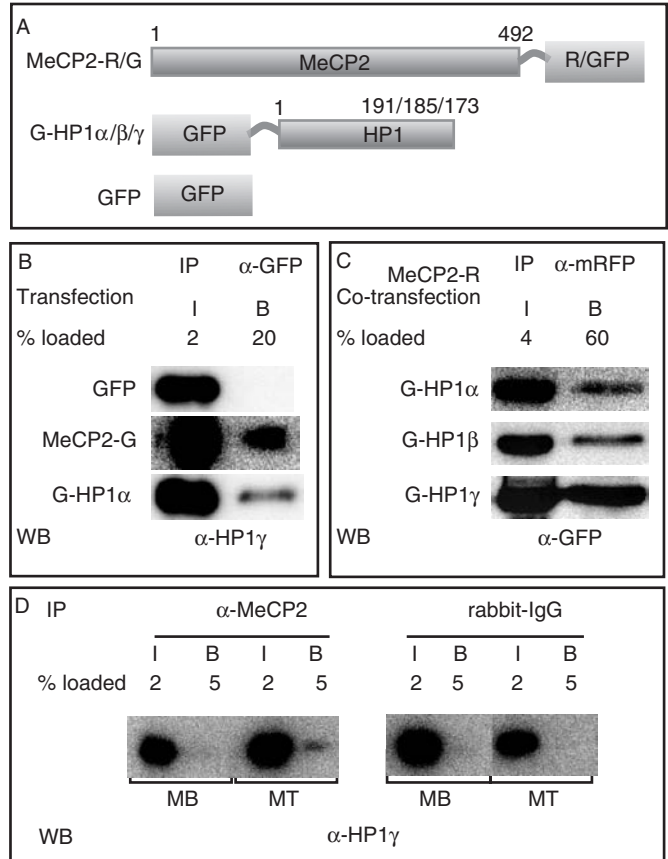


Figure 3. MeCP2 interacts with HP1 *in vivo*. (A) Schematic representation of the fusion proteins. Numbers represent amino acid coordinates. (B and C) HEK293-EBNA cells were transfected with the plasmids indicated and extracts prepared the next day. Immunoprecipitations were done using either anti-GFP (B) or anti-mRFP (C) antibody. (D) Extracts from MB and MT were subjected to immunoprecipitation using the antibodies, as indicated. Input (I) and bound (B) fractions were loaded in the percentages mentioned and analyzed by western blotting using anti-HP1 γ (B, D) or anti-GFP (C).

quantification of the recorded signals was done with the Image Gauge Ver.3.0 software (Fuji). Equal sized boxes were made around the recorded signals and for calculating the background. Integrated pixel intensity was measured for each band and the respective background signal was subtracted. Signals were normalized to the loading control (lamin B or histone H3) and the fold difference between the normalized signals in differentiated versus proliferating cultures was calculated. The mean and SDs were calculated from three independent experiments and plotted using Microsoft Excel software (Figure 1).

RESULTS AND DISCUSSION

Level of HP1 isoforms remains mostly constant during myogenesis

During cellular differentiation progressive inactivation of the genome occurs in parallel with the activation of tissue-specific gene expression patterns (24). We have shown that the level of methyl CpG-binding protein

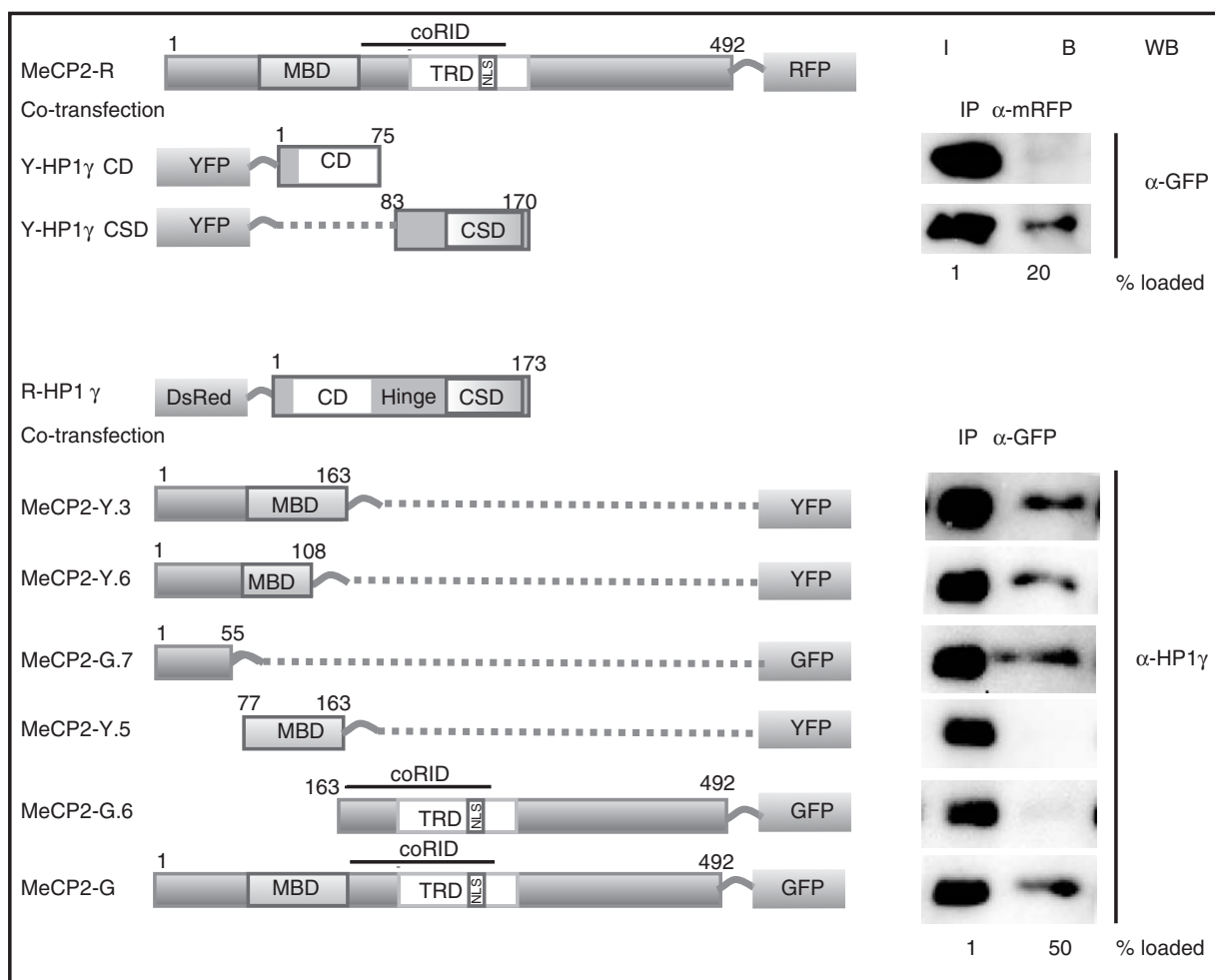


Figure 4. MeCP2 interacts via its N-terminal domain with the CSD domain of HP1. Schematic representation of the fusion proteins. Numbers represent amino acid coordinates. HEK293-EBNA cells were transfected with the plasmids indicated. Immunoprecipitations were done using either anti-mRFP or anti-GFP antibody. Input (I) and bound (B) fractions were loaded in the percentages mentioned and analyzed by western blotting using anti-GFP or anti-HP1 γ (shown here is the endogenous HP1 γ).

dramatically increased during muscle differentiation and induced large-scale aggregation of pericentric heterochromatin (16). A second major pathway associated with transcriptional silencing is mediated by HP1 binding of histone H3K9Me3. We therefore investigated whether the level of the different HP1 isoforms varied during cellular differentiation using a well-established *in vitro* culture system for myogenesis (Figure 1A). Pmi28 mouse myoblasts (MB) were induced to differentiate by incubation in horse-serum-containing medium. After three to four days, cells fused to form post-mitotic multinucleated myotubes (MT). These cultures still contained mononucleated not fully differentiated cells termed myocytes (MC). We quantified the level of HP1 in proliferating versus differentiated cell extracts by western blot analysis and normalized it to lamin B level as a loading control for nuclear proteins. The level of HP1 α , β , γ remained almost constant during differentiation (Figure 1B and C). However, the fraction of histone H3 that was trimethylated at lysine 9 position (H3K9Me3) increased about 3-fold in differentiated cells.

Association of HP1 γ with heterochromatin increases during differentiation and correlates with methyl CpG-binding protein presence

Previous studies have reported a cell cycle stage and isoform-specific localization of HP1 (18). To address this possibility, we examined the *in situ* localization of the HP1 isoforms as well as H3K9Me3 by immunofluorescence staining during myogenic differentiation. Pericentric heterochromatin organized in chromocenters was highlighted by counterstaining with the DNA dye 4',6-diamidino-2-phenylindole (DAPI). We found that the level of association of HP1 with pericentric heterochromatin differed between isoforms and changed during differentiation. While HP1 α protein could be found accumulated at pericentric heterochromatin in most of the MBs (89%; Supplementary Figure 1), HP1 β did not show such an accumulation (data not shown) and HP1 γ showed only a weak heterochromatin accumulation in about half of the MBs (61%; Figure 2). This weak accumulation was not due to the absence of H3K9Me3, since chromocenters of all MBs stained clearly positive for

this histone modification (Supplementary Figure 2) and is consistent with earlier reports showing HP1 γ mostly excluded from constitutive heterochromatin (25). We can also rule out epitope masking (26), as in the same population of MBs, there were cells where HP1 γ staining was detected at chromocenters (Figure 2A magnified nucleus). The fraction of MT nuclei with HP1 α and γ accumulated at heterochromatin increased to 100 and 90%, respectively (Supplementary Figure 1 and Figure 2). In contrast, upon differentiation there was no major change in the distribution of HP1 β (data not shown) even though there was an increase in the level of its binding site H3K9Me3 (Figure 1). We reasoned therefore, that this increase in heterochromatin association could depend on differentiation-specific factors other than the histone methylation mark *per se*. Since MeCP2 and other MBDs are present in a few MB only but increase during differentiation and label almost all chromocenters in MT (16), we tested whether the change in heterochromatin association of HP1 γ was correlated to MBD protein. Indeed we found a clear correlation of HP1 heterochromatin association in MB and the presence of either MeCP2 or MBD1. Almost all MeCP2 or MBD1 positive MB contained HP1 α (100%) and HP1 γ (95%) at chromocenters (Figure 2 and Supplementary Figure 1). Furthermore, 96 and 94% of MB cells ectopically expressing MeCP2-GFP fusion had HP1 γ and HP1 α accumulation at pericentric heterochromatin (Figure 2B and Supplementary Figure 1B). Altogether, these data showed that the chromocenter association of HP1 with particular emphasis for HP1 γ clearly increased upon myogenic differentiation and was positively correlated with the presence of MeCP2 and MBD1.

MeCP2 interacts via its N-terminal domain with the chromo shadow domain of HP1

Since the accumulation of HP1 at chromocenters correlated with the presence of MBD proteins at these sites, we tested whether they could physically interact. HEK293-EBNA cells, which express HP1 proteins, were transfected with plasmids coding for GFP, GFP-tagged MeCP2 or GFP-tagged HP1 (Figure 3A). Twelve hours later, cells were lysed and immunoprecipitations performed with an anti-GFP-specific antibody fragment [GFP binder; (23)]. Input and bound fractions were analyzed on western blots for precipitated GFP-tagged protein (data not shown) and for co-precipitated endogenous HP1 γ protein. HP1 γ did not bind to GFP alone but was co-precipitated with MeCP2-GFP (Figure 3B) and the same was true for HP1 α and β (data not shown). Since HP1 α , β and γ have been shown to form homodimers (12,13) as well as heterodimers [HP1 α - γ ; (12)], [HP1 α - β ; (27)], we reproduced this data as a positive control for our co-immunoprecipitation conditions. Moreover, the fraction of HP1 γ bound to HP1 α was comparable with the amount bound to MeCP2 (Figure 3B). Using a mRFP-tagged MeCP2, we co-immunoprecipitated GFP-tagged HP1 α , β and γ (Figure 3C). MeCP2-GFP proteins could likewise immunoprecipitate DsRed2-tagged HP1s (Figure 4 and data not shown) showing that the interaction of HP1 with MeCP2

was independent of the tags. Further, we tested whether endogenous HP1 and MeCP2 could interact. We performed immunoprecipitations using anti-MeCP2 antibody on Pmi28 MBs (expressing low level of MeCP2) and MTs (expressing higher level of MeCP2) (16). Indeed, the rabbit anti-MeCP2 antibody but not the control rabbit IgG could co-precipitate HP1 γ from MT extracts. Finally, to test whether MeCP2 could directly interact with HP1, we used GST pull down assays. Recombinant MeCP2 purified from bacteria was incubated with glutathione agarose coupled GST or GST-HP1 γ (Supplementary Figure 3). While no MeCP2 protein was detected in the GST-bound fraction, GST-HP1 γ was able to specifically pull down MeCP2. In summary, these results showed that MeCP2 and HP1 interact *in vivo* and at a level comparable to the dimerization of HP1 proteins.

The N terminus of HP1 contains the H3K9Me3-binding site (5) while the C terminus mediates dimerization of HP1 as well as interaction with other proteins (11,28). To test which domain would be involved in the interaction with MeCP2, we co-transfected HEK293-EBNA cells with plasmids coding for MeCP2-mRFP and with different YFP-tagged deletion constructs of HP1 isoforms coding either for the CD or the CSD. Co-immunoprecipitation assays demonstrated that the CSD of HP1s was necessary and sufficient for binding to MeCP2 *in vivo* (Figure 4 and data not shown). The CSD of HP1 has previously been shown to be important for the interaction of HP1 with other nuclear proteins (11). We then investigated which domain of MeCP2 binds to HP1 by using a series of fluorescently tagged deletion constructs of MeCP2. The results indicate that amino acids 1–55 of MeCP2 are primarily involved in binding HP1 (Figure 4), though weaker binding could be detected with other regions of MeCP2 as well (Supplementary Figure 4). We conclude that MeCP2 and HP1 interact via the CSD of HP1 and the N-terminal domain of MeCP2.

The domains of MeCP2 that have been better functionally characterized are the MBD, the transcriptional repressor domain (TRD) and the overlapping Sin3a co-repressor domain (coRID), all of which are in the central part of MeCP2 (29). Our data now implicate the N-terminal region before the MBD in binding to HP1, suggesting a direct physical link between the factors translating DNA and histone methylation. On the one hand, MeCP2 recognizes methyl CpGs and interacts with DNA methyltransferase 1 (30). On the other hand, HP1 binds to H3K9Me3 and associates with the histone H3K9 methyltransferase [Suv39h1; (31)]. Our data showing that HP1 and MeCP2 interact with each other interconnects these two major epigenetic pathways. Most recently, HP1 was also reported to interact with Dnmt1 (32). It is noteworthy that another MBD protein, MBD1 has been reported to interact with HP1 α via the MBD (33). Since other MBDs (Figure 2 and Supplementary Figure 1) were also able to enhance the accumulation of HP1 at heterochromatin, any single MBD knockout would not be expected to disrupt it. In line with this, we have previously shown that other MBDs have overlapping functions and knockout of MeCP2 alone did not affect heterochromatin reorganization during myogenic differentiation (16).

Significantly, we found that the heterochromatin association of HP1 γ increased during differentiation and that this was correlated with either MeCP2 or MBD1 presence. The differentiation-specific increase of the MBD proteins could enhance HP1 γ binding to constitutive heterochromatin, which would then recruit histone H3K9 methyltransferases leading to higher levels of H3K9 methylation. In Suv39h1/2 double knockout cells where H3K9 methylation at chromocenters is abrogated, MeCP2 still induced clustering (16), indicating that its interaction with HP1 is not required for its function in large-scale chromatin organization. We further propose that the multiple interactions of these factors with chromatin and with each other generate subnuclear silencing compartments, which stabilize the differentiated phenotype by reducing transcriptional noise. Individually these interactions are transient but their cumulative effect at heterochromatin increases the local concentration of repressing factors and thereby the efficiency of gene silencing.

SUPPLEMENTARY DATA

Supplementary Data are available at NAR Online.

ACKNOWLEDGEMENTS

We are indebted to R. Bastos, T. Misteli, Y. Hiraoka, P. Chambon and C.L. Woodcock for providing antibodies and plasmids. We thank Ingrid Grunewald for technical support and Jeffrey H. Stear for comments on the manuscript. T.H. was supported by the European Union (ESF Program). This work was funded by grants of the Deutsche Forschungsgemeinschaft to M.C.C. Funding to pay the Open Access publication charges for this article was provided by Deutsche Forschungsgemeinschaft (DFG).

Conflict of interest statement. None declared.

REFERENCES

- Nan, X., Meehan, R.R. and Bird, A. (1993) Dissection of the methyl-CpG binding domain from the chromosomal protein MeCP2. *Nucleic Acids Res.*, **21**, 4886–4892.
- Nan, X., Tate, P., Li, E. and Bird, A. (1996) DNA methylation specifies chromosomal localization of MeCP2. *Mol. Cell Biol.*, **16**, 414–421.
- Nan, X., Ng, H.H., Johnson, C.A., Laherty, C.D., Turner, B.M., Eisenman, R.N. and Bird, A. (1998) Transcriptional repression by the methyl-CpG-binding protein MeCP2 involves a histone deacetylase complex. *Nature*, **393**, 386–389.
- Eissenberg, J.C. and Elgin, S.C. (2000) The HP1 protein family: getting a grip on chromatin. *Curr. Opin. Genet. Dev.*, **10**, 204–210.
- Bannister, A.J., Zegerman, P., Partridge, J.F., Miska, E.A., Thomas, J.O., Allshire, R.C. and Kouzarides, T. (2001) Selective recognition of methylated lysine 9 on histone H3 by the HP1 chromo domain. *Nature*, **410**, 120–124.
- Lachner, M., O'Carroll, D., Rea, S., Mechtler, K. and Jenuwein, T. (2001) Methylation of histone H3 lysine 9 creates a binding site for HP1 proteins. *Nature*, **410**, 116–120.
- Saunders, W.S., Chue, C., Goebel, M., Craig, C., Clark, R.F., Powers, J.A., Eissenberg, J.C., Elgin, S.C., Rothfield, N.F. et al. (1993) Molecular cloning of a human homologue of Drosophila heterochromatin protein HP1 using anti-centromere autoantibodies with anti-chromo specificity. *J. Cell Sci.*, **104**, 573–582.
- Singh, P.B., Miller, J.R., Pearce, J., Kothary, R., Burton, R.D., Paro, R., James, T.C. and Gaunt, S.J. (1991) A sequence motif found in a Drosophila heterochromatin protein is conserved in animals and plants. *Nucleic Acids Res.*, **19**, 789–794.
- Paro, R. and Hogness, D.S. (1991) The Polycomb protein shares a homologous domain with a heterochromatin-associated protein of Drosophila. *Proc. Natl Acad. Sci. USA*, **88**, 263–267.
- Aasland, R. and Stewart, A.F. (1995) The chromo shadow domain, a second chromo domain in heterochromatin-binding protein 1, HP1. *Nucleic Acids Res.*, **23**, 3168–3173.
- Lechner, M.S., Schultz, D.C., Negorev, D., Maul, G.G. and Rauscher, F.J. III (2005) The mammalian heterochromatin protein 1 binds diverse nuclear proteins through a common motif that targets the chromo shadow domain. *Biochem. Biophys. Res. Commun.*, **331**, 929–937.
- Ye, Q., Callebaut, I., Pezhman, A., Courvalin, J.C. and Worman, H.J. (1997) Domain-specific interactions of human HP1-type chromodomain proteins and inner nuclear membrane protein LBR. *J. Biol. Chem.*, **272**, 14983–14989.
- Brasher, S.V., Smith, B.O., Fogh, R.H., Nietlispach, D., Thiru, A., Nielsen, P.R., Broadhurst, R.W., Ball, L.J., Murzina, N.V. et al. (2000) The structure of mouse HP1 suggests a unique mode of single peptide recognition by the shadow chromo domain dimer. *EMBO J.*, **19**, 1587–1597.
- Sugimoto, K., Yamada, T., Muro, Y. and Himeno, M. (1996) Human homolog of Drosophila heterochromatin-associated protein 1 (HP1) is a DNA-binding protein which possesses a DNA-binding motif with weak similarity to that of human centromere protein C (CENP-C). *J. Biochem.*, **120**, 153–159.
- Muchardt, C., Guilleme, M., Seeler, J.S., Trouche, D., Dejean, A. and Yaniv, M. (2002) Coordinated methyl and RNA binding is required for heterochromatin localization of mammalian HP1alpha. *EMBO Rep.*, **3**, 975–981.
- Brero, A., Easwaran, H.P., Nowak, D., Grunewald, I., Cremer, T., Leonhardt, H. and Cardoso, M.C. (2005) Methyl CpG-binding proteins induce large-scale chromatin reorganization during terminal differentiation. *J. Cell Biol.*, **169**, 733–743.
- Cheutin, T., McNairn, A.J., Jenuwein, T., Gilbert, D.M., Singh, P.B. and Misteli, T. (2003) Maintenance of stable heterochromatin domains by dynamic HP1 binding. *Science*, **299**, 721–725.
- Hayakawa, T., Haraguchi, T., Masumoto, H. and Hiraoka, Y. (2003) Cell cycle behavior of human HP1 subtypes: distinct molecular domains of HP1 are required for their centromeric localization during interphase and metaphase. *J. Cell Sci.*, **116**, 3327–3338.
- Kaufmann, U., Kirsch, J., Irintchev, A., Wernig, A. and Starzinski-Powitz, A. (1999) The M-cadherin catenin complex interacts with microtubules in skeletal muscle cells: implications for the fusion of myoblasts. *J. Cell Sci.*, **112**, 55–68.
- Sporbert, A., Gahl, A., Ankerhold, R., Leonhardt, H. and Cardoso, M.C. (2002) DNA polymerase clamp shows little turnover at established replication sites but sequential de novo assembly at adjacent origin clusters. *Mol. Cell*, **10**, 1355–1365.
- Mortusewicz, O., Rothbauer, U., Cardoso, M.C. and Leonhardt, H. (2006) Differential recruitment of DNA Ligase I and III to DNA repair sites. *Nucleic Acids Res.*, **34**, 3523–3532.
- Chaudhary, N. and Courvalin, J.C. (1993) Stepwise reassembly of the nuclear envelope at the end of mitosis. *J. Cell Biol.*, **122**, 295–306.
- Rothbauer, U., Zolghadr, K., Tillib, S., Nowak, D., Schermelleh, L., Gahl, A., Backmann, N., Conrath, K., Myuldermans, S. et al. (2006) Targeting and tracing antigens in live cells with fluorescent nanobodies. *Nat. Methods*, **3**, 887–889.
- Fisher, A.G. and Merkenschlager, M. (2002) Gene silencing, cell fate and nuclear organisation. *Curr. Opin. Genet. Dev.*, **12**, 193–197.
- Horsley, D., Hutchings, A., Butcher, G.W. and Singh, P.B. (1996) M32, a murine homologue of Drosophila heterochromatin protein 1 (HP1), localises to euchromatin within interphase nuclei and is largely excluded from constitutive heterochromatin. *Cytogenet. Cell Genet.*, **73**, 308–311.
- Minc, E., Courvalin, J.C. and Buendia, B. (2000) HP1gamma associates with euchromatin and heterochromatin in mammalian nuclei and chromosomes. *Cytogenet. Cell Genet.*, **90**, 279–284.
- Nielsen, A.L., Oulad-Abdelghani, M., Ortiz, J.A., Remboutsika, E., Chambon, P. and Losson, R. (2001) Heterochromatin formation in

- mammalian cells: interaction between histones and HP1 proteins. *Mol. Cell*, **7**, 729–739.
28. Cowieson, N.P., Partridge, J.F., Allshire, R.C. and McLaughlin, P.J. (2000) Dimerisation of a chromo shadow domain and distinctions from the chromodomain as revealed by structural analysis. *Curr. Biol.*, **10**, 517–525.
 29. Brero, A., Leonhardt, H. and Cardoso, M.C. (2006) Replication and translation of epigenetic information. *Curr. Top. Microbiol. Immunol.*, **301**, 21–44.
 30. Kimura, H. and Shiota, K. (2003) Methyl-CpG-binding protein, MeCP2, is a target molecule for maintenance DNA methyltransferase, Dnmt1. *J. Biol. Chem.*, **278**, 4806–4812.
 31. Yamamoto, K. and Sonoda, M. (2003) Self-interaction of heterochromatin protein 1 is required for direct binding to histone methyltransferase, SUV39H1. *Biochem. Biophys. Res. Commun.*, **301**, 287–292.
 32. Smallwood, A., Esteve, P.O., Pradhan, S. and Carey, M. (2007) Functional cooperation between HP1 and DNMT1 mediates gene silencing. *Genes Dev.*, **21**, 1169–1178.
 33. Fujita, N., Watanabe, S., Ichimura, T., Tsuruzoe, S., Shinkai, Y., Tachibana, M., Chiba, T. and Nakao, M. (2003) Methyl-CpG binding domain 1 (MBD1) interacts with the Suv39h1-HP1 heterochromatic complex for DNA methylation-based transcriptional repression. *J. Biol. Chem.*, **278**, 24132–24138.

SUPPLEMENTARY INFORMATION

Figure S1

Pericentric heterochromatin association of HP1 α increases during differentiation and correlates with the presence of MBD proteins. (A) Cells were stained with HP1 α and MeCP2 specific antibodies and DNA counterstained with DAPI, highlighting the chromocenters. The upper panel shows representative MB cells and the lower panel an overview of a differentiated culture. Scale bar: 20 μ m. (B) Percentage of cells with HP1 α at pericentric heterochromatin and correlation with MBD protein presence.

HP1 α protein could be found accumulated in chromocenters of 89% of MB (N= 131 cells). In contrast, the fraction of MT nuclei with HP1 α accumulated at heterochromatin increased to 100% (N= 100 cells). Indeed we found a correlation of HP1 heterochromatin association in MB and the presence of either MeCP2 or MBD1 with all MeCP2 or MBD1 positive MB (N=42 and 28 cells, respectively) containing HP1 α (100%) at chromocenters. Furthermore, 94% of MB cells ectopically expressing MeCP2-GFP fusion (N= 35 cells) had HP1 α accumulation at pericentric heterochromatin. Altogether, these data showed that the chromocenter association of HP1 α clearly increased upon myogenic differentiation and was positively correlated with the presence of MeCP2 and MBD1.

Figure S2

H3K9Me3 is present at chromocenters in MB and shows slight increase during differentiation. Cells were stained with H3K9Me3 specific antibody and DNA counterstained with DAPI. Scale bar: 20 μ m.

Figure S3

MeCP2 physically interacts with HP1 γ . Schematic representation of the constructs used in the experiment. GST and GST-HP1 γ were immobilized and incubated with purified MeCP2 (see supplemental method). Input (1%) and bound (15%) MeCP2 is shown. Whereas GST alone did not pull down MeCP2, an equivalent amount of GST-HP1 γ was able to specifically pull down MeCP2.

Figure S4

MeCP2 interacts preferentially via its N-terminal domain with the CSD domain of HP1. Schematic representation of the fusion proteins. Numbers represent amino acid coordinates. HEK293-EBNA cells were transfected with the plasmids indicated. Immunoprecipitations were done using anti-GFP antibody. Input (I) and bound (B) fractions were loaded in the percentages mentioned and analyzed by western blotting using anti-HP1 γ antibody. The ectopically expressed R-HP1 gamma binds to low and high affinity sites creating a competitive situation that reveals the preferential binding of the endogenous HP1 gamma protein to the N-terminus of MeCP2.

Supplemental Method

GST pull down assay

BL21 competent cells were transformed with Glutathione S Transferase (GST) expressing plasmid pGex2T1 (Pharmacia) and pGST-HP1 γ (1). Single colonies from each were inoculated in 4ml of LB-Amp separately and incubated with overnight shaking at 37°C. 2ml of this culture was used to inoculate 200ml of LB-Amp media and further incubated till O.D₆₀₀ reached to 0.6. 200 μ l of 1M IPTG (1mM final concentration) was added to each flask. After 3 hours of incubation, the culture was pelleted at 4000 rpm for 30 min 4°C. All the further steps were done at 4°C unless otherwise stated. Cells were lysed using a high pressure homogenizer (EmulsiFlex-C5, Avestin) and extracts loaded on pre-equilibrated Glutathione Superflow Resin (Clontech) for 2 hours with shaking. Bound GST and GST-HP1 γ were checked on a gradient NuPAGE 4-12% Bis-Tris gel using MOPS SDS running buffer, and stained with Simply Blue Safe Stain (Invitrogen) along with purified MeCP2. MeCP2 (pTYB1) was produced and purified as described (2). Equal amounts of GST and GST-HP1 γ were then incubated with purified MeCP2 overnight. Bound and flow through fractions were boiled in Laemmli sample buffer and analyzed on a gradient gel.

1. Nielsen, A.L., Oulad-Abdelghani, M., Ortiz, J.A., Remboutsika, E., Chambon, P. and Losson, R. (2001) Heterochromatin formation in mammalian cells: interaction between histones and HP1 proteins. *Mol Cell*, **7**, 729-739.
2. Georgel, P.T., Horowitz-Scherer, R.A., Adkins, N., Woodcock, C.L., Wade, P.A. and Hansen, J.C. (2003) Chromatin compaction by human MeCP2. Assembly of

novel secondary chromatin structures in the absence of DNA methylation. *J Biol Chem*, **278**, 32181-32188.

Figure S1

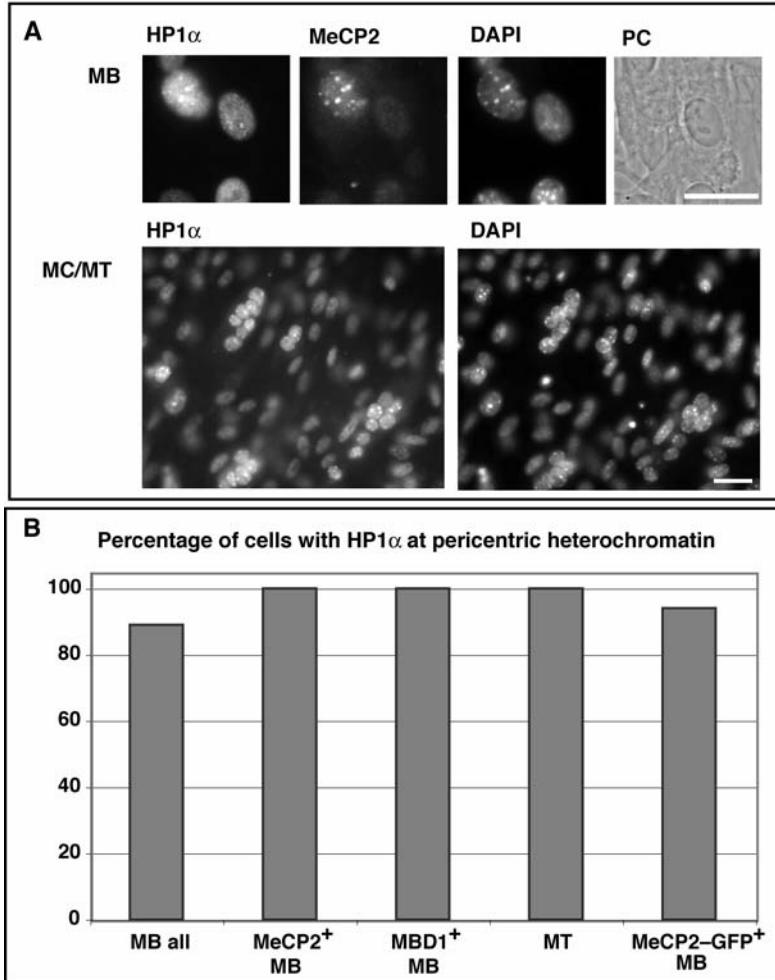


Figure S2

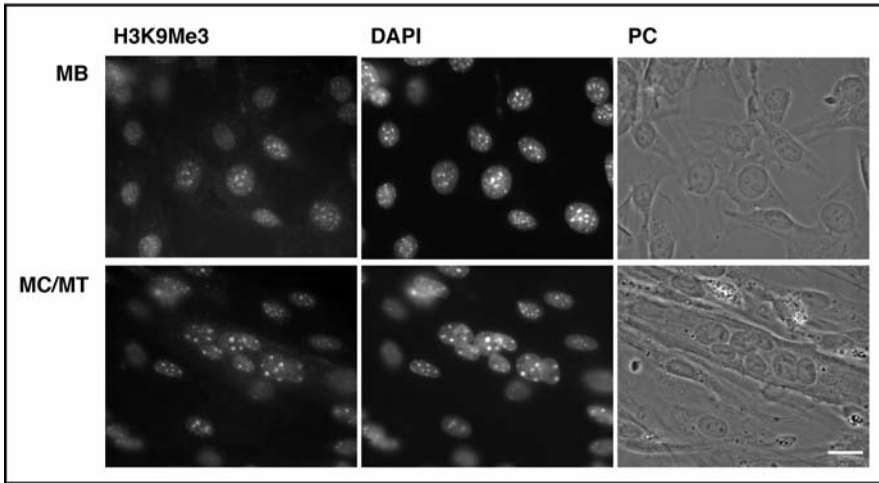


Figure S3

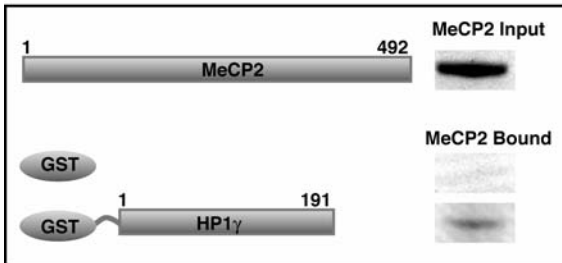
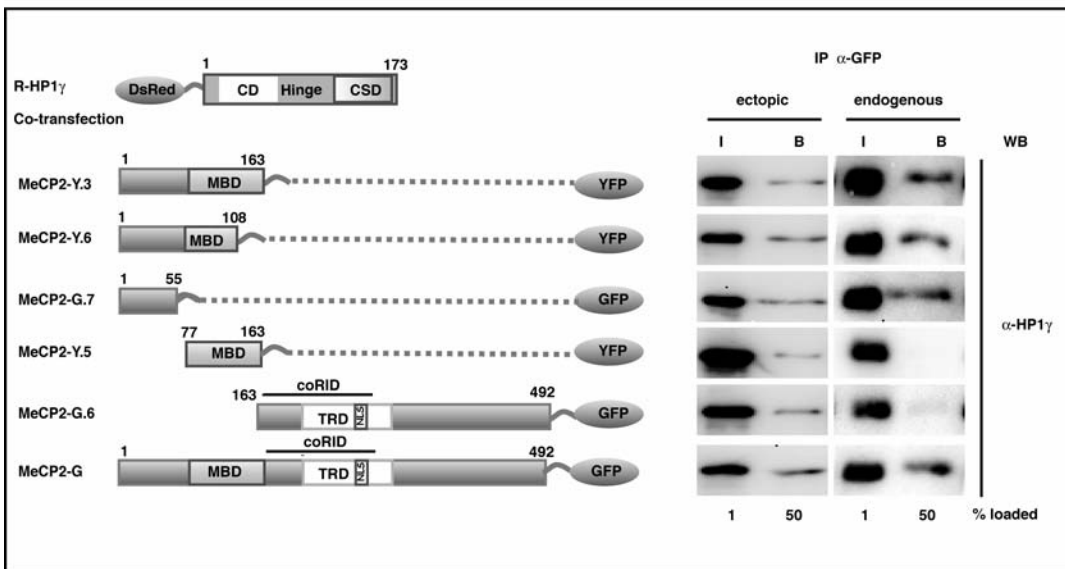


Figure S4



3.2. MeCP2 Rett mutations affect large scale chromatin organization

MeCP2 Rett mutations affect large scale chromatin organization

Noopur Agarwal¹, K. Laurence Jost^{1*}, Alessandro Brero^{1*}, Tanja Hardt^{1*}, Shinichi Kudo², Heinrich Leonhardt³, M. Cristina Cardoso^{1,4,#}

¹Max Delbrück Center for Molecular Medicine, 13125 Berlin, Germany

²Ludwig Maximilians University Munich, Department of Biology, 82152 Planegg-Martinsried, Germany

³Hokkaido Institute of Public Health, Sapporo, 060-0819, Japan

⁴Darmstadt University of Technology, Department of Biology, 64287 Darmstadt, Germany

Present address:

Tanja Hardt: Medical Proteomics Center, Ruhr University, 44801 Bochum, Germany

Alessandro Brero: Ludwig Maximilians University, Gene Center, 81377 Munich, Germany

* these authors contributed equally to this work

Key words: chromocenters, DNA methylation, MeCP2, methyl CpG binding domain, missense mutation, nuclear organization, pericentric heterochromatin, Rett syndrome

Abbreviations:

5mC → 5-methyl cytosine

MeCP2 → methyl CpG binding protein 2

MBD → methyl CpG binding domain

Running Title:

Rett mutations affect heterochromatin

#Correspondence to: M. Cristina Cardoso, Max Delbrück Center for Molecular

Medicine, Robert-Roessle-Str. 10, 13125 Berlin, Tel. +49-30-94062109, Fax +49-30-

94063343, E-mail: cardoso@mdc-berlin.de

All authors know and concur with the submission of this manuscript.

Rett syndrome is a neurological, X chromosomal-linked disorder associated with mutations in the MECP2 gene. We have recently found that MeCP2 induces large-scale heterochromatin remodeling. Therefore, we tested whether MeCP2 Rett mutations were affected in their ability to bind and induce aggregation of heterochromatin. We found that all 21 MeCP2 mutants analyzed accumulated at heterochromatin with the exception of R111G and surprisingly only a third of them were significantly affected. Furthermore, one third of all mutants showed also a significantly decreased ability to cluster heterochromatin. Yet both MeCP2 binding to and clustering of chromatin were not directly correlated but these two properties further allowed the separation of the mutants into two groups. Importantly, the mutations belonging to each group (binding or clustering impaired) segregated into two distinct surfaces of the MBD of MeCP2, thus ascribing novel chromatin functions of the MeCP2 MBD affected in Rett syndrome.

Rett syndrome (RTT, MIM 312750) is a postnatal neurological disorder, with an incidence of ~ 1/10,000 female births. The females develop normally until 6-18 months of age, but after that, the growth is drastically slowed down, followed by the development of stereotypical hand movements, autistic behaviour, loss of speech and motoric skills, respiratory disorders, etc. Mutations in the chromosome Xq28 region corresponding to the MECP2 gene have been shown to be linked to the disease ¹. MeCP2 recognizes methylated cytosines via a highly conserved methyl cytosine-binding domain (MBD) and is concentrated in the densely methylated pericentric heterochromatin ². Its ability to recruit transcription repression complexes and histone deacetylases via a region overlapping with its transcriptional repression domain (TRD) has been proposed to link both mechanisms of gene regulation by

stabilizing the heterochromatin state³. The mechanism(s) by which mutant MeCP2 causes Rett syndrome is though thus far unknown.

Several types of MECP2 gene mutations including deletions and also duplications have been found in Rett patients^{4 5}. A summary of MECP2 mutations along with their frequency is shown in Figure 1A (<http://mecp2.chw.edu.au/cgi-bin/mecp2/search/printGraph.cgi#MS>). The most common are missense mutations (black lines in frequency plot), which cluster within the MBD. The structure^{6 7} and conservation of this domain (in yellow) are depicted in Figure 1B and C, where the regions highlighted in blue recognize the methyl cytosines (displayed in white) and the residues making direct contacts with the cytosines are boxed in blue (Figure 1C). We have recently shown that the MBD of MeCP2 has the ability to reorganize and cluster pericentric heterochromatin⁸. Given that most Rett missense mutations affect this domain, we set out to investigate whether they were impaired on binding to and/or cluster heterochromatin.

We selected Pmi28 mouse myoblasts as our cellular assay system. This cell line was used before to characterize the dose-dependent effect of wild type MeCP2 on the spatial organization of chromocenters and it expresses very low to undetectable level of endogenous wild type MeCP2⁸. Moreover, it showed a stable and nearly normal karyotype (39, X0) (data not shown), resulting in moderate number of chromocenters compared to polyploid cell lines. Also, the stability of the karyotype minimized irreproducible variations of chromocenter number caused by variable numerical chromosome aberrations.

We used mammalian expression constructs containing the mutant human MECP2e2 isoform cDNAs fused at the C-terminus of the enhanced GFP coding sequence⁹. All 21 missense mutations within the MBD are highlighted in pink in Figure 1C and the

mutated forms of the wild type residues indicated below the sequence alignment.

Intranuclear localization of the fusion proteins and the induction of chromocenter clustering in transfected cells were assessed by epifluorescence microscopy using the AT-selective DNA dyes Hoechst 33258, DAPI or TOPRO-3 to independently visualize pericentric heterochromatin.

We first tested these MeCP2 Rett mutants for their protein accumulation at the chromocenters by taking a ratio of average mean intensity of protein bound at chromocenters versus nucleoplasm. The results indicate that all the mutant proteins showed an enrichment at chromocenters (ratio was greater than 1), but to very different extents (Figure 2). R111G mutant protein accumulated to the lowest extent. This mutant has been shown before to exhibit complete loss of function of MeCP2, and no longer repress Sp1-mediated transcriptional activation of methylated and unmethylated promoters⁹. We found that it mislocalizes to the nucleoli instead of pericentric heterochromatin (Figure 2 and Figure S1). Except for P101H, R133H, E137G, A140V, all the other analyzed mutant proteins accumulated at chromocenters less than the wild type, with more than half significantly affected in their accumulation ability as compared to wild type (p value shown in the table, Figure 2).

Since several mutants associated less efficiently with heterochromatin, we then tested whether they would be impaired in their ability to cluster heterochromatin *in vivo*. To assess the degree of heterochromatin clustering in a quantitative manner, we scored the number of chromocenters in cells expressing the wild type and mutant proteins (Figure 3). A statistical analysis was performed utilizing a Kolmogoroff-Smirnoff test comparing cumulative frequencies of chromocenter numbers. The potential of the proteins to induce clustering is reflected by the slope of the

cumulative frequency curve, which represents the percentage of nuclei with a certain number of chromocenters or less. A steeper curve consequently means a higher percentage of nuclei with a lower number of chromocenters. The Kolmogoroff-Smirnoff test revealed a significantly larger amount of chromocenters in cells expressing P101H mutant protein compared to wild type MeCP2 expressing cells. This was also the case for the R111G mutant, which though did not at all accumulated at heterochromatin. The A140V mutant on the other extreme behaved similarly to wild type MeCP2. This mutation has not only been reported in association with very mild clinical symptoms¹⁰. Altogether, a third of the mutant proteins were significantly affected and showed an intermediate clustering potential as compared to wild type. We further tested this effect in human cells expressing wild type or mutant MeCP2 by immunostaining in combination with fluorescence in situ hybridization using three DNA probes simultaneously to detect the major pericentric heterochromatin regions present in chromosomes 1, 9 and 16, and obtained a similar outcome (Figure S3A and B).

Next we tested whether the clustering of chromocenters generally reflected the amount of protein that accumulated at these regions. Hence, we plotted the median of chromocenter number versus the average accumulation at chromocenters (Figure 4A). Mutants falling onto an arbitrary line connecting the negative GFP alone control and the positive wild type MeCP2 control show an inverse correlation between binding to chromocenters and corresponding numbers of chromocenters, i.e. binding less is accompanied by more clustering. Interestingly, in the majority of the mutants neither a direct nor an inverse correlation between both parameters was found. In fact, several mutants were deficient in heterochromatin binding but only mildly affected in clustering of chromocenters and grouped to the left of the line (Figure 4A,

green) whereas the majority of mutants were mildly to non-affected in heterochromatin binding but disproportionately affected in clustering of chromocenters and grouped to the right of the line (Figure 4A, red). Interestingly, when we applied the same color code to label the residues in the MBD structure, the two subclasses nicely segregated onto two different surfaces of this domain (Figure 4B). The latter indicated that, in addition to the residues known to make contact with the methylated cytosines indicated in blue (Figures 1C and 4), this domain could be further functionally subdivided into a surface affecting primordially heterochromatin association (in green) and a second surface involved in clustering chromatin (in red). Mutants in these different MBD subdomains could be predicted to have different binding kinetics *in vivo*. Hence, we performed *in situ* extraction as well as fluorescence photobleaching recovery experiments on selected mutants that were either not affected in binding and clustering of chromatin (A140V), or affected only in clustering (P101H) or in both functions (R133L). The R133L mutation resulted in higher extractability and a much faster FRAP recovery, probably reflecting disruption of binding to the methylated cytosines. A minimal level of 5mC seems to be required for efficient accumulation of MeCP2 at heterochromatin, as shown by the lack of chromocenter localization of a GFP-tagged MBD fusion in Dnmt1/3a/3b triple knock-out cells ¹². Our live-cell kinetic data indeed indicated that albeit the ability to accumulate at heterochromatin to a low extent, the R133L mutant MeCP2 interacted only very transiently and with low affinity. Very similar FRAP kinetics were recently reported for different mutation of this residue, R133C ¹³. Both substitutions had similar heterochromatin clustering potential (Figure 3) although the R133L had a somehow lower ability to accumulate at heterochromatin (Figure 2). The *in vivo* accumulation of this mutant at chromatin may be either due to its retaining low affinity

recognition of 5mC and/or binding to DNA or other heterochromatin-associated proteins. On the other extreme, the A140V mutant protein performed in both assays, *in situ* extraction and FRAP kinetics, as the wild type or even more stably bound to chromatin (Figure 5). Importantly, the P101H mutant, which accumulated as the wild type at heterochromatin was drastically impaired in clustering chromocenters, and had an intermediate FRAP kinetics and was also easier to extract from heterochromatin. The FRAP kinetics follow the same trend for the different mutants independently of whether the region photobleached included only chromocenters (Figure 5B; which measures mostly the contribution of heterochromatin-bound MeCP2) or half of the nucleus (Figure 5C; with a higher contribution of the nucleoplasmic MeCP2 fraction) or was measured in human cells (Figure S2C). Since the P101 is located far away from the 5mC interacting pocket, these data suggest that it is primordially involved in connecting chromatin fibers either through direct DNA interaction or, more likely, interactions with other chromatin proteins. All other substitutions of P101 to L, R, S and T affected heterochromatin clustering albeit to different extent. This residue is located in N-terminal part of the MBD and likely induces a sharp turn before the two opposing beta-sheets ($\beta 1$ and $\beta 2$, Figure 1). Interference with this rigid conformation may be more significant upon replacement with the not very flexible histidine and less with more malleable amino acids. In summary, our analysis of the *in vivo* chromocenter clustering ability of the different mutations clearly indicated that all mutants where this property was significantly disrupted (including P101H) mapped to this same surface of the MBD three-dimensional structure and, importantly, these mutants were not concomitantly affected in chromatin binding. Such mutants would be able to bind to DNA quite well, as reflected by the chromatin accumulation data, but would be affected in binding to

other proteins present at chromatin and, therefore, could not induce chromocenter clustering resulting in faster binding dynamics at chromatin. Compared to other chromatin binders, the FRAP kinetics of wild type MeCP2 are much faster than the core histone components¹⁴ but close to the kinetics of linker histone H1^{15,16}. Both MeCP2 and H1 compete for binding to nucleosomes *in vitro*¹⁷ and bind to the linker DNA^{18,19}. Moreover, MeCP2 is able to condense chromatin *in vitro* at the same level as histone H1 and under physiological salt concentrations²⁰. These *in vitro* data suggest that MeCP2 can “crosslink” chromatin fibers together similar linker histone H1. We have previously shown that MeCP2 clusters chromatin *in vivo*⁸ and our present data suggests that mutations occurring in Rett patients are defective precisely in this function.

Our results and the results from literature²¹ on FRAP from other chromatin proteins like HP1, show that it is highly mobile with a very fast recovery kinetics (Figure S3). The results together point in the direction that proteins that serve/work as chromatin compacters, have a stronger binding at the chromatin and thus have a slow recovery kinetics. We propose that proteins that lead to higher order chromatin organization should not only have a good binding at the chromocenters through multiple modes of interactions, but also should stay there for a longer time. This longer residence time might help them to make multiple higher order contacts and thus can serve as linkers for DNA or chromatin.

Less stable MeCP2 heterochromatin binding and/or smaller heterochromatin domains within the nucleus could conceivably play a role in Rett syndrome etiology.

Acknowledgements

We are grateful to Akos Dobay for the analysis of kinetic data and to Ingrid Grunewald for excellent technical support. We thank M. Shirakawa for the MeCP2-MBD structure and T. Misteli for the GFP-HP1 expression construct. T.H. was supported by the European Union (ESF program). This work was funded by grants of the Deutsche Forschungsgemeinschaft to M.C.C.

References

1. Amir, R.E. et al. Rett syndrome is caused by mutations in X-linked MECP2, encoding methyl-CpG-binding protein 2. *Nat Genet* **23**, 185-8 (1999).
2. Nan, X., Tate, P., Li, E. & Bird, A. DNA methylation specifies chromosomal localization of MeCP2. *Mol Cell Biol* **16**, 414-21 (1996).
3. Nan, X., Cross, S. & Bird, A. Gene silencing by methyl-CpG-binding proteins. *Novartis Found Symp* **214**, 6-16; discussion 16-21, 46-50 (1998).
4. Archer, H.L. et al. Gross rearrangements of the MECP2 gene are found in both classical and atypical Rett syndrome patients. *J Med Genet* **43**, 451-6 (2006).
5. Pan, H. et al. Large deletions of the MECP2 gene in Chinese patients with classical Rett syndrome. *Clin Genet* **70**, 418-9 (2006).
6. Ohki, I. et al. Solution structure of the methyl-CpG binding domain of human MBD1 in complex with methylated DNA. *Cell* **105**, 487-97 (2001).
7. Wakefield, R.I. et al. The solution structure of the domain from MeCP2 that binds to methylated DNA. *J Mol Biol* **291**, 1055-65 (1999).
8. Brero, A. et al. Methyl CpG-binding proteins induce large-scale chromatin reorganization during terminal differentiation. *J Cell Biol* **169**, 733-43 (2005).
9. Kudo, S. et al. Heterogeneity in residual function of MeCP2 carrying missense mutations in the methyl CpG binding domain. *J Med Genet* **40**, 487-93 (2003).
10. Orrico, A. et al. MECP2 mutation in male patients with non-specific X-linked mental retardation. *FEBS Lett* **481**, 285-8 (2000).
11. Ho, K.L. et al. MeCP2 binding to DNA depends upon hydration at methyl-CpG. *Mol Cell* **29**, 525-31 (2008).
12. Tsumura, A. et al. Maintenance of self-renewal ability of mouse embryonic stem cells in the absence of DNA methyltransferases Dnmt1, Dnmt3a and Dnmt3b. *Genes Cells* **11**, 805-14 (2006).

13. Kumar, A. et al. Analysis of protein domains and Rett syndrome mutations indicate that multiple regions influence chromatin-binding dynamics of the chromatin-associated protein MECP2 in vivo. *J Cell Sci* **121**, 1128-37 (2008).
14. Kimura, H. Histone dynamics in living cells revealed by photobleaching. *DNA Repair (Amst)* **4**, 939-50 (2005).
15. Misteli, T., Gunjan, A., Hock, R., Bustin, M. & Brown, D.T. Dynamic binding of histone H1 to chromatin in living cells. *Nature* **408**, 877-81 (2000).
16. Lever, M.A., Th'ng, J.P., Sun, X. & Hendzel, M.J. Rapid exchange of histone H1.1 on chromatin in living human cells. *Nature* **408**, 873-6 (2000).
17. Nan, X., Campoy, F.J. & Bird, A. MeCP2 is a transcriptional repressor with abundant binding sites in genomic chromatin. *Cell* **88**, 471-481 (1997).
18. Ishibashi, T., Thambirajah, A.A. & Ausio, J. MeCP2 preferentially binds to methylated linker DNA in the absence of the terminal tail of histone H3 and independently of histone acetylation. *FEBS Lett* **582**, 1157-62 (2008).
19. Chandler, S.P., Guschin, D., Landsberger, N. & Wolffe, A.P. The methyl-CpG binding transcriptional repressor MeCP2 stably associates with nucleosomal DNA. *Biochemistry* **38**, 7008-18 (1999).
20. Georgel, P.T. et al. Chromatin compaction by human MeCP2. Assembly of novel secondary chromatin structures in the absence of DNA methylation. *J Biol Chem* **278**, 32181-8 (2003).
21. Cheutin, T. et al. Maintenance of stable heterochromatin domains by dynamic HP1 binding. *Science* **299**, 721-5 (2003).
22. Phair, R.D. et al. Global nature of dynamic protein-chromatin interactions in vivo: three-dimensional genome scanning and dynamic interaction networks of chromatin proteins. *Mol Cell Biol* **24**, 6393-402 (2004).

23. Kaufmann, U., Kirsch, J., Irintchev, A., Wernig, A. & Starzinski-Powitz, A. The M-cadherin catenin complex interacts with microtubules in skeletal muscle cells: implications for the fusion of myoblasts. *J Cell Sci* **112 (Pt 1)**, 55-68 (1999).
24. Agarwal, N. et al. MeCP2 interacts with HP1 and modulates its heterochromatin association during myogenic differentiation. *Nucleic Acids Res* **35**, 5402-8 (2007).
25. Schermelleh, L. et al. Dynamics of Dnmt1 interaction with the replication machinery and its role in postreplicative maintenance of DNA methylation. *Nucleic Acids Res* **35**, 4301-12 (2007).

Materials and methods

Expression plasmids

Expression vectors encoding GFP-tagged fusions of human wild type or mutant MeCP2 cDNA cloned into the pEGFP-C1 vector were described before⁹ as was GFP-HP1 α ²¹.

Cell culture, transfection and staining

Pmi28 mouse myoblasts were cultured as described²³. Cells were plated on glass coverslips or multiwell dishes (ibidi μ dishes 8 well; Ibidi GmbH, Munich, Germany) prior to transfection for fixed cell or live cell experiments, respectively. Cells were transfected using TransFectinTM (BioRad, Hercules, CA) following the manufacturer's protocol. Cultures were fixed and DNA stained as described²⁴. In short, cultures were rinsed in PBS and fixed in 3.7% formaldehyde in PBS. Nuclear DNA was counterstained using TOPRO-3 (Invitrogen, Carlsbad, CA), Hoechst 33258 or DAPI (4' -6'-diamidino-2-phenylindol) and samples were mounted in vectashield antifading medium (Vector Laboratories, Burlingame, CA) or moviol.

Microscopy and image analysis

Chromocenter clustering induced by GFP-tagged MeCP2 and mutants was assessed by visual inspection of GFP and/or DNA signals using widefield epifluorescence microscopy with appropriate filter sets (Axiovert 200 microscope; 63x Plan apochromat NA1.4 oil lens, Zeiss, Jena) and counting chromocenters in 50-55 nuclei. Cumulative frequencies of chromocenter numbers were tested for statistical significance differences using a Kolmogoroff-Smirnoff test with Microsoft Excel software and plotted with Origin 7.5 software (Origin Lab Corp).

To assess the chromocenter binding ability, we collected confocal Z stacks (voxel size: 0.05 x 0.05 x 0.3 μm) of 10-15 cells expressing similar levels of the GFP fusion protein on either Zeiss LSM510Meta or Leica SP5 microscopes, using 63x/1.4NA oil objective and 405nm DPSS (for Hoechst 33258, DAPI), 488nm argon (for GFP) and 633nm He-Ne (TOPRO-3) laser excitation. Care was taken in selecting the imaging conditions to avoid under and over exposed pixels, while keeping the imaging conditions constant. The heterochromatic foci were identified by staining with TOPRO-3, Hoechst 33258 or DAPI. Image analysis was done using ImageJ version 1.38x (<http://rsb.info.nih.gov/ij>). The average mean intensity at the chromocenters versus the nucleoplasm was assessed by selecting four regions of equal size in the two compartments, calculating the mean fluorescent intensity in each compartment and then taking a ratio between both. The formula used to calculate the accumulation of MeCP2 and mutants at chromocenters for each construct was:

Accumulation at chromocenter = average mean intensity at chromocenters / average mean intensity in nucleoplasm

In situ extraction of GFP-tagged wildtype MeCP2, and MeCP2 bearing mutants was done by transfecting the cells plated on ibidi dishes with the respective construct. Cells were first washed with PBS containing 0.5mM MgCl_2 , 0.5mM CaCl_2 and imaged. Then the solution was changed to PBS containing 0.5mM MgCl_2 , 0.5mM CaCl_2 and 0.5% Triton X-100. Confocal Z series were recorded over time on a Zeiss LSM510Meta microscope, using 63x/1.4NA oil objective. The microscope was equipped with a microscope cage incubation chamber (Oko-lab, Ottaviano, Italy) and the temperature was maintained at 37°C. GFP was excited with the 488nm argon laser line. Confocal Z stacks were acquired with a frame size of 1024 x 1024 pixels (voxel size: 0.20 x 0.20 and 1.0 μm), at 2 minutes time intervals for 14 minutes.

Quantitative evaluation was performed using ImageJ. The mean fluorescence intensities at the chromocenters for each cell and time point were calculated for PBS and PBS-Triton X-100. First, using ImageJ 'adjust threshold' plug-in the chromocenters were identified and then 'create selection' plug-in was used to assess the mean fluorescence intensity only at chromocenters. This procedure was repeated for each cell and time point. The whole data set for each cell was then normalized to the mean fluorescence intensities of the chromocenters before extraction with Triton X-100. The results were evaluated using Microsoft Excel and plotted using Origin 7.5 software (Origin Lab Corp).

Fluorescence recovery after photobleaching

Live cell imaging and FRAP experiments were performed on a LSM510Meta confocal microscope (Zeiss) using a 63x/1.4NA Plan-Apochromat oil immersion objective. The microscope was maintained at 37°C with the help of an Oko-lab cage incubation chamber. Confocal image series were recorded with a frame size of 512 x 512 pixels, a pixel size of 60 nm, and at 2 sec time intervals. 488nm argon laser line (25 mW) was used at 100% transmission to bleach and at 0.05% transmission to record GFP-tagged fluorophores over time, with the pinhole opened to 3 Airy units. Either a whole chromocenter or half of the nucleus was photobleached and 5-10 prebleach and 250-400 postbleach frames were recorded for each time series. Quantitative evaluation was performed using ImageJ and Microsoft Excel. The time series was first corrected for translational movements using 'stackreg' plug-in from ImageJ and the analysis of the FRAP data was performed exactly as described ²⁵.

Figures

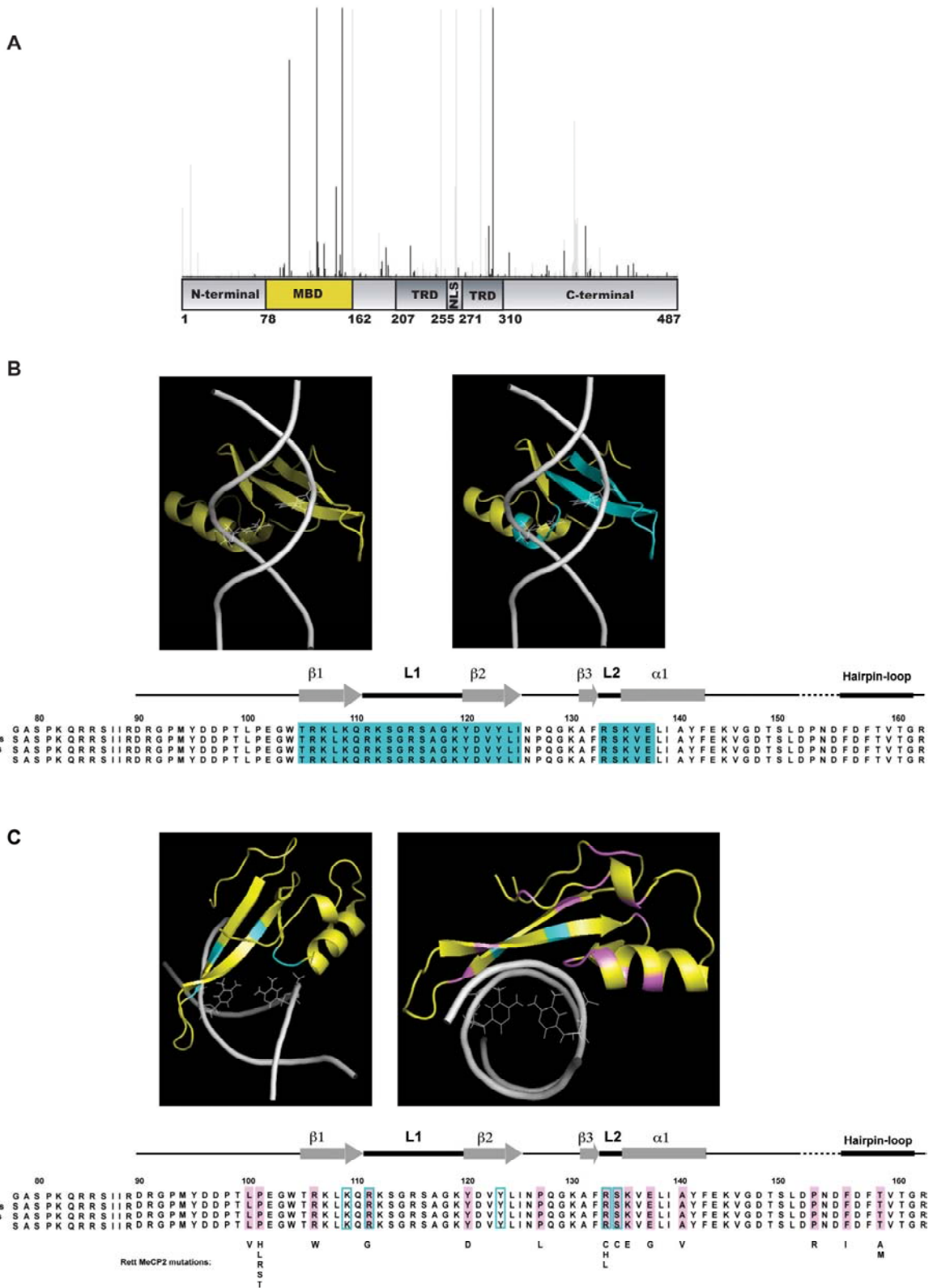


Figure 1: Summary of frequency and localization of MeCP2 Rett mutations.

(A) Mutation spectrum in Rett patients (IRSA <http://mecp2.chw.edu.au/cgi-bin/mecp2/search/printGraph.cgi#MS>), with missense mutations shown in black and the others in grey color. Location of individual mutations is indicated on a schematic representation of the MeCP2 protein (numbers are amino acids coordinates). MBD stands for methyl CpG binding domain, TRD for transcription repression domain and NLS for nuclear localization signal. (B) shows a model of the MBD of MeCP2 (yellow) interacting with its target 5mC within the DNA double helix ⁶. Structural data was displayed and annotated using PyMOL software (<http://pymol.sourceforge.net/>). The DNA backbone is shown in white along with the methylated cytosines. The MBD of MeCP2 is displayed in yellow. The parts of the MBD that make contacts with the 5mC on DNA are highlighted in blue in the structure on the left hand side and in the MeCP2 MBD sequence alignment shown below. (C) The five residues that directly interact with the two 5mC are shown in blue. The 21 mutations included in our study are listed below the corresponding wild type amino acid on MBD (pink).

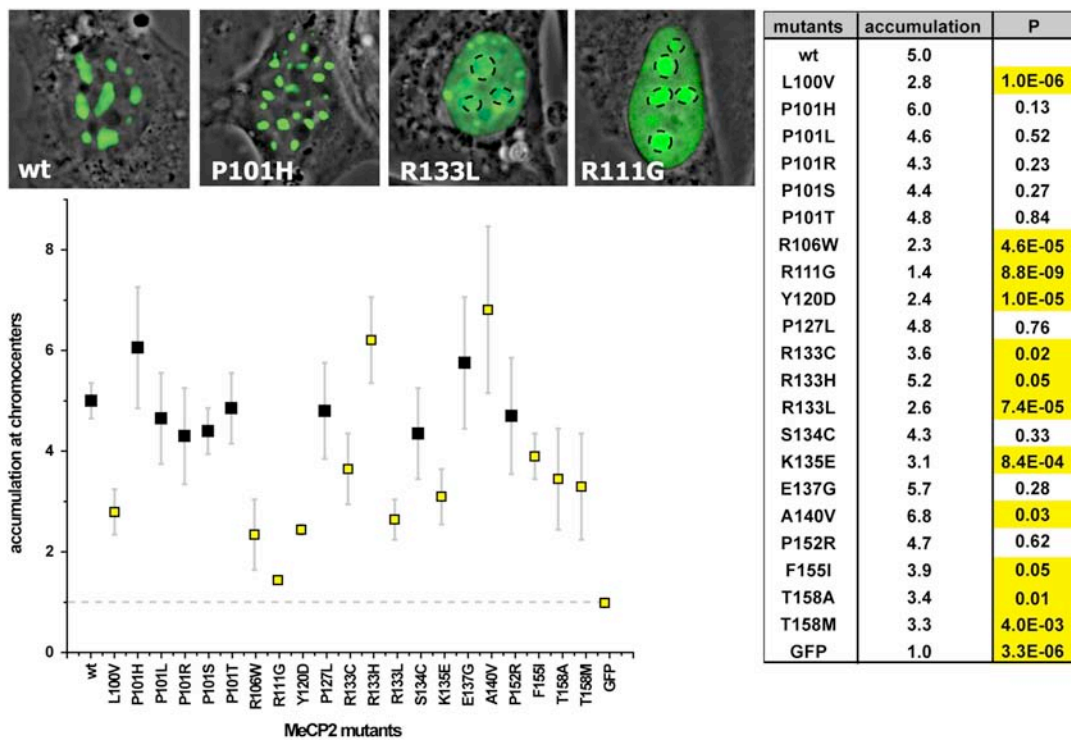


Figure 2: Mutant MeCP2 proteins accumulate at chromocenters *in vivo*, albeit to very different extent.

Representative overlay images of phase contrast and GFP fluorescence of cells expressing wild type MeCP2 and mutants, showing differential chromocenter accumulation ability. The dashed lines indicate the location of the nucleoli. The dot plot chart shows the fold accumulation at chromocenters of the 21 mutant proteins, the wild type MeCP2 and the EGFP tag alone as controls. All the mutants except R111G accumulate at chromocenters, but to very different extent. The yellow color highlights the mutants whose accumulation was significantly different ($p \leq 0.05$) from wild type. All mutants accumulated significantly different ($p \leq 0.05$) with respect to EGFP protein alone control (not shown). The table lists the average value of

accumulation of each protein at the chromocenters, along with their p value with respect to the wild type MeCP2. The experiment was repeated twice with 10-15 cells per mutant evaluated each time.

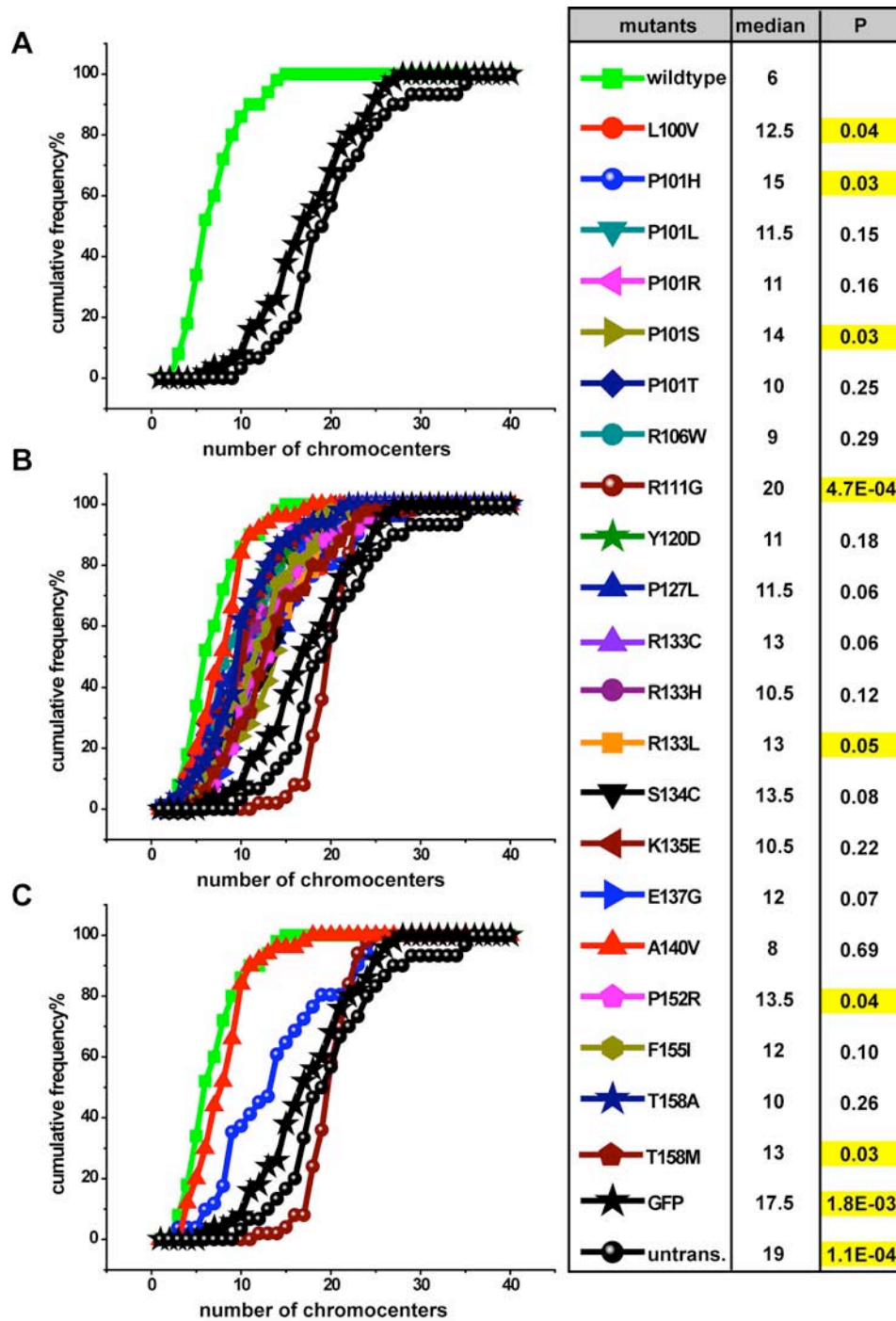
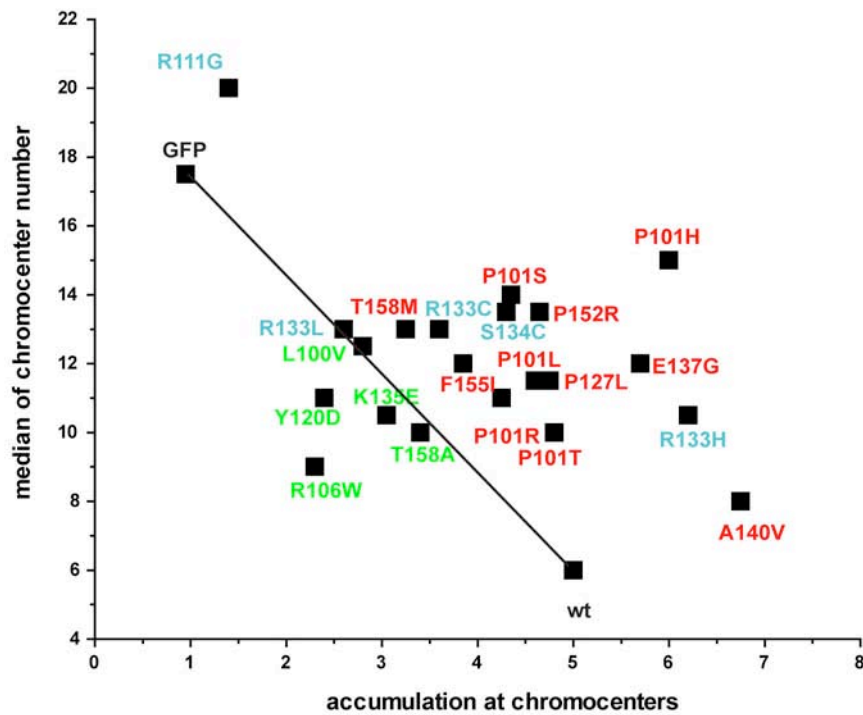


Figure 3: Rett mutant proteins are affected in their ability to cluster chromocenters.

(A) The plot shows the percentage cumulative frequencies of chromocenter numbers in cells expressing GFP-tagged wild type MeCP2 versus untransfected cells and

EGFP transfected cells. (B) Cumulative frequencies of chromocenter numbers in cells expressing each of the 21 GFP-tagged MeCP2 mutants. (C) depicts the MeCP2 Rett mutants that are either most affected (P101H), or less affected (A140V), as well as the extreme case of R111G that has lost its ability to bind chromatin, together with the controls (wild type MeCP2, EGFP alone and untransfected cells). The table lists the median number of chromocenters for each mutant along with the significance difference ($p \leq 0.05$, highlighted in yellow) of mutants with respect to wild type. All mutants except P101H and R111G had the median number of chromocenters significantly different ($p \leq 0.05$) with respect to untransfected cells (not shown). The experiment was repeated 2 times with 50 cells evaluated per mutant each time.

A



B

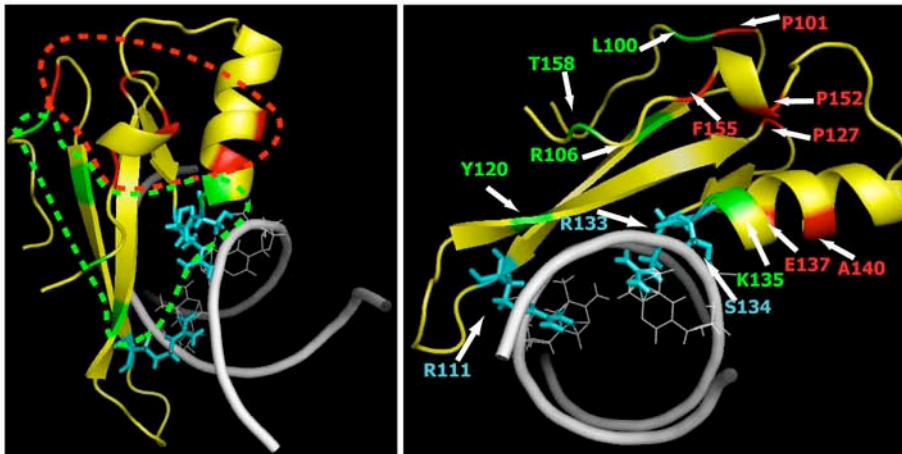
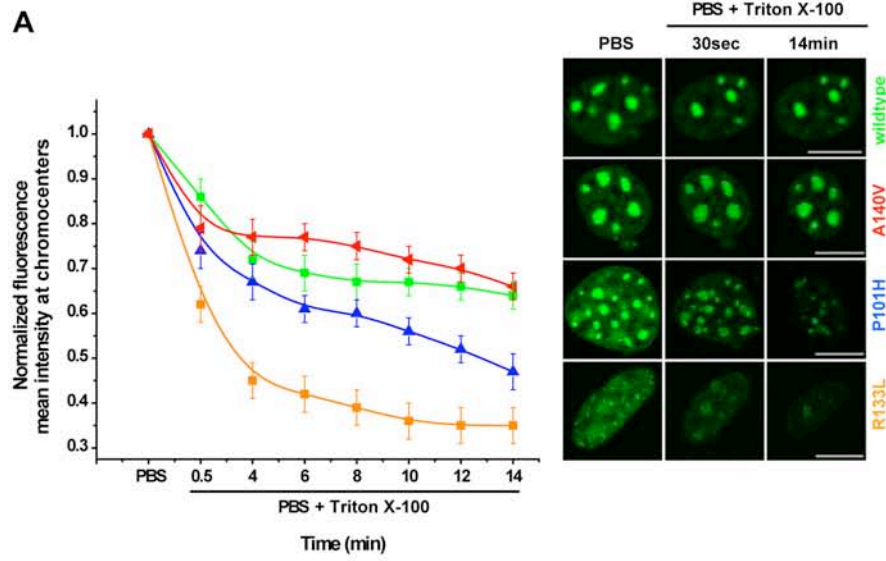


Figure 4: Correlation analysis of chromocenter clustering and accumulation at chromatin.

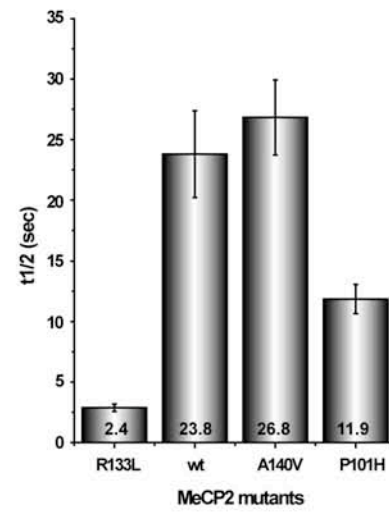
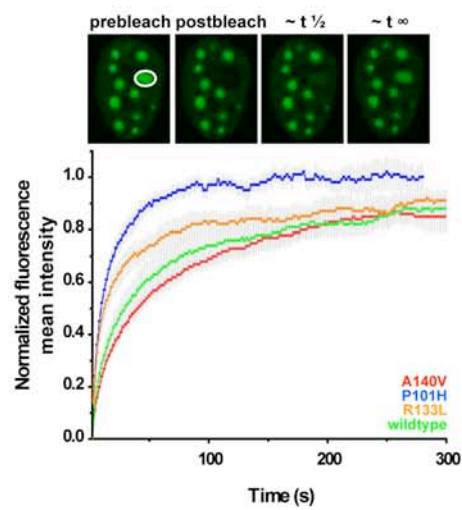
(A) Accumulation at chromocenters (see Figure 2) and median of chromocenter number (see Figure 3) were plotted on the X and Y-axis respectively. The scatter plot neither indicates an overall direct nor an inverse correlation. The theoretical line

connecting the GFP alone and GFP-MeCP2 delineates the indirect relationship between binding to chromatin and chromocenter number (clustering). Mutants grouping above the line are color coded in red and the ones grouping below the line are in green. Mutants in residues directly interacting with 5mC are shown in blue (see Figure 1C). (B) Structure of the MBD (in yellow) of MeCP2 in complex with DNA (in white) was displayed as in Figure 1. The residues were given the corresponding color as in part A. The location of the green and red residues within the MBD structure showed a similar separation in two groups as on the scatter plot.



B

Chromocenter FRAP



Half nucleus FRAP

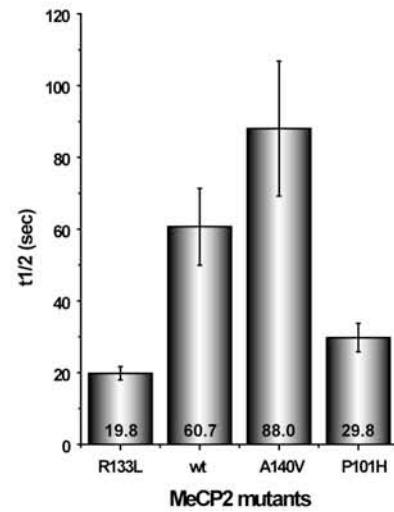
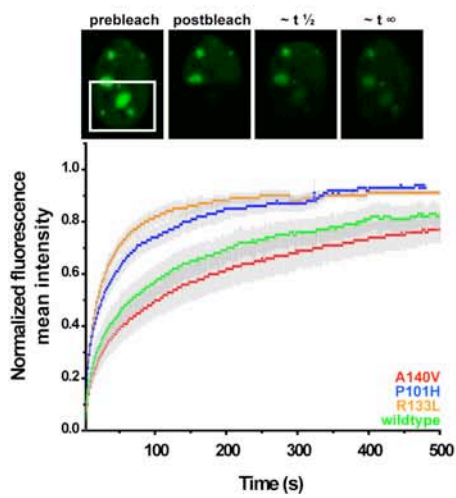


Figure 5: MeCP2 Rett mutant proteins show different kinetics in vivo.

To assess the mobility and binding kinetics of wild type MeCP2 versus mutants, we performed biochemical *in situ* as well as fluorescence photobleaching recovery experiments. (A) *In situ* extraction kinetics for GFP-tagged proteins was performed by permeabilizing the cells on the microscope stage with Triton X-100 and measuring the decrease of protein at chromocenters over time. The experiment was repeated twice and 7-10 cells were analyzed each time, for each mutant. The line graph shows the extraction kinetics of the mutants over time. Error bars represent the standard error of mean and representative mid section images are shown on the right. Scale bar represents 10 μ m. (B) FRAP curves of GFP-tagged wild type and mutant MeCP2 together with representative images before and after photobleaching. For FRAP analysis, either a whole chromocenter or half of the nucleus (marked in white) was photobleached. For each construct 15-20 cells were averaged and the mean curve as well as the standard error of the mean was calculated. Half times of recovery shown on the bar histograms were calculated from the mean curves and the error bars represent the standard error of mean.

Supplemental figures:

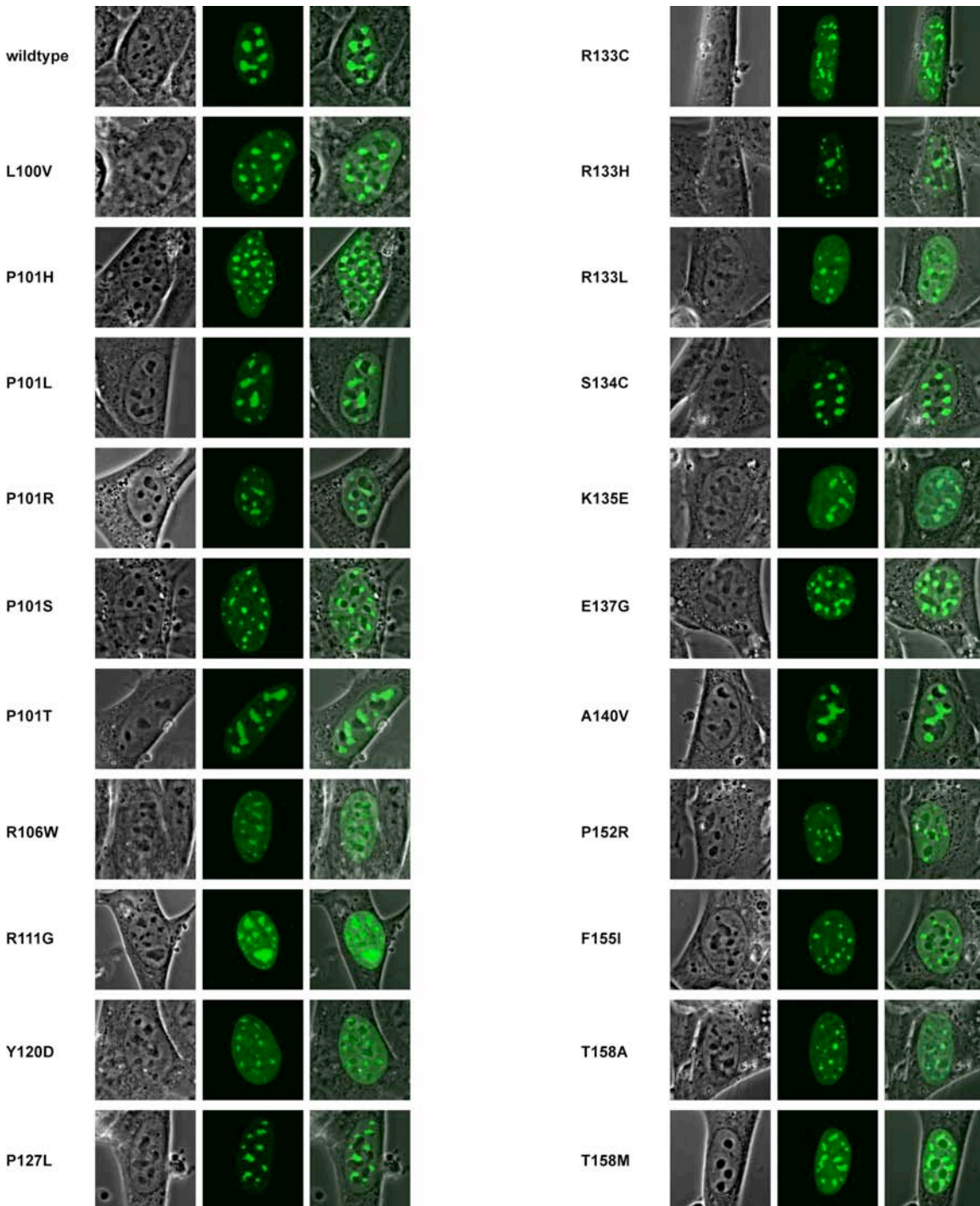


Figure S1: MeCP2 mutants differ in their ability to accumulate at chromocenters and to induce their clustering.

Representative confocal microscopy images of Pmi cells expressing GFP fusions to

wild type MeCP2 and each of the 21 MeCP2 Rett mutants used in this work. In the left panels, the phase contrast image is shown where the nucleus and nucleoli are seen. The middle panels depict the GFP fluorescence of a mid optical section and the right panels the overlay of both. Chromocenters were additionally visualized by counterstaining for DNA (data not shown). The ratio of protein enriched in heterochromatin versus nucleoplasm differs strongly between mutants (see also Figure 2), as does their ability to cluster the chromocenters (see also Figure 3). Furthermore, R111G mutant does not accumulate at chromocenters but rather at nucleoli, as can be seen by the overlay with the phase contrast image.

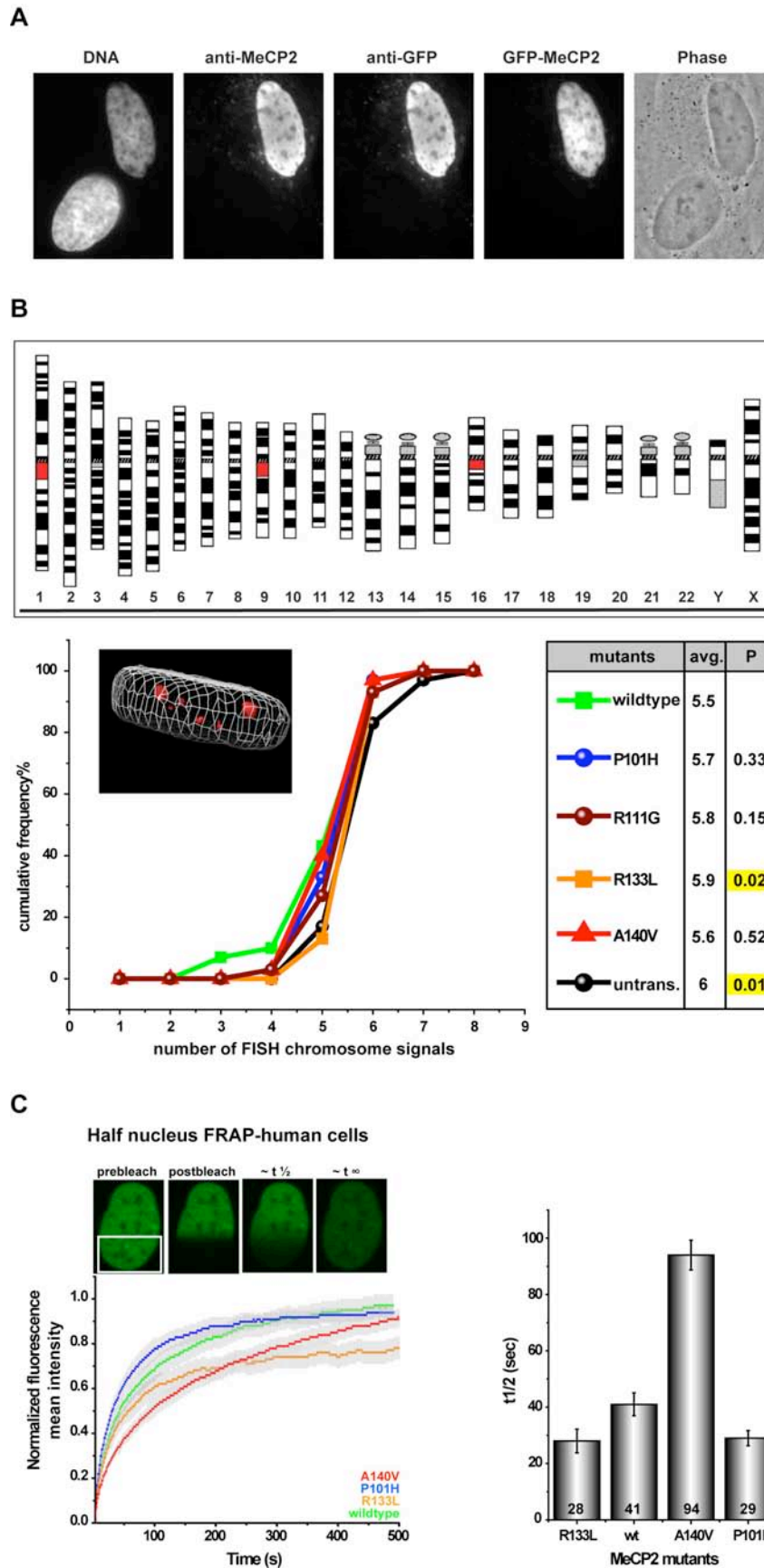


Figure S2: MeCP2 induces heterochromatin clustering in human diploid cells.

A) Human foreskin diploid fibroblasts (Bj-hTERT) were transfected with a plasmid encoding for GFP-tagged human MeCP2, fixed after 12h and immunostained with anti-MeCP2 and anti-GFP. The image shows one exemplary field including one transfected cell identified by direct GFP fluorescence as well as anti-GFP and anti-MeCP2 antibodies staining. The second cell was not transfected and hence shows no GFP or anti-GFP signals. The lack of any signal with the MeCP2-specific antibody in the untransfected cells indicates that Bj-hTERT cells, similarly to Pmi cells, do not contain detectable levels of endogenous MeCP2. (B) The top panel depicts an ideogram of G-banded human chromosomes (www.pathology.washington.edu/galleries/cytogallery/main.php?file=human%20karyotypes). Chromosomes 1, 9 and 16 contain the largest pericentric heterochromatin regions (marked in red), as compared to the other chromosomes, and were, thus, selected for our analysis of MeCP2-induced heterochromatin clustering. Cells were transfected with constructs coding for GFP-tagged wild type and mutant human MeCP2 and clustering of these heterochromatic regions analyzed by simultaneous hybridization with three DNA probes from the pericentric heterochromatin DNA of these three chromosomes. Cells expressing the GFP-tagged MeCP2 proteins were identified by immunostaining with anti-MeCP2 antibody and DNA was counterstained with DAPI. Confocal Z stacks of images from the GFP-MeCP2 signal, overall DNA signal and DNA FISH probes were then acquired. The three dimensional rendering of one such cell is shown where the contour of the nucleus is depicted by the white grid and the FISH signals of the three pericentric heterochromatin regions in red. The cumulative frequency % of the FISH signals counted in the presence of different MeCP2 mutants is shown together with the table listing the average number of chromosome signals and their p value with respect to the wild type MeCP2 ($p \leq 0.05$,

highlighted in yellow). Experiments were repeated twice with 30 cells evaluated each time per construct. Even with this extremely narrow dynamic range, between 3 and 6 chromosome signals, a significant difference could be measured in the number of FISH signals, which follows the one found in the chromocenter clustering analysis in mouse cells. (C) FRAP and the corresponding kinetic data analysis on the MeCP2 and mutants expressed in human Bj-hTERT cells. Half times of recovery were calculated from the mean curves and are shown in the bar chart. The error bars represent the standard error of mean. The experiment was repeated twice with 15-20 cells evaluated each time per construct.

Chromocenter FRAP

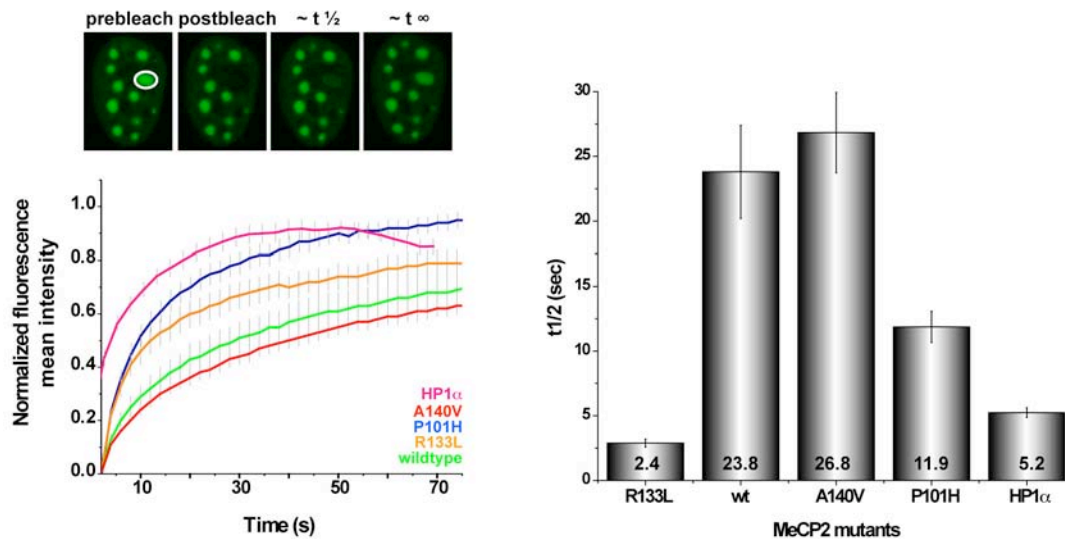


Figure S3: Comparison of the heterochromatin binding kinetics of MeCP2 Rett mutant proteins and HP1.

FRAP curves of GFP-tagged wild type MeCP2, mutant MeCP2 and HP1 α expressed in Pmi cells together with representative images before and after photobleaching of chromocenters (marked in white). For each construct 15-20 cells were averaged and the mean curve as well as the standard error of the mean was calculated. Half times were determined from the mean curves and are shown in the bar chart. The error bars represent the standard error of the mean.

Supplemental methods:

Human cell culture and transfection

The human foreskin fibroblast (Bj-hTERT) cell line (ATCC BJ-5ta) was derived by transfection of human foreskin fibroblasts with the pGRN145 hTERT expression plasmid and selection of stable immortalized cell clones ¹. It is a diploid human cell line with a modal chromosome number of 46 that occurred in 90% of the cells counted and karyotypically normal X and Y sex chromosomes.

Human Bj-hTERT fibroblasts were cultured in DMEM medium containing 10% FCS, glutamine and gentamicin. Cells were transfected using the Amaxa nucleofactor (Amaxa AG, Cologne, Germany) or TransFectin™ (BioRad, Hercules, CA) following the manufacturer's protocols.

ImmunoFISH

For fluorescence *in situ* hybridization, the following DNA probes were used: repetitive specific human DNA probe pUC 1.77 ² for chromosome 1, alphoid DNA probe pMR9A for the centromeric region 9q12 of chromosome 9 and alphoid DNA probe pHUR-195 for the centromeric region 16q11.2 of chromosome 16. These DNA probes were labeled by standard nick translation with Cy5-dUTP (Amersham, Buckinghamshire, UK). The labeled DNA was further purified by ethanol-precipitation and the pellet resuspended in hybridization solution (70% formamide, 2xSSC, 10% dextran sulfate, pH 7.0). The probes were denatured at 80 °C for 5 minutes.

For immunoFISH cells were fixed with 4% paraformaldehyde in PBS for 10 minutes and permeabilized with 0.25% Triton X-100 in PBS for another 10 minutes. Primary (rabbit polyclonal anti-MeCP2) and secondary (anti-rabbit IgG Alexa Fluor 568; Molecular probes, CA, USA) antibodies were diluted in PBS with 0.2% fish skin

gelatin and incubated sequentially for one hour each at room temperature. After immunostaining, the cells are post-fixed with 4% paraformaldehyde for 60 minutes followed by post-permeabilization with 0.5% Triton X-100 in PBS for 10 minutes, 0.1 M HCl for 10 minutes and 20% glycerol for 4 minutes. Probes were added to the cells and sealed with rubber cement to decrease evaporation of the probe over night. They were then denatured simultaneously at 75 °C for 5 minutes and hybridized over night at 37 °C. Non-hybridized probe was washed off using 50% formamide in SSC at 45 °C three times followed by two washes with 2xSSC. DNA was counterstained with DAPI and the cells were mounted using vectashield.

MeCP2 expressing cells were identified by the positive staining with the anti-MeCP2 antibody and complete Z stacks of images (voxel size: 80 x 80 x 200 nm) of the DAPI (excited at 405 nm) and Cy5 (excited at 633 nm) signals for whole DNA and chromosomes 1, 9 and 16 pericentric heterochromatin regions, respectively, were acquired on a Leica SP5 laser scanning microscope using a 63x/1.4NA oil objective. FISH signals were counted manually through these stacks. 3D rendering was done using UCSF chimera (www.cgl.ucsf.edu/chimera).

Supplemental references:

1. Bodnar, A.G. et al. Extension of life-span by introduction of telomerase into normal human cells. *Science* **279**, 349-52 (1998).
2. Cooke, H.J. & Hindley, J. Cloning of human satellite III DNA: different components are on different chromosomes. *Nucleic Acids Res* **6**, 3177-97 (1979).

4. DISCUSSION

In recent years, lot of research work has already been done on MeCP2 but still little is known about its role in chromatin reorganization during development and disease. In this study, using a combination of biochemical and microscopical techniques, I could show an interaction and interdependency between two major epigenetic factors, MeCP2 and HP1. Furthermore, I demonstrate that MeCP2 plays an important role in determining higher order chromatin organization and, disruption of this function, takes place on MeCP2 mutants found in patients with a neurological disorder termed Rett syndrome.

4.1. Chromatin clustering is induced by MeCP2 and not HP1 during differentiation

Recently, our group has shown that the MBD domain of MeCP2 is capable of causing chromosome clustering (Brero et al., 2005). In the present work, I have dissected this chromocenter clustering property of MeCP2 *in vivo*, during differentiation and disease. Recently, it has been shown that MeCP2 binds to nucleosomes in a very similar manner as linker histone H1 (Ishibashi et al., 2008) and, accordingly, MeCP2 was able to displace linker H1 pre-bound to chromatin (Nan et al., 1997). When the chromatin compacting properties of MeCP2 are compared with linker histones like H1 and H5, MeCP2 appears to have a stronger effect. As shown *in vitro* (Georgel et al., 2003) and *in vivo* (Brero et al., 2005), MeCP2 forms highly compacted condensed structures, whereas linker histones are shown to form a relatively decondensed zigzag conformation of nucleosomes and linker DNA (Bednar et al., 1998). In fact, histone H1-bound chromatin can reach an equivalent amount of compaction to MeCP2-bound chromatin but only at three times higher ionic strength (Hansen, 2002).

We have recently shown that HP1 does not cause chromocenter clustering *in vivo* (Brero et al., 2005). Also, in this work I could show that HP1 alone cannot cause chromocenter clustering, and the latter only occurred in cells co-expressing an MBD family member (Agarwal et al., 2007). Furthermore, it has been shown that HP1 α , does not have a similar binding mode to nucleosomal arrays as MeCP2 (Fan et al., 2004). MeCP2 has been shown to be capable of folding nucleosomal arrays (Georgel et al., 2003) *in vitro*, whereas HP1 α can only bind to folded nucleosomal arrays (Fan et al., 2004). Hence, HP1 α per se might only be able to induce local rearrangements of folded secondary chromatin structures, and does not seem to be able to cause the formation of

such structures themselves. The results of the kinetic FRAP analysis on HP1 α versus MeCP2 in this work indicated that HP1 is far more mobile on chromatin than MeCP2. The latter likely reflects the multiple chromatin binding modes of MeCP2 (Chahrour et al., 2008; Cohen et al., 2008), recognizing methylated cytosines as well as DNA, which could allow and/or facilitate intra/inter-chromatin fiber connections resulting in clustering and compaction of chromatin.

4.2. Chromatin clustering is affected by mutations in MeCP2

Mutations in MeCP2 gene are found in 80% of Rett syndrome patients (Trappe et al., 2001). The difference in phenotypic variability associated with different mutations on MeCP2 gene depends upon the pattern of X chromosome inactivation (XCI). In females, one of the two X chromosomes is active in each cell. This results in a mosaic situation, in terms of X chromosome gene expression (either maternal or paternal) and further complicates any gene therapy based approach.

Several reports in the literature point to the fact that missense mutations are mostly present on the MBD domain of MeCP2. Since our data showed that this domain is necessary and sufficient to cause chromatin clustering (Brero et al., 2005), I investigated whether these mutations affected this novel function of MeCP2. To determine the significance of these missense mutations on the chromatin compaction ability of MeCP2, I examined this effect on a total of 21 MBD missense Rett mutations. Through several assays, I could show in the present work that mutations on the MBD domain of MeCP2 can indeed result in disruption of distinct functions of MeCP2 like accumulation and dynamics of protein at chromocenters, and chromocenter clustering. I could also overlay the results from our analysis as a whole on the structure of the MBD domain of MeCP2.

I could show that P101H mutant protein revealed a significantly larger amount of chromocenter number as compared to wild type. Also, R111G mutant showed defect in chromocenter clustering ability and has been shown earlier to result in a complete loss of function of MeCP2 (Kudo et al., 2003) and, indeed, I could not detect any binding to heterochromatin. Replacement of proline with histidine at position 101 might result in large-scale changes in the protein structure, as proline provides a nick and rigidity at that position in the protein structure, whereas histidine being a flexible amino acid might prevent it. MeCP2 A140V mutant retained chromatin binding and clustering equivalent

to wild type. It has been shown that A140V mutation correlates with an almost normal clinical phenotype (Couvert et al., 2001; Orrico et al., 2000) and even males with this mutation can survive, being therefore a very mild mutation.

The analysis of the accumulation of protein at pericentric heterochromatin indicated that R106W and R111G, though still able to bind at chromocenters, show the lowest accumulation ability. R106W has been shown to lie on the β 2 sheet (Wakefield et al., 1999) and so has been predicted to strongly impair MBD function and inducing misfolding of MBD (Ballestar et al., 2000; Yusufzai and Wolffe, 2000). In addition to residue R111, residues R133 and S134 interact directly with the methylated cytosines. I tested three mutants of R133 residue, R133H accumulated better than wild type MeCP2, R133C accumulated less and R133L was the least able to accumulate, though all the three accumulated significantly different from wild type MeCP2. S134C mutant accumulated similarly to wild type MeCP2. R133 and S134 have been shown to be less critical for the MBD function than R111 (Kudo et al., 2003). K135E, E137G, T158A, T158M, Y120D, F155I showed intermediate impairment in chromatin binding.

To determine whether the MeCP2 MBD mutations affected the kinetics of chromatin binding, I performed *in vivo* kinetic studies (*in situ* extraction and FRAP) on selected mutants, which were either not affected in binding and clustering of chromatin (A140V), or affected only in clustering (P101H) or in both functions (R133L). R133L mutation resulted in higher extractability and a much faster FRAP recovery. This could be explained if we take into consideration the predicted NMR solution structure of MeCP2 with methylated DNA (Ohki et al., 2001; Ohki et al., 1999; Wakefield et al., 1999), indicating that this residue is involved in binding to the methylated cytosines. Furthermore, methyl cytosines seem to be required for efficient accumulation of MeCP2 at heterochromatin, as shown by the lack of chromocenter localization of a GFP-tagged MBD fusion in Dnmt1/3a/3b triple knock-out cells (Tsumura et al., 2006). Our live-cell kinetic data indeed indicates that albeit able of accumulate at heterochromatin to a low extent, the R133L mutant MeCP2 interacts only transiently and with low affinity. The *in vivo* accumulation of this mutant to chromatin may be either due to retaining a low affinity recognition of methylcytosine and/or binding to DNA or other heterochromatin-associated proteins. The results of kinetic data from P101H mutant highlight an intermediate ability to bind chromatin, whereas A140V mutant is quite similar to wild type MeCP2. In view of the position of the P101 residue in the MBD structure and the fact that this domain is not known to bind DNA (Nikitina et al., 2007b), I propose that this

surface of the MBD is likely involved in protein-protein interactions promoting connections between chromatin. My analysis of the *in vivo* chromocenter clustering ability of the different mutations clearly indicated that all mutants where this property was significantly disrupted (including P101H) mapped to this same surface of the MBD three-dimensional structure and, importantly, these mutants were not concomitantly affected in chromatin binding. Such mutants would be able to bind to DNA quite well, as is also clear from the chromatin accumulation data, but would be affected in binding to other proteins present at the chromatin and, therefore, could not induce chromocenter clustering resulting in faster binding dynamics at chromatin. Less stable MeCP2 heterochromatin binding and/or smaller heterochromatin domains within the nucleus could conceivably play a role in Rett syndrome etiology.

4.3. Modes of MeCP2 binding that lead to higher order chromatin structures

Based on our results and the results from other groups, I hypothesize that there are at least three binding classes for MeCP2: (a) binding to methylated and unmethylated chromatin (b) binding to other chromatin proteins (c) binding to itself.

4.3.1. Binding of MeCP2 to methylated or unmethylated chromatin

There are several lines of evidence in the literature showing the binding of MeCP2 to DNA and chromatin. It has been shown that MeCP2 forms discrete complexes with nucleosomal DNA associating with methyl-CpGs exposed in the major groove via the methyl-CpG-binding domain (MBD). The interaction of MBD domain of MeCP2 to methylated DNA is due to the presence of five highly conserved residues that form a hydrophobic patch (Ohki et al., 2001).

Furthermore, *in vitro* MeCP2 can bind to methylated as well as unmethylated DNA (Georgel et al., 2003). In addition to the MBD, the carboxyl-terminal segment of MeCP2 facilitates binding both to naked DNA and to the nucleosome core (Chandler et al., 1999).

4.3.2. Binding of MeCP2 to chromatin proteins

A connection between chromatin structure, DNA methylation and histone acetylation has been long known and discussed. MeCP2 could serve as an interconnecting element in this phenomenon. Evidence in that direction comes from the fact that, during

biochemical purifications of MeCP2, in both mammals and *Xenopus*, Sin3A was also co-purified (Jones et al., 1998; Nan et al., 1998), along with HDAC.

MeCP2 has been shown to interact in addition with several proteins as shown earlier in **Figure 6**. In this study, I also found a novel interacting partner of MeCP2, HP1 (Agarwal et al., 2007) which is involved in transcriptional silencing.

We have recent preliminary evidence indicating homo and heterodimerization between MBD protein family members (data not shown).

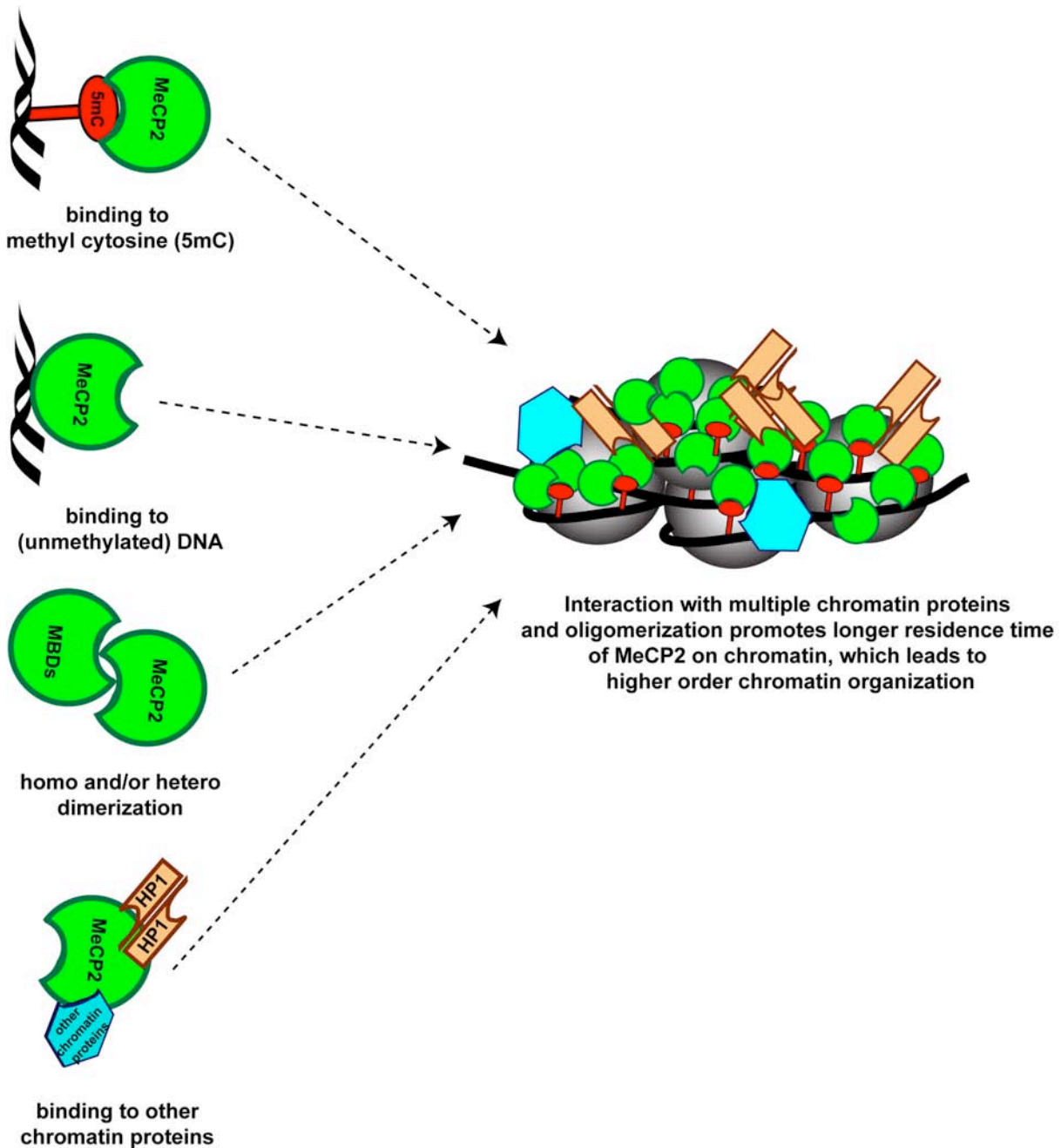


Figure 9. Model depicting different modes of MeCP2 binding and MeCP2 induced higher order chromatin structures.

The model in **Figure 9** highlights the different binding modes of MeCP2. Though no strict order of binding that can be predicted at this time, binding to methylated DNA could constitute a basic initial binding site for MeCP2. This is suggested by the lack of

heterochromatin association of the MBD domain of another family member MBD1 in the triple knockout ES cells for Dnmt1/a/3b (Tsumura et al., 2006). This basic binding of MBD proteins to methylated cytosines could be followed by binding of several other proteins to MeCP2 as well as the interaction between MeCP2 itself and other MBD protein family members. I suggest that the cooperation of all these binding modes, which individually may have low affinity, promotes ultimately stable association of MeCP2 at heterochromatin, as measured in the FRAP and *in situ* extraction experiments. This stable binding could facilitate connections within and between chromatin fibers and lead to a dynamic yet stable organization of heterochromatin domains with a modulating effect on the level of transcriptional noise.

5. OUTLOOK

Building upon the results obtained in this work, several lines of investigation could be pursued.

It would be interesting to elucidate the role of MeCP2, with special emphasis on the MBD domain in chromatin compaction *in vitro*. The goal of the project would be to know in detail, which part of the MBD domain is responsible for such an effect. This could be done by performing chromatin aggregation assays using recombinant purified MeCP2 starting with the particular Rett mutants identified in this analysis.

Another interesting set of parallel experiments would be to screen for interacting partners of MeCP2. This could be done in several ways: (a) yeast 2 hybrid approach (b) fluorescence 3 hybrid assay (c) mass spec analysis of MeCP2 co-precipitated proteins, followed by validation by GST pull down assays. This could be followed by comparing the proteins co-precipitating with wild type versus mutant MeCP2 thus would also allow to pinpoint which protein interaction(s) are relevant for chromatin clustering.

During this work, I got several preliminary results indicating that MeCP2 interacts with itself and other members of the MBD family. A detailed analysis of these interactions should be performed together with a better mapping of the domains involved. *In vivo* co-immunoprecipitation as well as *in vitro* pull-down assays together with deletion analysis should be performed as was done for the characterization of the HP1 interaction with MeCP2. In addition, the size of the MeCP2 containing complexes could be determined by gel filtration analysis of cell extracts as well as *in vitro* reconstituted complexes.

Finally, it would be very interesting to elucidate the structure of the mutant proteins analyzed in this study, in particular, P101H, R111G, R133L, A140V etc. This, together with the identification of binding partners (DNA or proteins) affected by the particular Rett mutations, should help elucidating the mechanism of chromatin higher-order organization by MeCP2.

6. REFERENCES

- Aasland, R. and Stewart, A.F. (1995) The chromo shadow domain, a second chromo domain in heterochromatin-binding protein 1, HP1. *Nucleic Acids Res*, **23**, 3168-3173.
- Agarwal, N., Hardt, T., Brero, A., Nowak, D., Rothbauer, U., Becker, A., Leonhardt, H. and Cardoso, M.C. (2007) MeCP2 interacts with HP1 and modulates its heterochromatin association during myogenic differentiation. *Nucleic Acids Res*, **35**, 5402-5408.
- Ainsztein, A.M., Kandels-Lewis, S.E., Mackay, A.M. and Earnshaw, W.C. (1998) INCENP centromere and spindle targeting: identification of essential conserved motifs and involvement of heterochromatin protein HP1. *J Cell Biol*, **143**, 1763-1774.
- Amir, R.E., Van den Veyver, I.B., Wan, M., Tran, C.Q., Francke, U. and Zoghbi, H.Y. (1999) Rett syndrome is caused by mutations in X-linked MECP2, encoding methyl-CpG-binding protein 2. *Nat Genet*, **23**, 185-188.
- Armstrong, D. (1997) Recent developments in neuropathology--electron microscopy--brain pathology. *Eur Child Adolesc Psychiatry*, **6 Suppl 1**, 69-70.
- Armstrong, D., Dunn, J.K., Antalffy, B. and Trivedi, R. (1995) Selective dendritic alterations in the cortex of Rett syndrome. *J Neuropathol Exp Neurol*, **54**, 195-201.
- Armstrong, D.D., Dunn, K. and Antalffy, B. (1998) Decreased dendritic branching in frontal, motor and limbic cortex in Rett syndrome compared with trisomy 21. *J Neuropathol Exp Neurol*, **57**, 1013-1017.
- Bachman, K.E., Rountree, M.R. and Baylin, S.B. (2001) Dnmt3a and Dnmt3b are transcriptional repressors that exhibit unique localization properties to heterochromatin. *J Biol Chem*, **276**, 32282-32287.

-
- Bailis, J.M., Bernard, P., Antonelli, R., Allshire, R.C. and Forsburg, S.L. (2003) Hsk1-Dfp1 is required for heterochromatin-mediated cohesion at centromeres. *Nat Cell Biol*, **5**, 1111-1116.
- Ballestar, E., Yusufzai, T.M. and Wolffe, A.P. (2000) Effects of Rett syndrome mutations of the methyl-CpG binding domain of the transcriptional repressor MeCP2 on selectivity for association with methylated DNA. *Biochemistry*, **39**, 7100-7106.
- Bannister, A.J., Zegerman, P., Partridge, J.F., Miska, E.A., Thomas, J.O., Allshire, R.C. and Kouzarides, T. (2001) Selective recognition of methylated lysine 9 on histone H3 by the HP1 chromo domain. *Nature*, **410**, 120-124.
- Bednar, J., Horowitz, R.A., Grigoryev, S.A., Carruthers, L.M., Hansen, J.C., Koster, A.J. and Woodcock, C.L. (1998) Nucleosomes, linker DNA, and linker histone form a unique structural motif that directs the higher-order folding and compaction of chromatin. *Proc Natl Acad Sci U S A*, **95**, 14173-14178.
- Bhattacharya, S.K., Ramchandani, S., Cervoni, N. and Szyf, M. (1999) A mammalian protein with specific demethylase activity for mCpG DNA. *Nature*, **397**, 579-583.
- Bhaumik, S.R., Smith, E. and Shilatifard, A. (2007) Covalent modifications of histones during development and disease pathogenesis. *Nat Struct Mol Biol*, **14**, 1008-1016.
- Bienvendu, T., Carrie, A., de Roux, N., Vinet, M.C., Jonveaux, P., Couvert, P., Villard, L., Arzimanoglou, A., Beldjord, C., Fontes, M., Tardieu, M. and Chelly, J. (2000) MECP2 mutations account for most cases of typical forms of Rett syndrome. *Hum Mol Genet*, **9**, 1377-1384.
- Brasher, S.V., Smith, B.O., Fogh, R.H., Nietlispach, D., Thiru, A., Nielsen, P.R., Broadhurst, R.W., Ball, L.J., Murzina, N.V. and Laue, E.D. (2000) The structure of mouse HP1 suggests a unique mode of single peptide recognition by the shadow chromo domain dimer. *Embo J*, **19**, 1587-1597.

-
- Braunschweig, D., Simcox, T., Samaco, R.C. and LaSalle, J.M. (2004) X-Chromosome inactivation ratios affect wild-type MeCP2 expression within mosaic Rett syndrome and *Mecp2*^{-/+} mouse brain. *Hum Mol Genet*, **13**, 1275-1286.
- Brero, A., Easwaran, H.P., Nowak, D., Grunewald, I., Cremer, T., Leonhardt, H. and Cardoso, M.C. (2005) Methyl CpG-binding proteins induce large-scale chromatin reorganization during terminal differentiation. *J Cell Biol*, **169**, 733-743.
- Buyse, I.M., Fang, P., Hoon, K.T., Amir, R.E., Zoghbi, H.Y. and Roa, B.B. (2000) Diagnostic testing for Rett syndrome by DHPLC and direct sequencing analysis of the MECP2 gene: identification of several novel mutations and polymorphisms. *Am J Hum Genet*, **67**, 1428-1436.
- Chahrour, M., Jung, S.Y., Shaw, C., Zhou, X., Wong, S.T., Qin, J. and Zoghbi, H.Y. (2008) MeCP2, a key contributor to neurological disease, activates and represses transcription. *Science*, **320**, 1224-1229.
- Chaillet, J.R., Vogt, T.F., Beier, D.R. and Leder, P. (1991) Parental-specific methylation of an imprinted transgene is established during gametogenesis and progressively changes during embryogenesis. *Cell*, **66**, 77-83.
- Chandler, S.P., Guschin, D., Landsberger, N. and Wolffe, A.P. (1999) The methyl-CpG binding transcriptional repressor MeCP2 stably associates with nucleosomal DNA. *Biochemistry*, **38**, 7008-7018.
- Cheadle, J.P., Gill, H., Fleming, N., Maynard, J., Kerr, A., Leonard, H., Krawczak, M., Cooper, D.N., Lynch, S., Thomas, N., Hughes, H., Hulten, M., Ravine, D., Sampson, J.R. and Clarke, A. (2000) Long-read sequence analysis of the MECP2 gene in Rett syndrome patients: correlation of disease severity with mutation type and location. *Hum Mol Genet*, **9**, 1119-1129.
- Chen, R.Z., Akbarian, S., Tudor, M. and Jaenisch, R. (2001) Deficiency of methyl-CpG binding protein-2 in CNS neurons results in a Rett-like phenotype in mice. *Nat Genet*, **27**, 327-331.

-
- Cheng, X. and Blumenthal, R.M. (2008) Mammalian DNA methyltransferases: a structural perspective. *Structure*, **16**, 341-350.
- Cheutin, T., McNairn, A.J., Jenuwein, T., Gilbert, D.M., Singh, P.B. and Misteli, T. (2003) Maintenance of stable heterochromatin domains by dynamic HP1 binding. *Science*, **299**, 721-725.
- Cohen, S., Zhou, Z. and Greenberg, M.E. (2008) Medicine. Activating a repressor. *Science*, **320**, 1172-1173.
- Collins, A.L., Levenson, J.M., Vilaythong, A.P., Richman, R., Armstrong, D.L., Noebels, J.L., David Sweatt, J. and Zoghbi, H.Y. (2004) Mild overexpression of MeCP2 causes a progressive neurological disorder in mice. *Hum Mol Genet*, **13**, 2679-2689.
- Cook, P.R. (2001) Principles of Nuclear Structure and Function. *New York, Wiley-Liss*.
- Couvert, P., Bienvenu, T., Aquaviva, C., Poirier, K., Moraine, C., Gendrot, C., Verloes, A., Andres, C., Le Fevre, A.C., Souville, I., Steffann, J., des Portes, V., Ropers, H.H., Yntema, H.G., Fryns, J.P., Briault, S., Chelly, J. and Cherif, B. (2001) MECP2 is highly mutated in X-linked mental retardation. *Hum Mol Genet*, **10**, 941-946.
- Coy, J.F., Sedlacek, Z., Bachner, D., Delius, H. and Poustka, A. (1999) A complex pattern of evolutionary conservation and alternative polyadenylation within the long 3'-untranslated region of the methyl-CpG-binding protein 2 gene (MeCP2) suggests a regulatory role in gene expression. *Hum Mol Genet*, **8**, 1253-1262.
- Cross, S.H., Meehan, R.R., Nan, X. and Bird, A. (1997) A component of the transcriptional repressor MeCP1 shares a motif with DNA methyltransferase and HRX proteins. *Nat Genet*, **16**, 256-259.
- D'Esposito, M., Quaderi, N.A., Ciccodicola, A., Bruni, P., Esposito, T., D'Urso, M. and Brown, S.D. (1996) Isolation, physical mapping, and northern analysis of the X-

linked human gene encoding methyl CpG-binding protein, MECP2. *Mamm Genome*, **7**, 533-535.

Dragich, J., Houwink-Manville, I. and Schanen, C. (2000) Rett syndrome: a surprising result of mutation in MECP2. *Hum Mol Genet*, **9**, 2365-2375.

Ellison, K.A., Fill, C.P., Terwilliger, J., DeGennaro, L.J., Martin-Gallardo, A., Anvret, M., Percy, A.K., Ott, J. and Zoghbi, H. (1992) Examination of X chromosome markers in Rett syndrome: exclusion mapping with a novel variation on multilocus linkage analysis. *Am J Hum Genet*, **50**, 278-287.

Fan, J.Y., Rangasamy, D., Luger, K. and Tremethick, D.J. (2004) H2A.Z alters the nucleosome surface to promote HP1alpha-mediated chromatin fiber folding. *Mol Cell*, **16**, 655-661.

Flemming, W. (1882) *Zellsubstanz, Kern and Zelltheilung*, Leipzig.

Fujita, N., Takebayashi, S., Okumura, K., Kudo, S., Chiba, T., Saya, H. and Nakao, M. (1999) Methylation-mediated transcriptional silencing in euchromatin by methyl-CpG binding protein MBD1 isoforms. *Mol Cell Biol*, **19**, 6415-6426.

Georgel, P.T., Horowitz-Scherer, R.A., Adkins, N., Woodcock, C.L., Wade, P.A. and Hansen, J.C. (2003) Chromatin compaction by human MeCP2. Assembly of novel secondary chromatin structures in the absence of DNA methylation. *J Biol Chem*, **278**, 32181-32188.

Goll, M.G., Kirpekar, F., Maggert, K.A., Yoder, J.A., Hsieh, C.L., Zhang, X., Golic, K.G., Jacobsen, S.E. and Bestor, T.H. (2006) Methylation of tRNA^{Asp} by the DNA methyltransferase homolog Dnmt2. *Science*, **311**, 395-398.

Gomperts, M., Garcia-Castro, M., Wylie, C. and Heasman, J. (1994) Interactions between primordial germ cells play a role in their migration in mouse embryos. *Development*, **120**, 135-141.

-
- Groudine, M. and Conkin, K.F. (1985) Chromatin structure and de novo methylation of sperm DNA: implications for activation of the paternal genome. *Science*, **228**, 1061-1068.
- Guy, J., Gan, J., Selfridge, J., Cobb, S. and Bird, A. (2007) Reversal of neurological defects in a mouse model of Rett syndrome. *Science*, **315**, 1143-1147.
- Guy, J., Hendrich, B., Holmes, M., Martin, J.E. and Bird, A. (2001) A mouse *Mecp2*-null mutation causes neurological symptoms that mimic Rett syndrome. *Nat Genet*, **27**, 322-326.
- Hansen, J.C. (2002) Conformational dynamics of the chromatin fiber in solution: determinants, mechanisms, and functions. *Annu Rev Biophys Biomol Struct*, **31**, 361-392.
- Heitz, E. (1928) Das Heterochromatin der Moose. *I. Jahrb. Wiss. Botanik*, **69**, 762-818.
- Hendrich, B. and Bird, A. (1998) Identification and characterization of a family of mammalian methyl-CpG binding proteins. *Mol Cell Biol*, **18**, 6538-6547.
- Hendrich, B., Guy, J., Ramsahoye, B., Wilson, V.A. and Bird, A. (2001) Closely related proteins MBD2 and MBD3 play distinctive but interacting roles in mouse development. *Genes Dev*, **15**, 710-723.
- Hendrich, B., Hardeland, U., Ng, H.H., Jiricny, J. and Bird, A. (1999) The thymine glycosylase MBD4 can bind to the product of deamination at methylated CpG sites. *Nature*, **401**, 301-304.
- Hendrich, B. and Tweedie, S. (2003) The methyl-CpG binding domain and the evolving role of DNA methylation in animals. *Trends Genet*, **19**, 269-277.
- Ho, K.L., McNae, I.W., Schmiedeberg, L., Klose, R.J., Bird, A.P. and Walkinshaw, M.D. (2008) MeCP2 binding to DNA depends upon hydration at methyl-CpG. *Mol Cell*, **29**, 525-531.

-
- Horn, P.J. and Peterson, C.L. (2002) Molecular biology. Chromatin higher order folding-wrapping up transcription. *Science*, **297**, 1824-1827.
- Horsley, D., Hutchings, A., Butcher, G.W. and Singh, P.B. (1996) M32, a murine homologue of *Drosophila* heterochromatin protein 1 (HP1), localises to euchromatin within interphase nuclei and is largely excluded from constitutive heterochromatin. *Cytogenet Cell Genet*, **73**, 308-311.
- Huisinga, K.L., Brower-Toland, B. and Elgin, S.C. (2006) The contradictory definitions of heterochromatin: transcription and silencing. *Chromosoma*, **115**, 110-122.
- Huppke, P., Laccone, F., Kramer, N., Engel, W. and Hanefeld, F. (2000) Rett syndrome: analysis of MECP2 and clinical characterization of 31 patients. *Hum Mol Genet*, **9**, 1369-1375.
- Ishibashi, T., Thambirajah, A.A. and Ausio, J. (2008) MeCP2 preferentially binds to methylated linker DNA in the absence of the terminal tail of histone H3 and independently of histone acetylation. *FEBS Lett*, **582**, 1157-1162.
- James, T.C. and Elgin, S.C. (1986) Identification of a nonhistone chromosomal protein associated with heterochromatin in *Drosophila melanogaster* and its gene. *Mol Cell Biol*, **6**, 3862-3872.
- Jones, P.L., Veenstra, G.J., Wade, P.A., Vermaak, D., Kass, S.U., Landsberger, N., Strouboulis, J. and Wolffe, A.P. (1998) Methylated DNA and MeCP2 recruit histone deacetylase to repress transcription. *Nat Genet*, **19**, 187-191.
- Jorgensen, H.F., Ben-Porath, I. and Bird, A.P. (2004) Mbd1 is recruited to both methylated and nonmethylated CpGs via distinct DNA binding domains. *Mol Cell Biol*, **24**, 3387-3395.
- Jugloff, D.G., Vandamme, K., Logan, R., Visanji, N.P., Brotchie, J.M. and Eubanks, J.H. (2008) Targeted delivery of an *Mecp2* transgene to forebrain neurons improves the behavior of female *Mecp2*-deficient mice. *Hum Mol Genet*, **17**, 1386-1396.

-
- Kafri, T., Ariel, M., Brandeis, M., Shemer, R., Urven, L., McCarrey, J., Cedar, H. and Razin, A. (1992) Developmental pattern of gene-specific DNA methylation in the mouse embryo and germ line. *Genes Dev*, **6**, 705-714.
- Kishi, N. and Macklis, J.D. (2004) MECP2 is progressively expressed in post-migratory neurons and is involved in neuronal maturation rather than cell fate decisions. *Mol Cell Neurosci*, **27**, 306-321.
- Klose, R.J., Sarraf, S.A., Schmiedeberg, L., McDermott, S.M., Stancheva, I. and Bird, A.P. (2005) DNA binding selectivity of MeCP2 due to a requirement for A/T sequences adjacent to methyl-CpG. *Mol Cell*, **19**, 667-678.
- Koike, N., Maita, H., Taira, T., Ariga, H. and Iguchi-Ariga, S.M. (2000) Identification of heterochromatin protein 1 (HP1) as a phosphorylation target by Pim-1 kinase and the effect of phosphorylation on the transcriptional repression function of HP1(1). *FEBS Lett*, **467**, 17-21.
- Kourmouli, N., Dialynas, G., Petraki, C., Pyrpasopoulou, A., Singh, P.B., Georgatos, S.D. and Theodoropoulos, P.A. (2001) Binding of heterochromatin protein 1 to the nuclear envelope is regulated by a soluble form of tubulin. *J Biol Chem*, **276**, 13007-13014.
- Kriaucionis, S. and Bird, A. (2003) DNA methylation and Rett syndrome. *Hum Mol Genet*, **12 Spec No 2**, R221-227.
- Kudo, S., Nomura, Y., Segawa, M., Fujita, N., Nakao, M., Schanen, C. and Tamura, M. (2003) Heterogeneity in residual function of MeCP2 carrying missense mutations in the methyl CpG binding domain. *J Med Genet*, **40**, 487-493.
- Lachner, M., O'Sullivan, R.J. and Jenuwein, T. (2003) An epigenetic road map for histone lysine methylation. *J Cell Sci*, **116**, 2117-2124.
- Lewis, J.D., Meehan, R.R., Henzel, W.J., Maurer-Fogy, I., Jeppesen, P., Klein, F. and Bird, A. (1992) Purification, sequence, and cellular localization of a novel chromosomal protein that binds to methylated DNA. *Cell*, **69**, 905-914.

-
- Li, E., Bestor, T.H. and Jaenisch, R. (1992) Targeted mutation of the DNA methyltransferase gene results in embryonic lethality. *Cell*, **69**, 915-926.
- Macleod, D., Clark, V.H. and Bird, A. (1999) Absence of genome-wide changes in DNA methylation during development of the zebrafish. *Nat Genet*, **23**, 139-140.
- Mann, M.R., Chung, Y.G., Nolen, L.D., Verona, R.I., Latham, K.E. and Bartolomei, M.S. (2003) Disruption of imprinted gene methylation and expression in cloned preimplantation stage mouse embryos. *Biol Reprod*, **69**, 902-914.
- Matarazzo, V. and Ronnett, G.V. (2004) Temporal and regional differences in the olfactory proteome as a consequence of MeCP2 deficiency. *Proc Natl Acad Sci U S A*, **101**, 7763-7768.
- McDowell, T.L., Gibbons, R.J., Sutherland, H., O'Rourke, D.M., Bickmore, W.A., Pombo, A., Turley, H., Gatter, K., Picketts, D.J., Buckle, V.J., Chapman, L., Rhodes, D. and Higgs, D.R. (1999) Localization of a putative transcriptional regulator (ATRX) at pericentromeric heterochromatin and the short arms of acrocentric chromosomes. *Proc Natl Acad Sci U S A*, **96**, 13983-13988.
- McGill, B.E., Bundle, S.F., Yaylaoglu, M.B., Carson, J.P., Thaller, C. and Zoghbi, H.Y. (2006) Enhanced anxiety and stress-induced corticosterone release are associated with increased Crh expression in a mouse model of Rett syndrome. *Proc Natl Acad Sci U S A*, **103**, 18267-18272.
- Meehan, R.R., Lewis, J.D., McKay, S., Kleiner, E.L. and Bird, A.P. (1989) Identification of a mammalian protein that binds specifically to DNA containing methylated CpGs. *Cell*, **58**, 499-507.
- Melcher, M., Schmid, M., Aagaard, L., Selenko, P., Laible, G. and Jenuwein, T. (2000) Structure-function analysis of SUV39H1 reveals a dominant role in heterochromatin organization, chromosome segregation, and mitotic progression. *Mol Cell Biol*, **20**, 3728-3741.

-
- Millar, C.B., Guy, J., Sansom, O.J., Selfridge, J., MacDougall, E., Hendrich, B., Keightley, P.D., Bishop, S.M., Clarke, A.R. and Bird, A. (2002) Enhanced CpG mutability and tumorigenesis in MBD4-deficient mice. *Science*, **297**, 403-405.
- Minc, E., Allory, Y., Worman, H.J., Courvalin, J.C. and Buendia, B. (1999) Localization and phosphorylation of HP1 proteins during the cell cycle in mammalian cells. *Chromosoma*, **108**, 220-234.
- Mnatzakanian, G.N., Lohi, H., Munteanu, I., Alfred, S.E., Yamada, T., MacLeod, P.J., Jones, J.R., Scherer, S.W., Schanen, N.C., Friez, M.J., Vincent, J.B. and Minassian, B.A. (2004) A previously unidentified MECP2 open reading frame defines a new protein isoform relevant to Rett syndrome. *Nat Genet*, **36**, 339-341.
- Monk, M., Boubelik, M. and Lehnert, S. (1987) Temporal and regional changes in DNA methylation in the embryonic, extraembryonic and germ cell lineages during mouse embryo development. *Development*, **99**, 371-382.
- Monros, E., Armstrong, J., Aibar, E., Poo, P., Canos, I. and Pineda, M. (2001) Rett syndrome in Spain: mutation analysis and clinical correlations. *Brain Dev*, **23 Suppl 1**, S251-253.
- Moretti, P., Bouwknecht, J.A., Teague, R., Paylor, R. and Zoghbi, H.Y. (2005) Abnormalities of social interactions and home-cage behavior in a mouse model of Rett syndrome. *Hum Mol Genet*, **14**, 205-220.
- Muchardt, C., Guilleme, M., Seeler, J.S., Trouche, D., Dejean, A. and Yaniv, M. (2002) Coordinated methyl and RNA binding is required for heterochromatin localization of mammalian HP1alpha. *EMBO Rep*, **3**, 975-981.
- Murzina, N., Verreault, A., Laue, E. and Stillman, B. (1999) Heterochromatin dynamics in mouse cells: interaction between chromatin assembly factor 1 and HP1 proteins. *Mol Cell*, **4**, 529-540.
- Nan, X., Campoy, F.J. and Bird, A. (1997) MeCP2 is a transcriptional repressor with abundant binding sites in genomic chromatin. *Cell*, **88**, 471-481.

-
- Nan, X., Cross, S. and Bird, A. (1998) Gene silencing by methyl-CpG-binding proteins. *Novartis Found Symp*, **214**, 6-16; discussion 16-21, 46-50.
- Nan, X., Meehan, R.R. and Bird, A. (1993) Dissection of the methyl-CpG binding domain from the chromosomal protein MeCP2. *Nucleic Acids Res*, **21**, 4886-4892.
- Ng, H.H., Jeppesen, P. and Bird, A. (2000) Active repression of methylated genes by the chromosomal protein MBD1. *Mol Cell Biol*, **20**, 1394-1406.
- Nielsen, A.L., Ortiz, J.A., You, J., Oulad-Abdelghani, M., Khechumian, R., Gansmuller, A., Chambon, P. and Losson, R. (1999) Interaction with members of the heterochromatin protein 1 (HP1) family and histone deacetylation are differentially involved in transcriptional silencing by members of the TIF1 family. *Embo J*, **18**, 6385-6395.
- Nielsen, A.L., Sanchez, C., Ichinose, H., Cervino, M., Lerouge, T., Chambon, P. and Losson, R. (2002) Selective interaction between the chromatin-remodeling factor BRG1 and the heterochromatin-associated protein HP1alpha. *Embo J*, **21**, 5797-5806.
- Nielsen, S.J., Schneider, R., Bauer, U.M., Bannister, A.J., Morrison, A., O'Carroll, D., Firestein, R., Cleary, M., Jenuwein, T., Herrera, R.E. and Kouzarides, T. (2001) Rb targets histone H3 methylation and HP1 to promoters. *Nature*, **412**, 561-565.
- Nikitina, T., Ghosh, R.P., Horowitz-Scherer, R.A., Hansen, J.C., Grigoryev, S.A. and Woodcock, C.L. (2007a) MeCP2-chromatin interactions include the formation of chromatosome-like structures and are altered in mutations causing Rett syndrome. *J Biol Chem*, **282**, 28237-28245.
- Nikitina, T., Shi, X., Ghosh, R.P., Horowitz-Scherer, R.A., Hansen, J.C. and Woodcock, C.L. (2007b) Multiple modes of interaction between the methylated DNA binding protein MeCP2 and chromatin. *Mol Cell Biol*, **27**, 864-877.

-
- Nonaka, N., Kitajima, T., Yokobayashi, S., Xiao, G., Yamamoto, M., Grewal, S.I. and Watanabe, Y. (2002) Recruitment of cohesin to heterochromatic regions by Swi6/HP1 in fission yeast. *Nat Cell Biol*, **4**, 89-93.
- Ohki, I., Shimotake, N., Fujita, N., Jee, J., Ikegami, T., Nakao, M. and Shirakawa, M. (2001) Solution structure of the methyl-CpG binding domain of human MBD1 in complex with methylated DNA. *Cell*, **105**, 487-497.
- Ohki, I., Shimotake, N., Fujita, N., Nakao, M. and Shirakawa, M. (1999) Solution structure of the methyl-CpG-binding domain of the methylation-dependent transcriptional repressor MBD1. *Embo J*, **18**, 6653-6661.
- Okano, M., Takebayashi, S., Okumura, K. and Li, E. (1999) Assignment of cytosine-5 DNA methyltransferases Dnmt3a and Dnmt3b to mouse chromosome bands 12A2-A3 and 2H1 by in situ hybridization. *Cytogenet Cell Genet*, **86**, 333-334.
- Okano, M., Xie, S. and Li, E. (1998) Dnmt2 is not required for de novo and maintenance methylation of viral DNA in embryonic stem cells. *Nucleic Acids Res*, **26**, 2536-2540.
- Olins, A.L. and Olins, D.E. (1974) Spheroid chromatin units (v bodies). *Science*, **183**, 330-332.
- Olins, D.E. and Olins, A.L. (2003) Chromatin history: our view from the bridge. *Nat Rev Mol Cell Biol*, **4**, 809-814.
- Orrico, A., Lam, C., Galli, L., Dotti, M.T., Hayek, G., Tong, S.F., Poon, P.M., Zappella, M., Federico, A. and Sorrentino, V. (2000) MECP2 mutation in male patients with non-specific X-linked mental retardation. *FEBS Lett*, **481**, 285-288.
- Pak, D.T., Pflumm, M., Chesnokov, I., Huang, D.W., Kellum, R., Marr, J., Romanowski, P. and Botchan, M.R. (1997) Association of the origin recognition complex with heterochromatin and HP1 in higher eukaryotes. *Cell*, **91**, 311-323.

-
- Peters, A.H., Kubicek, S., Mechtler, K., O'Sullivan, R.J., Derijck, A.A., Perez-Burgos, L., Kohlmaier, A., Opravil, S., Tachibana, M., Shinkai, Y., Martens, J.H. and Jenuwein, T. (2003) Partitioning and plasticity of repressive histone methylation states in mammalian chromatin. *Mol Cell*, **12**, 1577-1589.
- Polioudaki, H., Kourmouli, N., Drosou, V., Bakou, A., Theodoropoulos, P.A., Singh, P.B., Giannakouros, T. and Georgatos, S.D. (2001) Histones H3/H4 form a tight complex with the inner nuclear membrane protein LBR and heterochromatin protein 1. *EMBO Rep*, **2**, 920-925.
- Rai, K., Chidester, S., Zavala, C.V., Manos, E.J., James, S.R., Karpf, A.R., Jones, D.A. and Cairns, B.R. (2007) Dnmt2 functions in the cytoplasm to promote liver, brain, and retina development in zebrafish. *Genes Dev*, **21**, 261-266.
- Razin, A. and Szyf, M. (1984) DNA methylation patterns. Formation and function. *Biochim Biophys Acta*, **782**, 331-342.
- Reichwald, K., Thiesen, J., Wiehe, T., Weitzel, J., Poustka, W.A., Rosenthal, A., Platzer, M., Stratling, W.H. and Kioschis, P. (2000) Comparative sequence analysis of the MECP2-locus in human and mouse reveals new transcribed regions. *Mamm Genome*, **11**, 182-190.
- Reik, W. and Walter, J. (2001) Evolution of imprinting mechanisms: the battle of the sexes begins in the zygote. *Nat Genet*, **27**, 255-256.
- Saito, M. and Ishikawa, F. (2002) The mCpG-binding domain of human MBD3 does not bind to mCpG but interacts with NuRD/Mi2 components HDAC1 and MTA2. *J Biol Chem*, **277**, 35434-35439.
- Sanford, J.P., Clark, H.J., Chapman, V.M. and Rossant, J. (1987) Differences in DNA methylation during oogenesis and spermatogenesis and their persistence during early embryogenesis in the mouse. *Genes Dev*, **1**, 1039-1046.
- Scholzen, T., Endl, E., Wohlenberg, C., van der Sar, S., Cowell, I.G., Gerdes, J. and Singh, P.B. (2002) The Ki-67 protein interacts with members of the

heterochromatin protein 1 (HP1) family: a potential role in the regulation of higher-order chromatin structure. *J Pathol*, **196**, 135-144.

Seeler, J.S., Marchio, A., Sitterlin, D., Transy, C. and Dejean, A. (1998) Interaction of SP100 with HP1 proteins: a link between the promyelocytic leukemia-associated nuclear bodies and the chromatin compartment. *Proc Natl Acad Sci U S A*, **95**, 7316-7321.

Shahbazian, M., Young, J., Yuva-Paylor, L., Spencer, C., Antalffy, B., Noebels, J., Armstrong, D., Paylor, R. and Zoghbi, H. (2002) Mice with truncated MeCP2 recapitulate many Rett syndrome features and display hyperacetylation of histone H3. *Neuron*, **35**, 243-254.

Shahbazian, M.D. and Zoghbi, H.Y. (2002) Rett syndrome and MeCP2: linking epigenetics and neuronal function. *Am J Hum Genet*, **71**, 1259-1272.

Sirianni, N., Naidu, S., Pereira, J., Pillotto, R.F. and Hoffman, E.P. (1998) Rett syndrome: confirmation of X-linked dominant inheritance, and localization of the gene to Xq28. *Am J Hum Genet*, **63**, 1552-1558.

Song, K., Jung, Y., Jung, D. and Lee, I. (2001) Human Ku70 interacts with heterochromatin protein 1alpha. *J Biol Chem*, **276**, 8321-8327.

Srinivasan, P.R. and Borek, E. (1964) Enzymatic Alteration of Nucleic Acid Structure. *Science*, **145**, 548-553.

Stallcup, M.R. (2001) Role of protein methylation in chromatin remodeling and transcriptional regulation. *Oncogene*, **20**, 3014-3020.

Stancheva, I. and Meehan, R.R. (2000) Transient depletion of xDnmt1 leads to premature gene activation in *Xenopus* embryos. *Genes Dev*, **14**, 313-327.

Strahl, B.D. and Allis, C.D. (2000) The language of covalent histone modifications. *Nature*, **403**, 41-45.

- Tachibana, M., Sugimoto, K., Fukushima, T. and Shinkai, Y. (2001) Set domain-containing protein, G9a, is a novel lysine-preferring mammalian histone methyltransferase with hyperactivity and specific selectivity to lysines 9 and 27 of histone H3. *J Biol Chem*, **276**, 25309-25317.
- Tate, P., Skarnes, W. and Bird, A. (1996) The methyl-CpG binding protein MeCP2 is essential for embryonic development in the mouse. *Nat Genet*, **12**, 205-208.
- Thomas, G.H. (1996) High male:female ratio of germ-line mutations: an alternative explanation for postulated gestational lethality in males in X-linked dominant disorders. *Am J Hum Genet*, **58**, 1364-1368.
- Trappe, R., Laccone, F., Cobilanschi, J., Meins, M., Huppke, P., Hanefeld, F. and Engel, W. (2001) MECP2 mutations in sporadic cases of Rett syndrome are almost exclusively of paternal origin. *Am J Hum Genet*, **68**, 1093-1101.
- Tsumura, A., Hayakawa, T., Kumaki, Y., Takebayashi, S., Sakae, M., Matsuoka, C., Shimotohno, K., Ishikawa, F., Li, E., Ueda, H.R., Nakayama, J. and Okano, M. (2006) Maintenance of self-renewal ability of mouse embryonic stem cells in the absence of DNA methyltransferases Dnmt1, Dnmt3a and Dnmt3b. *Genes Cells*, **11**, 805-814.
- Vassallo, M.F. and Tanese, N. (2002) Isoform-specific interaction of HP1 with human TAFII130. *Proc Natl Acad Sci U S A*, **99**, 5919-5924.
- Wade, P.A., Geronne, A., Jones, P.L., Ballestar, E., Aubry, F. and Wolffe, A.P. (1999) Mi-2 complex couples DNA methylation to chromatin remodelling and histone deacetylation. *Nat Genet*, **23**, 62-66.
- Wakefield, R.I., Smith, B.O., Nan, X., Free, A., Soteriou, A., Uhrin, D., Bird, A.P. and Barlow, P.N. (1999) The solution structure of the domain from MeCP2 that binds to methylated DNA. *J Mol Biol*, **291**, 1055-1065.
- Wong, E., Yang, K., Kuraguchi, M., Werling, U., Avdievich, E., Fan, K., Fazzari, M., Jin, B., Brown, A.M., Lipkin, M. and Edelman, W. (2002) Mbd4 inactivation

-
- increases Cright-arrowT transition mutations and promotes gastrointestinal tumor formation. *Proc Natl Acad Sci U S A*, **99**, 14937-14942.
- Wu, C. and Morris, J.R. (2001) Genes, genetics, and epigenetics: a correspondence. *Science*, **293**, 1103-1105.
- Xiang, F., Buervenich, S., Nicolao, P., Bailey, M.E., Zhang, Z. and Anvret, M. (2000) Mutation screening in Rett syndrome patients. *J Med Genet*, **37**, 250-255.
- Yamamoto, K., Sonoda, M., Inokuchi, J., Shirasawa, S. and Sasazuki, T. (2004) Polycomb group suppressor of zeste 12 links heterochromatin protein 1alpha and enhancer of zeste 2. *J Biol Chem*, **279**, 401-406.
- Ye, Q., Callebaut, I., Pezhman, A., Courvalin, J.C. and Worman, H.J. (1997) Domain-specific interactions of human HP1-type chromodomain proteins and inner nuclear membrane protein LBR. *J Biol Chem*, **272**, 14983-14989.
- Young, J.I. and Zoghbi, H.Y. (2004) X-chromosome inactivation patterns are unbalanced and affect the phenotypic outcome in a mouse model of rett syndrome. *Am J Hum Genet*, **74**, 511-520.
- Yusufzai, T.M. and Wolffe, A.P. (2000) Functional consequences of Rett syndrome mutations on human MeCP2. *Nucleic Acids Res*, **28**, 4172-4179.
- Zhang, C.L., McKinsey, T.A. and Olson, E.N. (2002) Association of class II histone deacetylases with heterochromatin protein 1: potential role for histone methylation in control of muscle differentiation. *Mol Cell Biol*, **22**, 7302-7312.
- Zhao, T., Heyduk, T., Allis, C.D. and Eisenberg, J.C. (2000) Heterochromatin protein 1 binds to nucleosomes and DNA in vitro. *J Biol Chem*, **275**, 28332-28338.

7. ANNEX

7.1. Abbreviations

5mC	5-methyl cytosine
Brm	Brahma
CBX	chromobox homolog
CD	chromodomain
CDKL5	cyclin dependent kinase like 5
CoREST	co repressor of repressor element RE-1 silencing transcription factor
CSD	chromoshadow domain
Dnmt	DNA methyl transferase
FBP11	formin binding protein 11
FRAP	Fluorescence recovery after photobleaching
HAT	histone acetyl transferase
HDAC	histone deacetylases
HMGB1	high mobility group protein 1
HMT	histone methyl transferase
HP1	heterochromatin protein 1
LANA	latency associated nuclear antigen
MeCP2	Methyl CpG binding protein 2
MBD1	methyl CpG binding protein 1
MBD	methyl CpG binding domain
N6mA	N6-methyladenine
NLS	nuclear localization signal
NMR	nuclear magnetic resonance
NuRD	nucleosome remodeling and histone deacetylation
PAC	P1-derived artificial chromosome
PU.1	Ets family transcription factor
RTT	Rett syndrome
SAM	S-adenosyl-L-methionine
SET domain	Su(var)3-9, Enhancer of Zeste, Trithorax domain
TFIIB	transcription factor II B
TRD	transcription repression domain
UTR	untranslated region

XCI	X chromosome inactivation
YB1	Y box binding protein 1

Abbreviations listed in the publications are not mentioned here.

7.2. Acknowledgements

I would like to thank all people, without whose support this PhD would have not been possible. First of all, I would like to thank Prof. Dr. M. Cristina Cardoso. Cristina has been more to me than a supervisor to me, sometimes a friend and sometimes a colleague. Working with her, has helped me improve myself in several aspects. She has always encouraged me to embrace the new techniques. I found her very open and supportive to any activity that would not only benefit scientific research, but also to any activity that would be helpful for my own scientific career. She is very understanding and is always by the side of her coworkers, whether it be thick or thin. I would also very much like to thank Prof. Dr. Heinrich Leonhardt, my doctor father, who from time to time has motivated me, with the way I should plan my work, thesis, experiments and move forward on. I have always admired Heinrich for his innovative ideas and it has been great to have Heinrich as a doctor father.

Jeff deserves special mention and appreciation for all his support. He has been an excellent coworker and a great advisor. Also, he is one of the key persons who took out time to go through my thesis in detail and provide valuable comments. I would also like to thank Volker, who not only extended his helpful hand always but also helped me learn the basics of microscopy and then provided me with useful comments to improve this thesis.

I would also like to mention the love and support that Gilla always extended to me from the very beginning, since I joined this group. She is a gem of a person with a golden heart filled with love for everyone. Sandro, Sabine, Tanja and Joke were there with me during the first year of my joining in the lab, and ever since then we have been in touch and all these people have been very supportive always. I would like to express my heartily felt thanks to Petra and Marion for their endless support throughout, especially during my pregnancy. Corella, Laurence, Danny, Maria, Gohar, Robert, and Anne have provided a nice working environment for me to work in the lab. They all have been great friends. I would cherish their friendship for the rest of my life.

Last but not the least, I would like to thank all the coworkers in Munich for their extended support during this thesis.

I would further like to acknowledge my family. It was their dedication, love and support that brought me here. Lastly, but most importantly I would like to thank my husband, Shashank for his untiring support all the time during this thesis. He has stood by my

side through all the thick and thin during this period. He has been extremely supportive, whether it be a matter related to science, or to our sweet home. He has gifted me with the most precious thing of my life, my son Shivank. Shivank, my dear son I love you so much.

Thanks to all of you, for making this time so enjoyable and productive.

Anchor Side Chains of Short Peptide Fragments Trigger Ligand-Exchange of Class II MHC Molecules

Shashank Gupta¹, Sabine Höpner¹, Bernd Rupp², Sebastian Günther¹, Katharina Dickhaut^{1,3}, Noopur Agarwal¹, M. Cristina Cardoso¹, Ronald Kühne², Karl-Heinz Wiesmüller⁴, Günther Jung⁴, Kirsten Falk^{1*}, Olaf Röttschke^{1*}

1 Max-Delbrück-Center for Molecular Medicine (MDC), Berlin, Germany, **2** Leibniz-Institute for Molecular Pharmacology (FMP), Berlin, Germany, **3** Charite Berlin, Berlin, Germany, **4** University of Tübingen, Tübingen, Germany

Abstract

Class II MHC molecules display peptides on the cell surface for the surveillance by CD4⁺ T cells. To ensure that these ligands accurately reflect the content of the intracellular MHC loading compartment, a complex processing pathway has evolved that delivers only stable peptide/MHC complexes to the surface. As additional safeguard, MHC molecules quickly acquire a 'non-receptive' state once they have lost their ligand. Here we show now that amino acid side chains of short peptides can bypass these safety mechanisms by triggering the reversible ligand-exchange. The catalytic activity of dipeptides such as Tyr-Arg was stereo-specific and could be enhanced by modifications addressing the conserved H-bond network near the P1 pocket of the MHC molecule. It affected both antigen-loading and ligand-release and strictly correlated with reported anchor preferences of P1, the specific target site for the catalytic side chain of the dipeptide. The effect was evident also in CD4⁺ T cell assays, where the allele-selective influence of the dipeptides translated into increased sensitivities of the antigen-specific immune response. Molecular dynamic calculations support the hypothesis that occupation of P1 prevents the 'closure' of the empty peptide binding site into the non-receptive state. During antigen-processing and -presentation P1 may therefore function as important "sensor" for peptide-load. While it regulates maturation and trafficking of the complex, on the cell surface, short protein fragments present in blood or lymph could utilize this mechanism to alter the ligand composition on antigen presenting cells in a catalytic way.

Citation: Gupta S, Höpner S, Rupp B, Günther S, Dickhaut K, et al. (2008) Anchor Side Chains of Short Peptide Fragments Trigger Ligand-Exchange of Class II MHC Molecules. PLoS ONE 3(3): e1814. doi:10.1371/journal.pone.0001814

Editor: Mauricio Martins Rodrigues, Federal University of São Paulo, Brazil

Received: January 10, 2008; **Accepted:** February 11, 2008; **Published:** March 19, 2008

Copyright: © 2008 Gupta et al. This is an open-access article distributed under the terms of the Creative Commons Attribution License, which permits unrestricted use, distribution, and reproduction in any medium, provided the original author and source are credited.

Funding: B. Rupp, R. Kühne, G. Jung, O. Röttschke and K. Falk were supported by the BMBF-sponsored network grant 'MHCenhancer' (www.MHCenhancer.de). S. Gupta was supported by the EC-funded Marie-Curie Research Training Network (MC-RTN) 'Drugs for therapy'. S. Höpner and S. Günther were supported by grants awarded by MDC Ph.D. stipend programs.

Competing Interests: The authors have declared that no competing interests exist.

* E-mail: falk@mdc-berlin.de (KF); roetzsch@mdc-berlin.de (OR)

Introduction

The endosomal route is considered to be the default pathway for the loading of class II MHC molecules. Here the MHC molecule encounters internalized proteins serving as antigen source inside the cell in an acidic lysosomal-like compartment (MIIC) [1,2]. However, experiments with fixed cells or MHC expressing cells lacking key components of the processing pathway indicate that MHC loading can take place also directly on the cell surface. This applies not only for optimally sized peptides but also for larger polypeptide chains or even full-length proteins [3–5]. In particular immature dendritic cells (DC) could utilize this pathway. These DC contain a large fraction of 'empty' class II MHC molecules on the cell surface, which may allow the direct capturing of antigens from the extracellular space [6,7].

While for these cells cell-surface processing seems to represent a major antigen-loading pathway, on other cells it could cause irregular immune responses. Namely on mature DC or activated B cells the ligands presented on the cell surface should accurately reflect the peptide composition inside the MIIC compartment. Presumably as safeguard, a mechanism has evolved that prevents the 'accidental' loading of class II MHC molecules. MHC molecules, once they have lost their ligand, rapidly convert into

a stable inactive state that is 'non-receptive' for free peptides [8,9]. Neither the receptive nor the non-receptive conformation has been structurally defined yet, so that they are characterized solely by their kinetic parameters.

While in principle the conversion between the two forms is reversible, the equilibrium is largely shifted towards the non-receptive conformation. As a consequence, cell surface loading is usually very inefficient, which hinders the induction of productive immune responses during peptide vaccinations. In the endosomal processing pathway MHC-loading is facilitated by HLA-DM, a chaperone stabilizing the 'peptide receptive' state [10,11]. In previous studies we have shown that surprisingly also small organic compounds can exhibit this effect [12,13]. Similarly to HLA-DM, these 'MHC-loading enhancers' (MLE) stabilize a peptide receptive state resulting in accelerated antigen-loading and ligand exchange. Here we demonstrate that not only simple organic chemicals but also amino acid side chains can mediate this effect. In experiments with short dipeptides we could demonstrate that they can provoke both ligand exchange and peptide loading when targeted to the conserved P1 anchor pocket of the class II MHC molecule. The presence of 'peptide-MLE' during T cell assays therefore significantly improved the cell surface loading of antigen presenting cells (APC) with peptide antigens, which directly

translated into an increased sensitivity of antigen-specific T cell responses.

Results

Studies with synthetic organic MHC ligand-exchange catalysts pointed already to the P1-pocket as specific target site for 'MHC-loading enhancer' (MLE) [12]. The pocket is located in the binding groove close to the N-terminal side of the peptide ligand. In the ligand-complex the pocket accommodates the side chain of a key anchor residue of the peptide (Fig. 1A). It was therefore assumed that the MLE-effect may also be achieved with small natural-like compounds consisting of amino acids. In order to test this assumption soluble HLA-DR1 molecules were incubated with the high-affinity peptide ligand HA306-318 in the presence of amino acids or very short peptides. While free amino acids did not exhibit any effect (data not shown) the simple dipeptide Tyr-Arg (YR) accelerated the MHC-loading with the HA306-318 peptide in a dose-dependent way (Fig. 1B). No effect was observed with the Ala-Arg (AR) dipeptide lacking the aromatic anchor side chain, indicating that the replacement of tyrosine by alanine completely abrogated the MLE-effect.

As illustrated in Fig. 1A the stability of the MHC/ligand complex is maintained by an H-bond network formed with the backbone of the peptide. A considerable number of these bonds is formed in the immediate vicinity of the P1-pocket. To further stabilize the dipeptide by maximizing the number of H-bonds, acetyl- and amide-groups were introduced to the N- and C-termini of the dipeptides. Computational docking of acetylated dipeptide amide Ac-YR-NH₂ to the P1-pocket of HLA-DR1 indicates that as much as five of the conserved H-bonds can be formed with this minimal peptide (coordinates of the docking is enclosed in the supplemental PDB-file PDB_Coordinates S1). Compared to the free dipeptide YR a more than 10 fold increase in the catalytic activity was observed with Ac-YR-NH₂ (Fig. 2A). A partial MLE-

effect was observed also with Ac-YR and YR-NH₂, whereas Ac-AR-NH₂ was still completely inactive. To confirm the importance of a natural peptide structure, a dipeptide analogue to Ac-YR-NH₂ was employed in which tyrosine was replaced by β -homotyrosine (b3hY). The introduction of this amino acid increased the distance between the side chains by an additional CH₂-group and resulted in a total loss of activity (Fig. 2B). Likewise any replacement of the standard L-amino acids by the respective D-enantiomer abrogated the catalytic activity. Also the dipeptide Ac-ry-NH₂ composed of D-amino acids in inverse sequence did not show any effect, indicating a strict stereospecificity of the catalyst (Fig. 2C).

Steric requirements, H-bond usage and in particular the failure of dipeptides lacking the aromatic side chain further supported the assumption that the effect was mediated by the dimorphic P1 pocket. The pocket of HLA-DR1 (DRB1*0101) contains the residue β 86G, which results in a preference for aromatic and, to a lower extent, for aliphatic anchor residues [14]. To determine whether these preferences are reflected in the catalytic activity of peptide-MLE, a collection of acetylated dipeptide amides was tested in which the tyrosine residue of Ac-YR-NH₂ was replaced by one of the two other aromatic amino acids phenylalanine (F) and tryptophan (W) and by the aliphatic amino acids leucine (L), methionine (M), isoleucine (I), and valine (V). In line with expectation, strongest increase was observed with the dipeptides containing F, Y or W, while the dipeptides with aliphatic side chains showed weaker activity (Fig. 2D). No enhancement was detected with Ac-ER-NH₂ where tyrosine was substituted by glutamate (E) which belongs to the residues not fitting in the P1 pocket of HLA-DR1 [15].

The mean catalytic MLE-activity is summarized in Table 1. For soluble HLA-DR1 (DRB1*0101) the catalytic rate enhancement coefficient was determined to be 6.5 mM⁻¹, 3.7 mM⁻¹ and 3.5 mM⁻¹, for minimal peptide-MLE containing F, Y and W

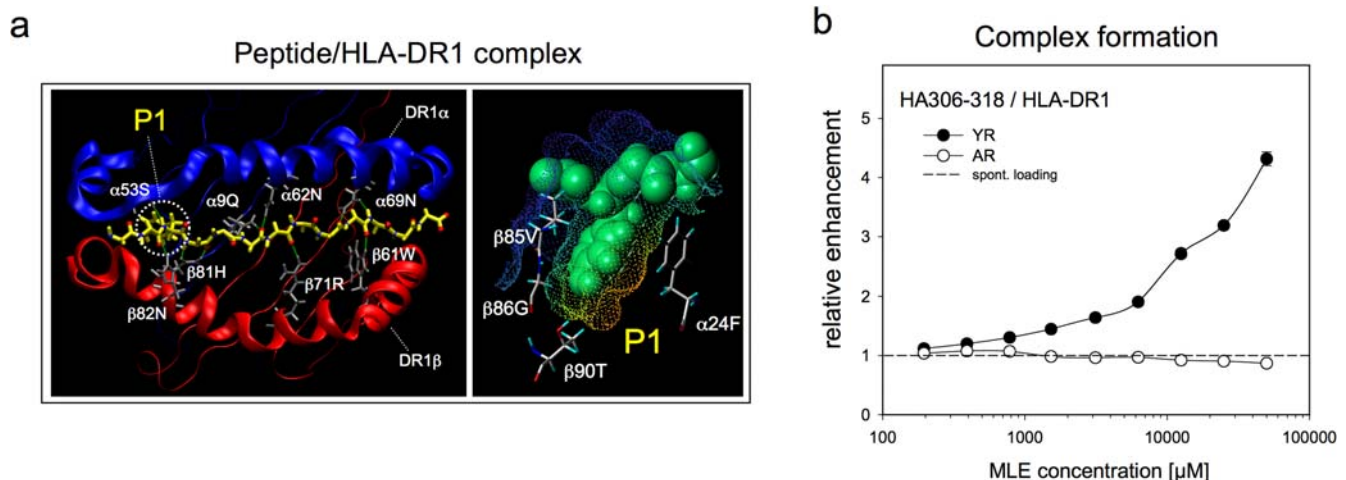


Figure 1. Amino acid side chains of short peptide fragments can catalyze the formation of MHC/ligand complexes. a) Location of P1 and the H-bond network in class II MHC molecules. Left panel: top view on the peptide binding site of the class II MHC molecule HLA-DR1. Only the α_1 - (blue ribbon) and the β_1 -domain of the MHC molecule (red ribbon) are depicted; position of P1 is indicated. The backbone of the peptide ligand HA306-318 and the anchor side chain filling the P1 pocket are shown in grey; MHC residues forming H-bonds with the backbone are labelled in grey. Right panel: side view of a P1 pocket loaded with the tyrosine anchor side chain. Surface of the pocket is indicated in yellow; amino acid residues forming this pocket are indicated; the peptide is shown in spacefill mode (green). Images are based on the crystal structure of HA306-318/HLA-DR1 (PDB: 1DLH) [38]. b) The catalytic impact of dipeptide side chains on the formation of antigen-complexes. The influence of short peptides on the complex formation-rate between HA306-318 and soluble HLA-DR1 was determined. The loading reaction was carried out in the presence of titrated amounts of the dipeptides Tyr-Arg (YR, filled circle) or Ala-Arg (AR, open circle) or in the absence of these dipeptides (dashed line). Complex formation was determined by ELISA and is expressed as relative enhancement in reference to the spontaneous complex formation in the absence of any catalyst. The amount of catalytic peptide fragments (MLE concentration) is indicated on the x-axis.
doi:10.1371/journal.pone.0001814.g001

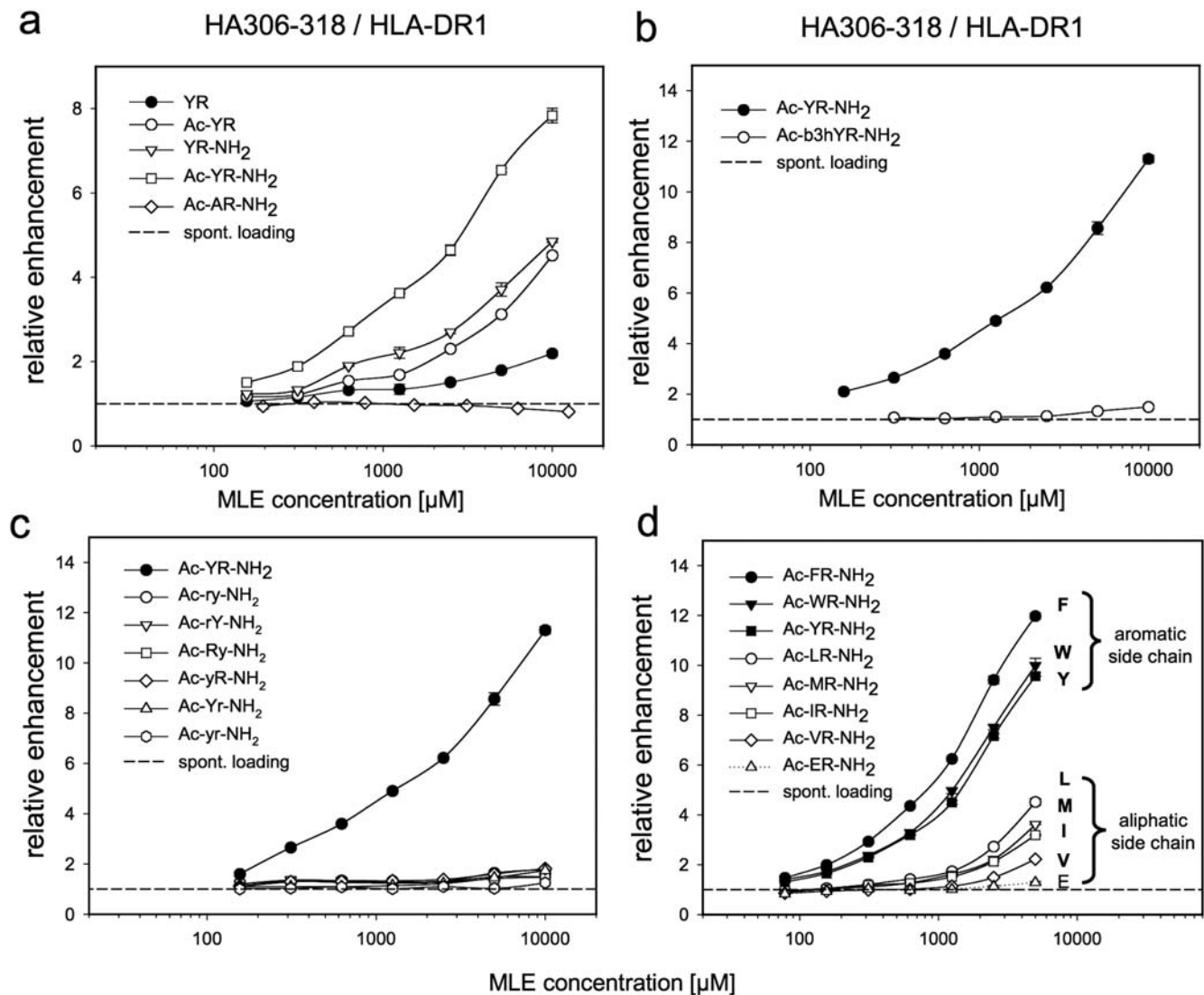


Figure 2. Structure/activity relationships of catalytic dipeptides. a) Role of H-bonds for the catalytic activity of dipeptides. Various H-bond bridges proximal to the P1 pocket stabilize the ligand complex (compare Fig. 1a). N-terminal acetylation and C-terminal amidation was introduced to the YR dipeptide to facilitate the utilization of this H-bond network by minimal peptide-MLE catalysts. The influence was demonstrated in loading reactions with HA306-318 and sol. HLA-DR1 in the presence of titrated amounts of YR (filled circle), Ac-YR (open circle), YR-NH₂ (open triangle), Ac-YR-NH₂ (open square) and as control Ac-AR-NH₂ (open diamond). b) Impact of elongated side chain spacing. A dipeptide derivative was used in which the side chain spacing was elongated a single CH₂-group by using the L- β -homotyrosine (Ac-b3hYR-NH₂; open circle) instead of tyrosine (Ac-YR-NH₂; filled circle). c) Influence of D-amino acids. Complex formation was carried out in the presence of titrated amounts of Ac-YR-NH₂ (filled circle), Ac-ry-NH₂ (open circle), Ac-rY-NH₂ (open triangle), Ac-Ry-NH₂ (open square), Ac-yR-NH₂ (open diamond), Ac-Yr-NH₂ (open triangle up), Ac-yr-NH₂ (open hexagon). D-amino acids are indicated by small letters. d) Structural requirements of the catalytic anchor side chain. The P1 pocket of HLA-DR1 interacts preferably with bulky hydrophobic anchor side chains. To compare the catalytic activity with the known structural preferences of P1 the complex formation of HA306-318/HLA-DR1 is shown for Ac-FR-NH₂ (filled circle), Ac-WR-NH₂ (filled triangle down), Ac-YR-NH₂ (filled square), Ac-LR-NH₂ (open circle), Ac-MR-NH₂ (open triangle down), Ac-IR-NH₂ (open square), Ac-VR-NH₂ (open diamond), Ac-ER-NH₂ (open triangle up). doi:10.1371/journal.pone.0001814.g002

respectively. Compared to Ac-FR-NH₂, the dipeptides with aliphatic MLE side chains exhibited only between 12% (L) and 4% (V) of the activity. Similar catalytic activity was also detected for some unmodified tripeptides as well as for two peptides derived from invariant chain (LRMK, LRMKLPK) [16]. As 'i-key' they had been described to facilitate MHC-loading by targeting an allosteric invariant chain binding site located outside the P1 pocket. Their activity, however, was not significantly higher than that of the unmodified tripeptides and the combined use with the more active peptide-MLE Ac-FR-NH₂ did not show any cooperativity (data not shown). Notably, no effect was observed

for the N-terminal fragment of the invariant chain octapeptide (LRKPPKPV). Although the fragment was reported to facilitate antigen-loading and catalyze the self-release of the invariant chain peptide IC106-120 (CLIP) [17] at least in this experimental system no catalytic effect was observed.

So far, the impact of peptide-MLE was determined only on the loading of empty MHC molecules. To evaluate their influence on complex dissociation soluble class II MHC molecules were preloaded with the medium affine CLIP peptide (Fig. 3). Although the peptide binds to HLA-DR1 with lower affinity than HA306-318 there was virtually no spontaneous decay detectable (left

Table 1. Catalytic activity of short peptides on the loading of soluble HLA-DR1 with HA306-318

	Compound*	Catalytic Rate Enhancement** [$\times 10^3$ M ⁻¹]	rel. cat. Activity*** [%]
a) Minimal peptide-MLE			
1	Ac-FR-NH ₂	6.5 \pm 1.2	100
2	Ac-YR-NH ₂	3.7 \pm 1.0	57
3	Ac-WR-NH ₂	3.5 \pm 0.9	54
4	Ac-LR-NH ₂	0.76 \pm 0.08	12
5	Ac-MR-NH ₂	0.52 \pm 0.00	8
6	Ac-IR-NH ₂	0.43 \pm 0.01	7
7	Ac-VR-NH ₂	0.25 \pm 0.02	4
8	Ac-ER-NH ₂	0.02 \pm 0.02	0
9	Ac-AR-NH ₂	0.00 \pm 0.00	0
b) Catalytic tripeptides			
10	YFR	0.68 \pm 0.29	11
11	YKT	0.59 \pm 0.12	9
12	KYV	0.51 \pm 0.15	8
13	GYV	0.49 \pm 0.16	8
c) 'Invariant Chain'-derived peptides			
14	LRMKLPK	0.98 \pm 0.21	15
15	LRMK	0.53 \pm 0.15	8
16	LRKPPKPV	0.00 \pm 0.00	0

*'Minimal peptide-MLE' and 'catalytic tripeptides' are introduced in this study, catalytic activity for 'invariant chain derived peptides' has been reported for LRMK and LRMKLPK [16] and for LRKPPKPV [17].

**The 'Catalytic Rate Enhancement' coefficient (k) represents the relative increase of the spontaneous loading rate (r_{spont}) in the presence of the catalytic peptide (P_{cat}). The total rate (r_{tot}) can be calculated by ($r_{\text{tot}} = r_{\text{spont}} + k [P_{\text{cat}}] r_{\text{spont}}$).

***'rel. cat. Activity' indicates the relative catalytic activity of peptide derivatives and is expressed as percentage in reference to the catalytic rate enhancement of Ac-FR-NH₂.

doi:10.1371/journal.pone.0001814.t001

panel). The same applies also when the experiment was carried out in the presence of dipeptide-MLE. The situation looked different when HA306-318 peptide was added (right panel). In less than 2 h, 50% of the HLA-DR1/CLIP complex disappeared when Ac-FR-NH₂ was present during dissociation. Notably, in the absence of catalyst more than 80% of the complex still remained intact even after 64 h of incubation indicating that the dipeptide-MLE is able to increase also the off-rate of peptide-ligands. In the presence of Ac-YR-NH₂ and Ac-LR-NH₂ the half-life was shortened to <4 h and <10 h while Ac-AR-NH₂ had only a very limited effect. The reversible acceleration of both complex formation and complex dissociation could therefore be correlated with the anchor preference of the P1 pocket.

In order to formally demonstrate that the catalytic side chains of peptide-MLE act through the P1 pocket, mutants of HLA-DR1 were generated in which the glycine residue $\beta 86$ at the floor of P1 was replaced either by valine ($\beta 86V$) or by tyrosine ($\beta 86Y$) (Fig. 4). In HLA-DR, $\beta 86V$ represents the natural dimorphic alternate to $\beta 86G$. Occupation of $\beta 86$ by valine produces a shallow hydrophobic pocket that is able to accommodate aliphatic side chains but, in contrast to $\beta 86G$ -pockets, is too small for bulky aromatic residues [18]. The non-natural substitution $\beta 86Y$ has been shown to produce MHC molecules that are highly receptive but contain a P1 pocket blocked by the tyrosine residue [19]. Here, only those peptides can bind where the binding does not depend on the P1 pocket. Therefore, loading experiments were therefore carried out with ABL908-922, a pentadecapeptide derived from the ABL kinase that can form a complex with all three variants (Höpner et al. manuscript in preparation) (Fig. 4, upper panels). In the absence of any peptide-MLE, ABL908-922 binds equally strong to wt HLA-DR1 ($\beta 86G$) and HLA-DR1 ($\beta 86G \rightarrow V$). Due to the inherently increased receptiveness of the mutant [19], it exhibits the highest spontaneous on-rate with HLA-DR1 ($\beta 86G \rightarrow Y$). Also here the addition of peptide-MLE resulted in increased loading reactions (Fig. 4, lower panel). With wt HLA-DR1 ($\beta 86G$) the enhancement of ABL908-922 loading corresponded to the result obtained with HA306-318, in which the aromatic dipeptides showed stronger enhancements than the aliphatic Ac-LR-NH₂ peptide. The pattern was reversed for HLA-DR1 ($\beta 86G \rightarrow V$). In line with the anchor preferences of the shallow P1 pocket, best enhancement was obtained with Ac-LR-

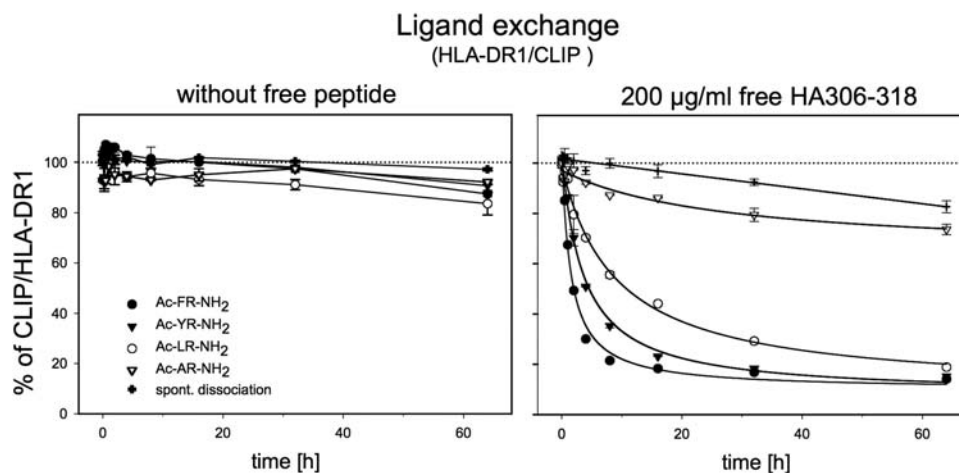


Figure 3. Catalytic dipeptides trigger reversible ligand exchange. To demonstrate that peptide-MLE can catalyze the reversible ligand exchange, complex dissociation of CLIP/HLA-DR1 induced by the peptide-MLE was determined in the absence (left panel) or presence of 200 $\mu\text{g/ml}$ free HA306-318 (right panel). In this experiment 10 mM Ac-FR-NH₂ (filled circle), Ac-YR-NH₂ (filled triangle), Ac-LR-NH₂ (open circle), Ac-AR-NH₂ (open triangle) or no catalysts (cross) was used. The percentage of CLIP/HLA-DR1 complex remaining after indicated time points was determined by ELISA. doi:10.1371/journal.pone.0001814.g003

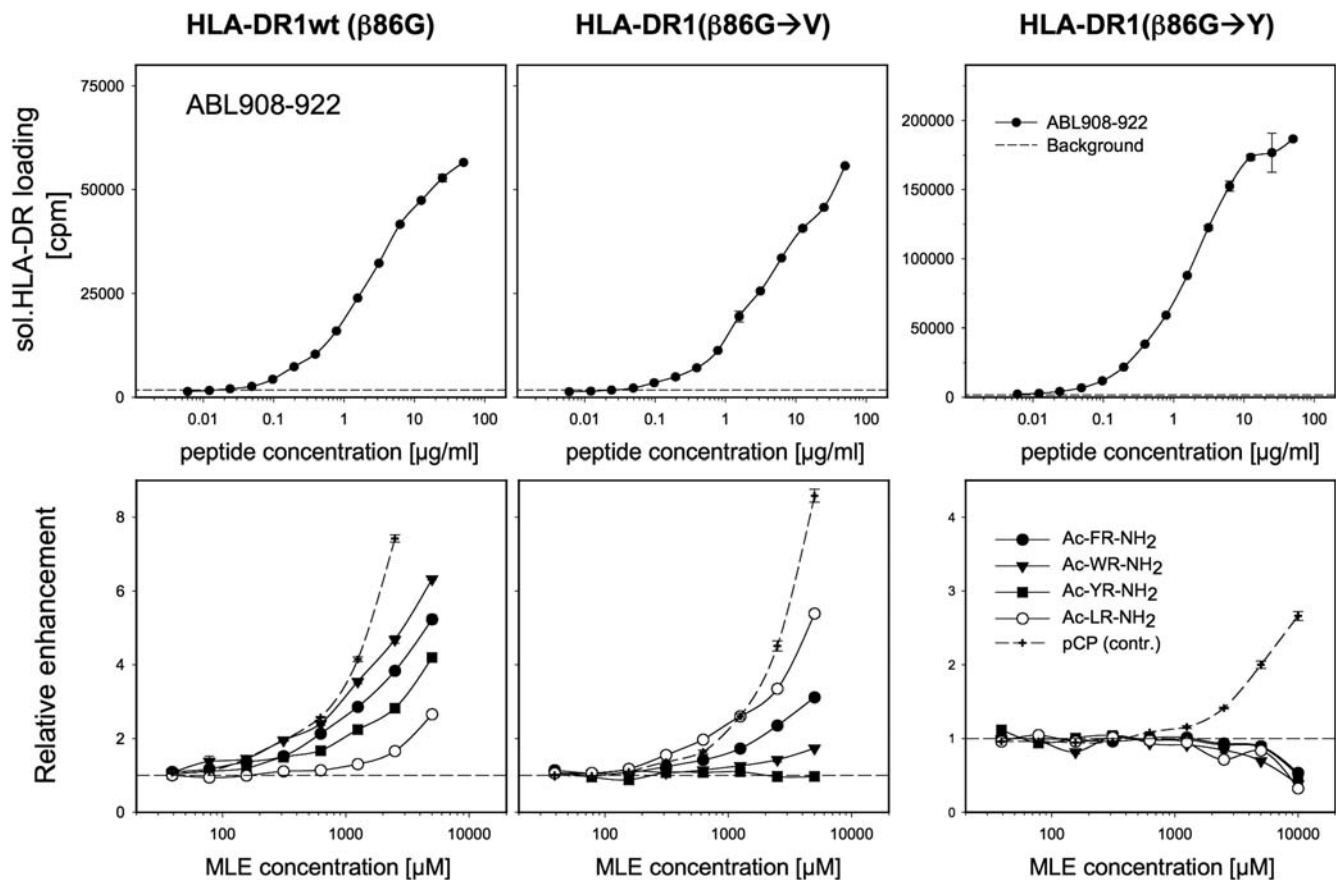


Figure 4. Allele selectivity of catalytic dipeptides. Recombinant soluble HLA-DR1 molecules were mutated inside the P1 pocket and used in loading experiments with ABL908-922, a peptide able to bind to wt as well as to the mutated forms of HLA-DR1 (S. Höpner, unpublished). Upper panels: the spontaneous loading of ABL908-922 is shown for wt HLA-DR1 ($\beta 86G$), for HLA-DR1 ($\beta 86G \rightarrow V$) and HLA-DR1 ($\beta 86G \rightarrow Y$). The formation of ABL908-922/HLA-DR complex is expressed in counts per minute (cpm); dashed line indicates background signal. Lower panels: The allele-selective effect of catalytic dipeptides is shown. The influence on HLA-DR loading is shown for Ac-FR-NH₂ (filled circle), Ac-WR-NH₂ (filled triangle down), Ac-YR-NH₂ (filled square) and Ac-LR-NH₂ (open circle) and for p-chlorophenol (pCP; cross with dashed line), a simple aromatic MLE compound acting independent of P1 [13]. 1.5 $\mu\text{g/ml}$ ABL908-922 were used for wt HLA-DR1 and HLA-DR1 ($\beta 86G \rightarrow V$) and 0.2 $\mu\text{g/ml}$ for HLA-DR1 ($\beta 86G \rightarrow Y$). Complex formation is expressed as relative enhancement in reference to the spontaneous complex formation in the absence of any catalyst. The loading was determined by ELISA.

doi:10.1371/journal.pone.0001814.g004

NH₂ while weaker amplification was detected with aromatic dipeptides. No enhancement was observed with HLA-DR1 ($\beta 86G \rightarrow Y$). Even a slight reduction was detected at the highest dipeptide concentration used, while 4-chlorophenol (pCP), a simple disubstituted benzene known to act independent of P1 [12,13], still exhibited an MLE-effect.

Exposure of cells to synthetic organic MLE facilitated the antigen loading directly on cell surface MHC molecules [12,13]. To determine whether this applies also for peptide-MLE, 721.221 cells expressing HLA-DR1-GFP fusion proteins (721.221-DRb1GFP) were incubated in the absence or presence of Ac-FR-NH₂ with biotinylated HA306-318 peptide. After staining with fluorescence-labelled streptavidin, imaging of the cells by confocal laser scanning microscopy revealed a striking increase in the amount of peptide bound to the cell surface in the presence of Ac-FR-NH₂ (Fig. 5A). While almost no HA306-318 peptide was detectable when the loading was carried out in the absence of the dipeptide-MLE, the addition of the catalyst resulted in a bright surface staining that colocalized with the HLA-DR1-GFP fusion protein.

In a more detailed analysis the peptide loading of cells was analyzed by FACS (Fig. 5B). For these experiments fibroblast cells were used that do not express endogenous class II MHC molecules

but were transfected with full length versions of wt HLA-DR1 ($\beta 86G$) and mutated HLA-DR1 ($\beta 86G \rightarrow V$). As in the previous experiment the cells were incubated with biotinylated MHC-binding peptide ABL908-922 in the absence or presence of titrated amounts of catalytic dipeptides (Fig. 5B, upper panels). Quantification of peptide-loading by FACS revealed a similar pattern as observed before with soluble MHC molecules (compare Fig. 4). On fibroblasts expressing wt HLA-DR1 the strongest enhancement was observed with aromatic dipeptides, while the aliphatic Ac-LR-NH₂ peptide showed the weakest effect. Similar effects were also observed with bone-marrow derived dendritic cells obtained from HLA-DR1 transgenic mice (data not shown). On cells expressing the mutated $\beta 86G \rightarrow V$ molecule, the aliphatic Ac-LR-NH₂ was more effective than the peptide-MLE with aromatic side chains. Thus, also the enhancement cell surface loading correlated with the allele-specific anchor preferences of P1.

Importantly, the increased loading efficiency translated directly into improved CD4⁺ T cell responses (Fig. 5B, lower panels). CD4⁺ T cell hybridoma specific for the ABL epitope (SaABL/G2) showed the strongest response when they were stimulated with fibroblast cells that had been loaded before in the presence of the dipeptides. The pattern of enhancement reflected the catalytic

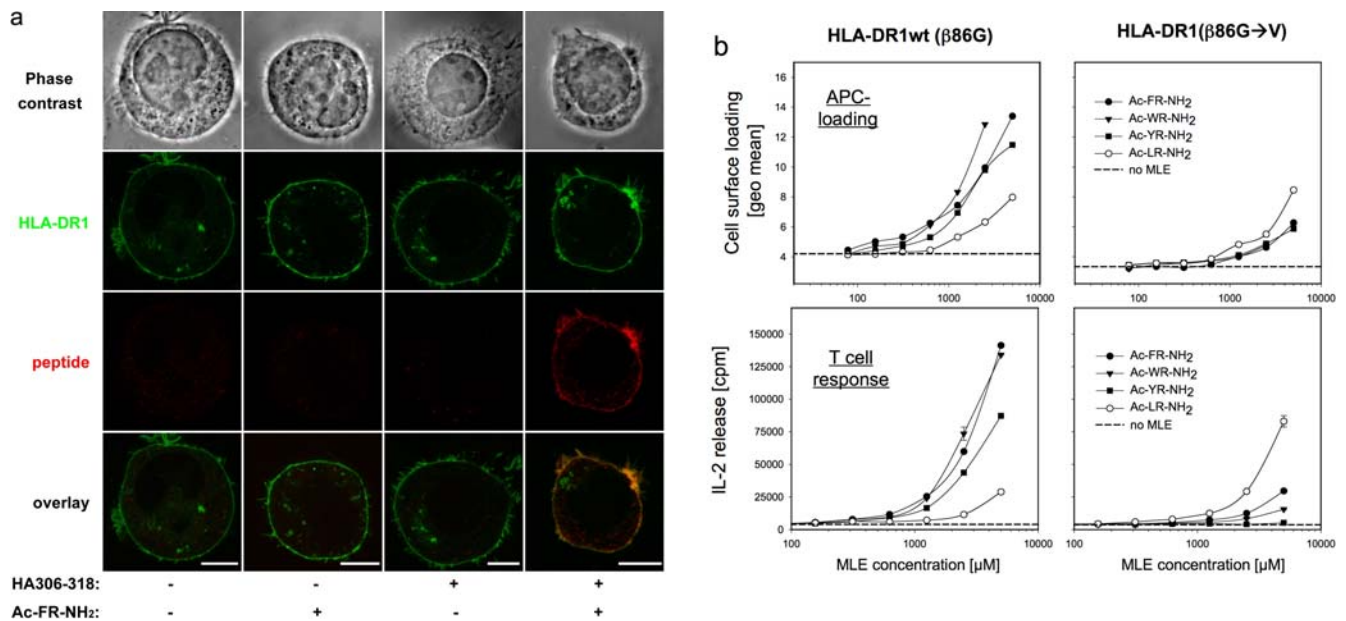


Figure 5. Enhanced loading of cell surface MHC by peptide-MLE. a) Confocal laser scanning analysis of cell surface loading. 721.221-DRb1GFP cells expressing a GFP-tagged HLA-DR1 molecule were incubated with biotinylated HA306-318 peptide in the absence or presence of Ac-FR-NH₂. After staining with streptavidin-Cy5 images were taken by confocal laser scanning microscopy. Scale bar represents 10 µm. b) Impact on APC loading and T cell response. Fibroblast transfectants expressing either wt HLA-DR1 (left panels) or mutated HLA-DR1 ($\beta 86G \rightarrow V$; right panels) were incubated with ABL908-922 in the presence of titrated amounts of Ac-FR-NH₂ (filled circle), Ac-WR-NH₂ (filled triangle), Ac-YR-NH₂ (filled square), Ac-LR-NH₂ (open circle) or in the absence of any peptide-MLE. Upper panels: Analysis of cell surface loading by FACS. Fibroblast cells were incubated with 12 µg/ml biotinylated ABL908-922. After 4h peptide loading was determined by FACS and is expressed as geometrical mean (geo. mean). Lower panels: Enhancement of the ABL908-922-specific T cell response. Fibroblast cells expressing wt HLA-DR1 or HLA-DR1 ($\beta 86G \rightarrow V$) were incubated for 4 h with 150 ng/ml or 300 ng/ml ABL908-922, washed and used to challenge SaABL1/G2, an ABL908-922 specific T cell hybridoma that recognizes the peptide on both HLA-DR1 molecules. The response is expressed as IL-2 release; dashed lines represent the T cell response triggered in the absence of any MLE compounds.

doi:10.1371/journal.pone.0001814.g005

effect on antigen loading as it directly correlated with the allele-specific P1-anchor preference. Aromatic dipeptides were most efficient on wt HLA-DR1 ($\beta 86G$) while the aliphatic Ac-LR-NH₂ showed best stimulation with cells expressing the mutated HLA-DR1 ($\beta 86G \rightarrow V$) with the shallow P1 pocket.

The influence of catalytic dipeptides on the CD4⁺ T cell response was further studied in *in vitro* T cell assays in which T cells and APC were exposed to free peptide antigens and peptide-MLE. In these experiments HA306-318 was used as antigen to challenge two different HLA-DR-restricted CD4⁺ T cells, the mouse T cell hybridoma EvHA/X5 (Fig. 6A, upper panels) and the human T cell line PD2 (Fig. 6A, lower panels). For both cell lines the presence of peptide-MLE resulted in a drastic increase in the sensitivity of the T cell response. Titration of the peptide-MLE at suboptimal antigen dosage revealed maximal enhancement of the T cell response at concentrations around 2–3 mM (left panels). At these concentrations the dose response curves for the HA306-318 antigen were shifted up to 50-fold towards lower concentrations (right panels). While a half-maximal response in the absence of catalyst was detected at a concentration of 31 ng/ml for EvHA/X5 and of 14 ng/ml for PD2, Ac-FR-NH₂ lowered the threshold to 0.65 ng/ml and 0.23 ng/ml, respectively. In line with the previous data weaker effects were determined with Ac-LR-NH₂.

Lastly, to confirm that peptide-MLE mediated enhancement can be observed also with primary cells, lymph node cells from HLA-DR1tg mice were challenged *ex vivo* in the absence or presence of Ac-FR-NH₂. The mice were primed either with HA306-318 or with NY-ESO-1 89-101, a CD4⁺ T cell epitope derived from the NY-ESO-1 protein associated with various solid tumours [20]. After 12 days the antigen-specific *ex vivo* response

was determined by an IFN- γ ELISPOT assay (Fig. 6B). In line with the previous results, the catalytic dipeptide was found to significantly increase the sensitivity of the assay. At concentrations of 5 ng/ml HA306-318 (upper panel) and of 50 ng/ml NY-ESO-1 89-101 (lower panel) the number of spots representing single IFN- γ secreting cells was significantly higher when the Ac-FR-NH₂ was added. Thus, short peptides exhibiting MLE-like activity can amplify immune responses also in primary cultures containing ‘natural’ CD4⁺ T cells and professional APC.

Discussion

Our experimental data show that short peptide fragments can influence the ligand composition of class II MHC molecules in a catalytic way. By placing an amino acid side chain into a defined pocket of the MHC molecule they trigger ligand-exchange and antigen-loading. Mutational analysis indicated already that the occupation of pocket P1 is crucial for the catalytic effect of organic MLE compounds [12]. As demonstrated here for the human molecule HLA-DR1, a similar role could also be established for the ligand exchange driven by short peptides. P1 is present in all MHC class II molecules. It is located within the peptide binding site and accommodates the side chain of a key-anchor residue of the peptide ligand. While the location of the pocket is conserved, it contains polymorphic residues that determine allele-specific preferences for anchor residues. Since the same structural requirements also dictate the interaction with ‘catalytic’ side chains of short peptides, they exhibit their effect in an allele-selective way.

As shown before for simple organic compounds the MLE mechanism is based on the stabilization of the peptide-receptive

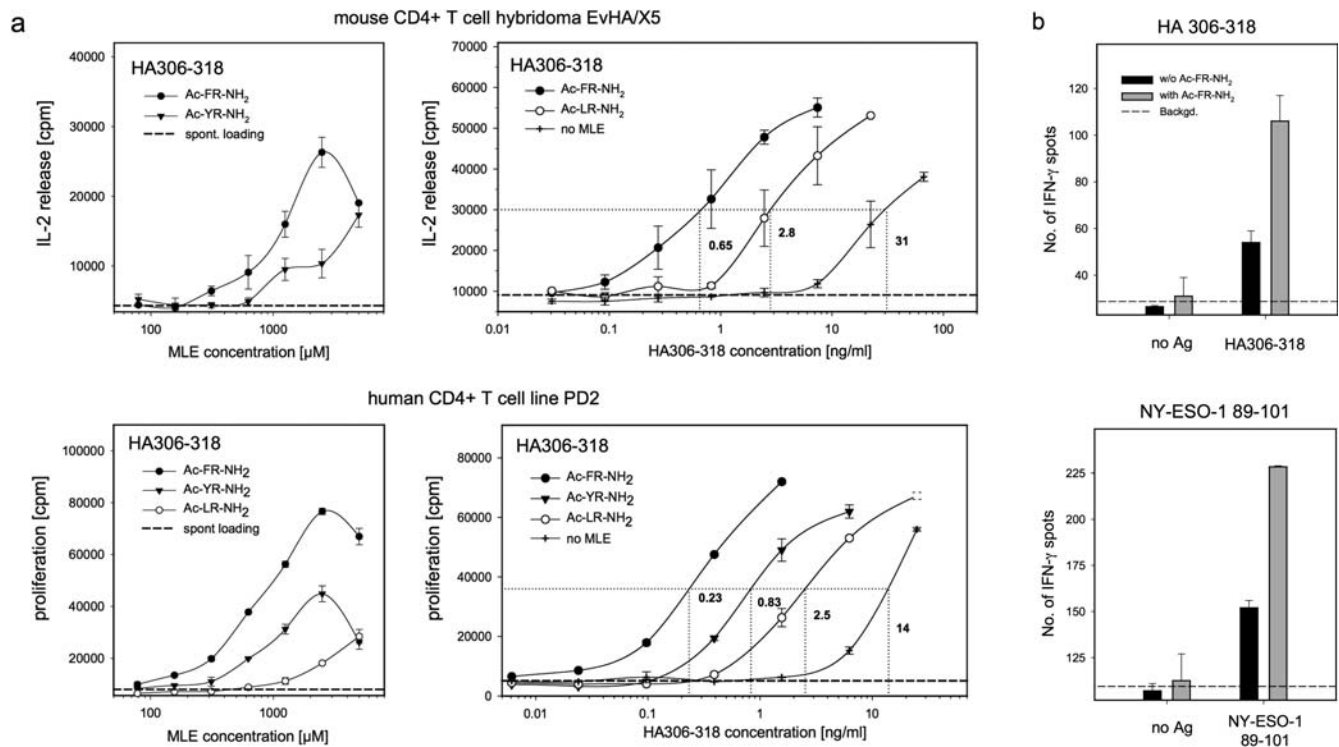


Figure 6. Amplification of the antigen-specific T cell response. a) Enhancement of the *in vitro* T cell response. The influence of catalytic peptides on the antigen-specific CD4+ T cell response was tested with a mouse T cell hybridoma EvHA/X5 (upper panels) and a human T cell line PD2 (lower panels). Both recognize the HA306-318 antigen in the context of HLA-DR1. The left panels show the influence of titrated amounts of Ac-FR-NH₂ (filled circle), Ac-YR-NH₂ (filled triangle) or Ac-LR-NH₂ (open circle) by EvHA/X5 and PD2 in the presence of 15 or 2 ng/ml HA306-318, respectively. The response in the absence any catalyst is indicated as a dashed line. The right panels are showing the dose response curves of HA306-318 in the presence of 5 mM Ac-FR-NH₂ (filled circle) or Ac-LR-NH₂ (open circle), 3 mM Ac-YR-NH₂ (filled triangle) or in the absence of any peptide-MLE (cross). Dashed line indicates the background. b) Enhancement of the *ex vivo* T cell response. Lymph node cells were isolated from HLA-DR1tg mice primed with HA306-318 peptide or NY-ESO-1 89-101. The *ex vivo* response was determined by an IFN- γ ELISPOT assay by challenging the cells with 5 ng/ml HA306-318 (upper panel) or 50 ng/ml NY-ESO-1 89-101 (lower panel), respectively. The bars represent the number of spots detected in the absence (black bar) or presence of 2.5 mM Ac-FR-NH₂ (grey bar). Each spot originates from a single IFN- γ secreting cell; dashed line indicates the background signal. doi:10.1371/journal.pone.0001814.g006

conformation [12]. Earlier studies showed already that the substitution of residue β 86G by tyrosine resulted in a ‘filled’ P1 pocket and produced an MHC molecule with elevated receptiveness [21]. P1 is located proximal to the binding site of HLA-DM and binding studies suggested that HLA-DM interacts specifically with the flexible empty hydrophobic P1-pocket [21]. While the active conversion of a non-receptive molecule by HLA-DM has recently been questioned [22], it is undisputed that the chaperone interacts with a region proximal to P1 to stabilize the peptide receptive conformation [10,11,23,24].

In a recent publication we introduced a model in which the transition to the non-receptive state is directly correlated with structural changes inside pocket P1. Experimental evidence was taken from the observation that P1-targeting MLE compounds prevent this transition [12]. The strict correlation of the catalytic activity with the structural requirements of P1 introduced by this study provides additional support to the hypothesis that the stabilization of P1 prevents the transition into the non-receptive state. A molecular dynamic (MD) simulation confirmed that the pocket P1 is indeed quickly lost when the peptide ligand is stripped off from the MHC molecule (Rupp et al. manuscript in preparation) (Fig. 7). Calculations based on the coordinates of the crystal structure of the HLA-DR1/HA306-318 complex revealed that the most significant transitions were detected near the P1 pocket. While these shifts resulted in a narrowing of the two α -helices by more than 7 Å (Fig. 7A), they also led to a complete

loss of the P1 pocket. In less than 15 ns the P1 cavity was filled with side chains or removed by distortions (Fig. 7C,D). Notably, this collapse was prevented when prior to the MD simulation the Ac-FR-NH₂ was docked into the P1 pocket (Fig. 7B).

Based on this model even the partial occupation of the binding site by a very short peptide is sufficient to stabilize the receptive state as long as it positions an anchor side chain inside the P1-pocket (supplemental PDB file PDB_Coordinates S1). P1 therefore seems to function as a sensor for the peptide load where occupation leads to a stabilization of the ‘open’ conformation required to accommodate the peptide ligand. Studies by other groups have already shown that the loading status of P1 plays a crucial role as indicator in the intracellular antigen-processing pathway. The interaction with HLA-DM seems to depend on the loading state [21] and its catalytic activity was reported to be mediated by β H81, a conserved residue located on top of the P1 pocket [24].

While inside the cell the occupational state of P1 seems to control the interaction with key-components of the processing pathway, on the cell surface it may regulate the transition into the non-receptive conformation. Here, it functions as trigger for a safeguard mechanism that closes the binding site as soon as the ligand is lost. In this study we showed that small peptide fragments can by-pass this mechanism in a catalytic way. Particularly striking is the effect on the ligand exchange. Peptide-MLE were able to increase not only the loading of empty HLA-DR molecules but also the dissociation of HLA-DR molecules preloaded with lower-

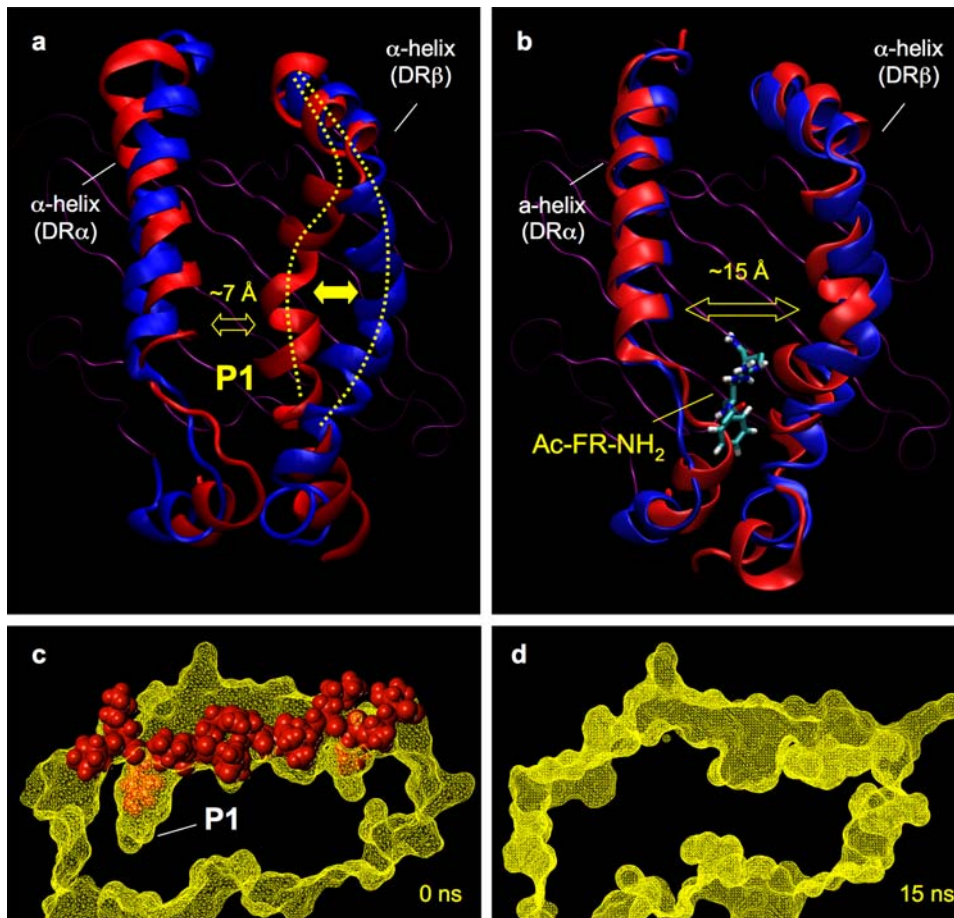


Figure 7. Molecular dynamic (MD) calculation of 'empty' and peptide-MLE stabilized HLA-DR1. The coordinates of the MHC component of the crystallized HLA-DR1/HA306-318 complex (1DHL) were used to carry out a 15 ns MD calculation with an 'empty' MHC molecule. a) Dynamic of the empty MHC molecule. The floor composed of the β -plated sheets is depicted in magenta, the α -helices of the starting structure are shown in red, α -helices of the structure obtained after 15 ns are shown in blue. The approximate position of P1 is indicated. While the dynamic was carried out with all extracellular domains, only the binding site is shown (α_1 , β_1 -domain). b) Dynamic of the peptide-MLE stabilized MHC molecule. The same MD calculation was carried out as in Fig. 7a except that coordinates of an HLA-DR1 molecule were used, in which prior to the MD calculation the peptide-MLE Ac-FR-NH₂ was docked into the P1 pocket. c) P1 pocket in the peptide loaded MHC complex. The image shows a cross-section of the HLA-DR1/HA306-318 complex. The surface of the MHC molecule is shown in yellow, the peptide ligand in red; position of the P1 pocket is indicated. d) Loss of P1 in the empty MHC molecule. The same cross-section shown in Fig. 7c for the peptide-loaded MHC is shown here for the empty molecule obtained after 15 ns of MD calculation. In this structure the P1 pocket can no longer be located.
doi:10.1371/journal.pone.0001814.g007

affinity ligands in a reversible reaction. Both effects should account for the increased antigen-loading of cell surface MHC molecules, which translated directly into improved CD4+ T cell responses. As molecular tool MLE compounds may therefore find applications in experimental and therapeutic settings in which improved antigen loading is desired. A particular suitable field may be peptide-based tumour immune interventions, where the exposure of antigen to a hostile proteolytic environment is extended by the limited access to receptive MHC molecules on the surface of professional APC.

While the importance of CD4+ T cells for productive tumour immune responses has just begun to be fully discovered [25] their role in the induction of autoimmune responses has long been acknowledged [26]. It is evident for instance in the strong genetic link to class II MHC molecules and in the fact that experimental autoimmune diseases can often be induced by the adoptive transfer of auto-aggressive CD4+ T cells. In this respect 'accidental' loading of these cells with self-antigens by peptide-MLE may therefore trigger unwanted auto-aggressive responses. *In vitro* we have shown already that the presence of simple organic MLE compounds can enhance encephalitogenic T cell responses

[12,13]. The same may also apply for colitis or celiac disease. Intestinal dendritic cells are known to penetrate gut epithelia cells [27] and expose their dendrites inside the gut lumen to extremely high polypeptide concentrations originating from the diet or commensal debris. Capture of soluble antigens by immature DC from lymph or blood, on the other hand, also seems to be an important mechanism for tolerance induction [28] and direct cell surface loading has been discussed as an alternative processing pathway of immature dendritic cells [6,7]. Natural protein fragments present in blood or lymph acting as peptide-MLE may therefore participate in this process by mediating the direct transfer of antigens onto cell surface MHC molecules.

Materials and Methods

Compounds and reagents

The following peptides were used: IC106-120 (KMRMATPL-LMQALPM; 'CLIP' peptide) [29], HA306-318 (PKYVKQNT-LKLAT) [30], NY-ESO-1 89-101 (EFYLAMPFATPME) [20] and human ABL 908-922 (KGKLSRLKAPPPPP) (Hopner et al.,

unpublished). N-terminal biotinylation was introduced using two 6-amino hexanoic acid spacer units. Stock solutions of short peptides (100 mM) were prepared with DMSO/PBS after ultrasound sonication at the following DMSO concentrations: YR, AR (0%); LRMK, YFR, GYV, Ac-AR-NH₂, Ac-ry-NH₂, Ac-rY-NH₂, Ac-Ry-NH₂, Ac-yR-NH₂, Ac-Yr-NH₂ and Ac-b3hYR-NH₂ (10%); Ac-FR-NH₂, Ac-YR-NH₂, Ac-LR-NH₂, Ac-ER-NH₂ (15%); LPKPPKPV (20%); Ac-WR-NH₂ (25%); Ac-VR-NH₂, Ac-MR-NH₂, Ac-IR-NH₂, Ac-RY-NH₂ (100%). All peptides were produced by EMC microcollections GmbH (Tübingen, Germany) and analyzed by RP-HPLC (214 nm) and ESI-MS.

Antibodies and soluble HLA-DR1

Phycoerythrin- (PE) conjugated streptavidin was purchased from Caltag, α -HLA-DR-PE (L243) was obtained from BD Biosciences. Unlabelled α -HLA-DR (L243) and α -IFN- γ (AN18.1724 and R4-6A2) were purified from hybridoma supernatant by Prot.A and Prot.G columns (GE Healthcare). R4-6A2 was labeled with NHS-Biotin according to the manufactures recommendation (Pierce). Soluble wt HLA-DR1 (DRA*0101, DRB1*0101) [31] was produced in S2 insect cells as described [13]. Mutant forms of HLA-DR1 were expressed in a baculovirus expression system. Briefly, DNA coding for the extracellular domains of DRA*0101 and DR1B*0101 was separately cloned into the transfer vector pFastbac 1 (Invitrogen). Leucine zipper domains were added to the C-termini of the α - and β -chain as described [32]. Site-directed mutagenesis of HLA-DR1 β -chain was carried out using the QuickChange site-directed mutagenesis kit (Stratagene). Recombinant viruses were generated in *S. frugiperda* cells (Sf21). For expression of proteins, cells were co-infected with viruses for the α - and β -chain.

Cells

The following class II expressing cell lines were used: L929 fibroblasts (ATCC) transfected with wt (DRB1*0101) or mutated HLA-DR1 (HLA-DRB1*0101 β 86V) [12], EBV-transformed B cell 721.221 (ATCC) and HTR [33]. 721.221-DRb1GFP cells were produced by stably transfecting 721.221 cells with a HLA-DR β -chain (DRB1*0101) C-terminally fused to EGFP (Falk et al. unpublished). The following T cells were used: DRB1*0101-restricted, HA306-318-specific mouse hybridoma line EvHA/X5 [12] and human CD4+ T cell line PD2 [33]; the ABL 908-922-specific T cell hybridoma SaABL/G2 was generated after fusing a CD4+ T cell line generated in HLA-DR1 tg mice [34] with BW cells (Hopner et al., unpublished).

Peptide loading of soluble HLA-DR1 molecules

Loading experiments with soluble MHC molecules were carried out as described [13]. Briefly, 100 nM HLA-DR1 was incubated with 50 μ g/ml of biotinylated HA306-318 peptide (PBS, pH 7.4, 37°C, 1 h). The amount of peptide/MHC complex formed was determined by ELISA with the α -HLA-DR capture antibody (L243, ATCC) and Eu³⁺-labelled streptavidin (DELFLIA,Wallac) using a Victor 3V reader (Perkin Elmer). Ligand exchange experiments were carried out with preloaded HLA-DR1/CLIP complexes (1.5 μ M HLA-DR1, 50 μ g/ml biotinylated CLIP, 18-20 h, pH 7.4, 5% ethanol/PBS) diluted 1:15 and incubated with or without 200 μ g/ml HA peptide in presence and absence of 10 mM dipeptide [12]. All experiments are carried out at 2 or 3 times.

Peptide loading of cell surface MHC molecules

Loading experiments were carried out as described [12]. Briefly, 1×10^5 HLA-DR expressing cells/well were incubated with biotinylated MHC-binding peptides in presence and absence of

catalytic dipeptides (4 h, 37°C, DMEM, 5% FCS, 96 well V-bottom plates). For FACS analysis cells were stained with streptavidin-PE and analyzed on a FACScalibur instrument (BD Biosciences). Dead cells were excluded by propidium iodide staining. Experiments were carried out twice.

Confocal laser scanning microscopy

Briefly, 1×10^5 HLA-DR1 expressing cells (721.221-DRb1GFP) per well were incubated with 20 μ g/ml of biotinylated HA 306-318 peptide in presence and absence of 2.5 mM Ac-FR-NH₂ (4 h, 37°C, DMEM, 5% FCS, 96 well V-bottom plates). Cells were then washed and were incubated on poly-L-lysine (sigma) coated plates for 30 min. at 37°C in RPMI medium (Gibco), followed by a 15 min. 3.7% formaldehyde fixation. After washing cells were stained with streptavidin-Cy5 (Amersham) and mounted with vectashield (vector labs). Fixed cell microscopy was performed with a Zeiss LSM510Meta confocal setup (63 \times phase contrast planapochromat oil objective). Experiments were carried out twice.

T cell assays

T cell assays were carried out as described [13]. Briefly, 5×10^4 HLA-DR expressing cells/well were incubated with MHC-binding peptides in presence and absence of catalytic dipeptides (37°C, DMEM, 5% FCS, 96 well round-bottom plates). In assays with antigen-pulsed APC, cells were washed after 4 h before 5×10^4 T cells were added, in permanent exposure assays the T cells were added directly without prior removal of the peptides. In experiments with T cell hybridoma the culture supernatant was removed after 24 h and the T cell response was determined by measuring IL-2 release in a secondary assay with CTLL cells (ATCC) as described previously [35]. In experiments with T cell lines, APC were radiated with 60.7 Gy and ³H-thymidine was added after 48h and the incorporation was determined using a 1450 Microbeta counter (Wallac). Experiments were carried out twice.

Detection of ex vivo response by ELISPOT assay

HLA-DR1tg mice were primed with 5 μ g HA306-318 or 10 μ g NY-ESO-1 89-101 in incomplete Freud's adjuvant (Sigma)/50 μ g CpG OND 1826 (BioTez GmbH). On day 12, lymph node cells were isolated and incubated in ELISPOT-plates (Multiscreen HTS 96 well Filtration plate; Millipore) coated with α -IFN- γ (clone AN18.1724). Cells were incubated at a density of 1×10^6 splenocytes/well with indicated amounts of HA306-318 and Ac-FR-NH₂ peptide (20–40 h, 37°C, 5% CO₂, RPMI 5% FCS). Detection was carried out according to manufacturer's recommendation using the biotinylated α -IFN- γ detection antibody (clone R4-6A2), avidin-HRP enzyme conjugate (Sigma) and 3,3 diaminobenzidine tablets (Sigma). Spots were counted using Immunospot reader (C.T.L Europe GmbH). Experiments were carried out twice.

Calculation of the 'catalytic rate enhancement'

The 'catalytic rate enhancement' coefficient was determined in loading assays with 100 nM soluble HLA-DR1 and 50 μ g/ml HA306-318 with titrated amounts of the catalytic peptide-MLE (1 h, 37°C, pH 7.4). A curve fit was carried out by a hyperbola regression ($f(x) = ax/(b+x)$) using the Sigmaplot Version 9.0 software (Systat Software Inc.) and the coefficient was determined by forming the average of the starting slope (a/b) of 2–4 independent experiments.

Docking and 'Molecular Dynamics' calculation

The benzene ring of the phenylalanine residue and the backbone of the Ac-FR-NH₂ dipeptide were superimposed to the residues Y308 and V309 of the HA306-318 peptide in the

HA306-318/HLA-DR1 crystal structure 1DLH, followed by a conformation search with the arginine side chain of the dipeptide to find an optimal orientation. Subsequently, the complex structure was minimized using the Tripos software (SYBYL 7.3, Tripos Inc., St. Louis, USA) and the GROMACS force field [36]. For both, the empty MHC structure and the Ac-FR-NH₂/MHC-complex, a 15 ns molecular dynamic simulation in the GROMACS force field was performed (Rupp et al., manuscript in preparation). The simulations were done under physiological conditions (0.9% NaCl, 310 K) after equilibration over a period of 500 ps using a positional restraint of 1000 kJmol⁻¹nm⁻². Frames were stored every 5 ps, visualisation of trajectories and arrangement of the figures were realised using VMD [37].

Supporting Information

PDB_Coordinates S1 The text file contains the calculated coordinates of the complex Ac-FR-NH₂/HLA-DR1 in PDB-file format. For the docking of Ac-FR-NH₂ the benzene ring of the phenylalanine residue and the backbone of the dipeptide were

superimposed to the residue Y308 (located within the P1 pocket) and V309 of the HA306-318 peptide in the HA-306-318/HLA-DR1 crystal structure 1DLH. Subsequently, the complex was minimized using Tripos and the GROMACS force field. Chain A: HLA-DR1 α -chain (DRA*0101); chain B: HLA-DR1 β -chain (DRB1*0101); chain C: Ac-FR-NH₂
Found at: doi:10.1371/journal.pone.0001814.s001 (0.26 MB TXT)

Acknowledgments

We thank S. Kleißle for technical assistance and S. Giering for help in preparing the manuscript.

Author Contributions

Conceived and designed the experiments: OR SG SH RK GJ KF. Performed the experiments: SG SH SG KD NA BR. Analyzed the data: OR KW SG SH SG KD NA RK GJ KF BR. Contributed reagents/materials/analysis tools: MC KW GJ BR. Wrote the paper: OR KF.

References

- Stern LJ, Potoличchio I, Santambrogio L (2006) MHC class II compartment subtypes: structure and function. *Curr Opin Immunol* 18: 64–69.
- Watts C (2001) Antigen processing in the endocytic compartment. *Curr Opin Immunol* 13: 26–31.
- Pinet V, Vergelli M, Martin R, Bakke O, Long EO (1995) Antigen presentation mediated by recycling of surface HLA-DR molecules. *Nature* 375: 603–606.
- Vergelli M, Pinet V, Vogt AB, Kalbus M, Malnati M, et al. (1997) HLA-DR-restricted presentation of purified myelin basic protein is independent of intracellular processing. *Eur J Immunol* 27: 941–951.
- Marin-Esteban V, Falk K, Rotzschke O (2003) Small-molecular compounds enhance the loading of APC with encephalitogenic MBP protein. *J Autoimmun* 20: 63–69.
- Santambrogio L, Sato AK, Carven GJ, Belyanskaya SL, Strominger JL, et al. (1999) Extracellular antigen processing and presentation by immature dendritic cells. *Proc Natl Acad Sci U S A* 96: 15056–15061.
- Santambrogio L, Sato AK, Fischer FR, Dorf ME, Stern LJ (1999) Abundant empty class II MHC molecules on the surface of immature dendritic cells. *Proc Natl Acad Sci U S A* 96: 15050–15055.
- Natarajan SK, Assadi M, Sadegh-Nasseri S (1999) Stable peptide binding to MHC class II molecule is rapid and is determined by a receptive conformation shaped by prior association with low affinity peptides. *J Immunol* 162: 4030–4036.
- Rabinowitz JD, Vrljic M, Kasson PM, Liang MN, Busch R, et al. (1998) Formation of a highly peptide-receptive state of class II MHC. *Immunity* 9: 699–709.
- Denzin LK, Hammond C, Cresswell P (1996) HLA-DM interactions with intermediates in HLA-DR maturation and a role for HLA-DM in stabilizing empty HLA-DR molecules. *J Exp Med* 184: 2153–2165.
- Kropshofer H, Arndt SO, Moldenhauer G, Hammerling GJ, Vogt AB (1997) HLA-DM acts as a molecular chaperone and rescues empty HLA-DR molecules at lysosomal pH. *Immunity* 6: 293–302.
- Hopner S, Dickhaut K, Hofstatter M, Kramer H, Ruckerl D, et al. (2006) Small organic compounds enhance antigen loading of class II major histocompatibility complex proteins by targeting the polymorphic P1 pocket. *J Biol Chem* 281: 38535–38542.
- Marin-Esteban V, Falk K, Rotzschke O (2004) “Chemical analogues” of HLA-DM can induce a peptide-receptive state in HLA-DR molecules. *J Biol Chem* 279: 50684–50690.
- Rammensee H-G, Bachmann J, Stevanovic S (1997) MHC Ligands and Peptide Motifs. Austin, TX: Springer-Verlag; Landis Biosciences.
- Fleckenstein B, Kalbacher H, Muller CP, Stoll D, Halder T, et al. (1996) New ligands binding to the human leukocyte antigen class II molecule DRB1*0101 based on the activity pattern of an undecapeptide library. *Eur J Biochem* 240: 71–77.
- Xu M, Li J, Gulfo JV, Von Hofe E, Humphreys RE (2001) MHC class II allosteric site drugs: new immunotherapeutics for malignant, infectious and autoimmune diseases. *Scand J Immunol* 54: 39–44.
- Kropshofer H, Vogt AB, Stern LJ, Hammerling GJ (1995) Self-release of CLIP in peptide loading of HLA-DR molecules. *Science* 270: 1357–1359.
- Ong B, Wilcox N, Wordsworth P, Beeson D, Vincent A, et al. (1991) Critical role for the Val/Gly86 HLA-DR beta dimorphism in autoantigen presentation to human T cells. *Proc Natl Acad Sci U S A* 88: 7343–7347.
- Natarajan SK, Stern LJ, Sadegh-Nasseri S (1999) Sodium dodecyl sulfate stability of HLA-DR1 complexes correlates with burial of hydrophobic residues in pocket 1. *J Immunol* 162: 3463–3470.
- Chen Q, Jackson H, Parente P, Luke T, Rizkalla M, et al. (2004) Immunodominant CD4+ responses identified in a patient vaccinated with full-length NY-ESO-1 formulated with ISCOMATRIX adjuvant. *Proc Natl Acad Sci U S A* 101: 9363–9368.
- Chou CL, Sadegh-Nasseri S (2000) HLA-DM recognizes the flexible conformation of major histocompatibility complex class II. *J Exp Med* 192: 1697–1706.
- Grottenbreg GM, Nicholson MJ, Fowler KD, Wilbuer K, Octavio L, et al. (2007) Empty Class II Major Histocompatibility Complex Created by Peptide Photolysis Establishes the Role of DM in Peptide Association. *J Biol Chem* 282: 21425–21436.
- Doebele RC, Busch R, Scott HM, Pashine A, Mellins ED (2000) Determination of the HLA-DM interaction site on HLA-DR molecules. *Immunity* 13: 517–527.
- Narayan K, Chou CL, Kim A, Hartman IZ, Dalai S, et al. (2007) HLA-DM targets the hydrogen bond between the histidine at position beta81 and peptide to dissociate HLA-DR-peptide complexes. *Nat Immunol* 8: 92–100.
- Corthay A, Skovseth DK, Lundin KU, Rosjo E, Omholt H, et al. (2005) Primary antitumor immune response mediated by CD4+ T cells. *Immunity* 22: 371–383.
- Jones EY, Fugger L, Strominger JL, Siebold C (2006) MHC class II proteins and disease: a structural perspective. *Nat Rev Immunol* 6: 271–282.
- Rescigno M, Urbano M, Valzasina B, Francolini M, Rotta G, et al. (2001) Dendritic cells express tight junction proteins and penetrate gut epithelial monolayers to sample bacteria. *Nat Immunol* 2: 361–367.
- Hochweller K, Sweeney CH, Anderton SM (2006) Immunological tolerance using synthetic peptides—basic mechanisms and clinical application. *Curr Mol Med* 6: 631–643.
- Riberdy JM, Newcomb JR, Surman MJ, Barbosa JA, Cresswell P (1992) HLA-DR molecules from an antigen-processing mutant cell line are associated with invariant chain peptides. *Nature* 360: 474–477.
- Lamb JR, Eckels DD, Lake P, Woody JN, Green N (1982) Human T-cell clones recognize chemically synthesized peptides of influenza haemagglutinin. *Nature* 300: 66–69.
- Sloan VS, Cameron P, Porter G, Gammon M, Amaya M, et al. (1995) Mediation by HLA-DM of dissociation of peptides from HLA-DR. *Nature* 375: 802–806.
- Fourneau JM, Cohen H, van Endert PM (2004) A chaperone-assisted high yield system for the production of HLA-DR4 tetramers in insect cells. *J Immunol Methods* 285: 253–264.
- Falk K, Rotzschke O, Strominger JL (2000) Antigen-specific elimination of T cells induced by oligomerized hemagglutinin (HA) 306-318. *Eur J Immunol* 30: 3012–3020.
- Rosloniec EF, Brand DD, Myers LK, Whittington KB, Gumanovskaya M, et al. (1997) An HLA-DR1 transgene confers susceptibility to collagen-induced arthritis elicited with human type II collagen. *J Exp Med* 185: 1113–1122.
- Falk K, Lau JM, Santambrogio L, Esteban VM, Puentes F, et al. (2002) Ligand exchange of major histocompatibility complex class II proteins is triggered by H-bond donor groups of small molecules. *J Biol Chem* 277: 2709–2715.
- Van Der Spoel D, Lindahl E, Hess B, Groenhof G, Mark AE, et al. (2005) GROMACS: fast, flexible, and free. *J Comput Chem* 26: 1701–1718.
- Humphrey W, Dalke A, Schulten K (1996) VMD: visual molecular dynamics. *J Mol Graph* 14: 33–3827–38.
- Stern LJ, Brown JH, Jardetzky TS, Gorga JC, Urban RG, et al. (1994) Crystal structure of the human class II MHC protein HLA-DR1 complexed with an influenza virus peptide. *Nature* 368: 215–221.

7.4. Contributions

Declaration of contributions to “MeCP2 interacts with HP1 and modulates its heterochromatin association during myogenic differentiation.”

I laid out the project aims and conceived the study together with Cristina Cardoso. Alessandro Brero and Danny Nowak did the initial experiments. Annete Becker generated the DsRed-HP1 γ construct. Ulrich Rothbauer and Heinrich Leonhardt provided sepharose-conjugated GFP-binder and scientific advice. Tanja performed the initial experiments on Figure 2. My contributions to this publication include: design and performance of all immunoprecipitation and microscopy experiments, data analysis, preparation of the figures and manuscript with help from Cristina Cardoso.

Declaration of contributions to “Rett mutations affect heterochromatin organization.”

This project was initiated by Alessandro Brero, Tanja Hardt and Cristina Cardoso. I picked up the project and laid out the project aims and goals and conceived the study together with Cristina Cardoso. My contributions to this publication include: design and performance of all microscopy and photobleaching experiments, data analysis, preparation of the figures and manuscript with help from Cristina Cardoso. Laurence Jost contributed part a and b of the supplementary Figure 2. Shinichi Kudo provided us with GFP tagged mutant constructs used in the study.

Declaration of contributions to “Anchor side chains of short peptide fragments trigger ligand-exchange of class II MHC molecules.”

The project is done as collaboration with the laboratory of Olaf Rötzschke. I contributed the microscopy experiments and subsequent data analysis. In addition, I prepared Figure 5a of the manuscript and wrote the corresponding Figure legend and Material and Methods section.

Declaration according to the "Promotionsordnung der LMU München für die Fakultät Biologie"

Betreuung: Hiermit erkläre ich, dass die vorgelegte Arbeit an der LMU von Herrn Prof. Dr. Heinrich Leonhardt betreut wurde

Anfertigung: Hiermit versichere ich ehrenwörtlich, dass die Dissertation von mir selbstständig und ohne unerlaubte Hilfsmittel angefertigt wurde. Über Beiträge, die im Rahmen der kumulativen Dissertation in Form von Manuskripten in der Dissertation enthalten sind, wurde im Kapitel 7.3 Rechenschaft abgelegt und die eigenen Leitungen wurden aufgelistet.

Prüfung: Hiermit erkläre ich, dass die Dissertation weder als ganzes noch in Teilen an einem anderen Ort einer Prüfungskommission vorgelegt wurde. Weiterhin habe ich weder an einem anderen Ort eine Promotion angestrebt oder angemeldet oder versucht eine Doktorprüfung abzulegen.

(Noopur Agarwal)

7.5. Curriculum Vitae

Name: **Noopur Agarwal**
Address: Max Delbrück Center for Molecular Medicine
Robert - Rössle Str. 10
13125 Berlin, Germany
Date of Birth: 16/ 06/ 1978
Place of Birth: Bareilly

Education:

1993 Class X (81.4%)
St. Mary's convent school,
Dhampur, India.

1995 Class XII (71.4%)
Tulsidas Kilachand intermediate college,
Bareilly, India.

1997-2001 Bachelor in pharmaceutical sciences (9.4 on the scale of 10)
I.E.T M.J.P Rohilkhand University,
Bareilly, India.

2002- 2003 Masters in Engineering (Biotechnology) (9.6 on the scale of 10)
Birla Institute of Technology and Sciences,
Pilani, India.

2005- contd. PhD thesis at the Department of Biology, Ludwig Maximilians
University, Munich.
Max Delbrück Center for Molecular Medicine, Berlin, Germany.

Positions and teaching:

2003 lecturer in Saroj Institute of technology and management

2004 lecturer in Career Institute of technology and management
2004-2005 project associate in National Brain Research Center

Lists of publications:

Agarwal, N., T. Hardt, A. Brero, D. Nowak, U. Rothbauer, A. Becker, H. Leonhardt, and M.C. Cardoso. 2007. MeCP2 interacts with HP1 and modulates its heterochromatin association during myogenic differentiation. *Nucleic Acids Res.* 35:5402-8.

Gupta, S., S. Hopner, B. Rupp, S. Gunther, K. Dickhaut, **N. Agarwal**, M.C. Cardoso, R. Kuhne, K.H. Wiesmuller, G. Jung, K. Falk, and O. Rotzschke. 2008. Anchor side chains of short peptide fragments trigger ligand-exchange of class II MHC molecules. *PLoS ONE.* 3:e1814.

Agarwal, N., K.L. Jost, A. Brero, T. Hardt, S. Kudo, H. Leonhardt, and M.C. Cardoso. MeCP2 Rett mutations affect large-scale chromatin organization. *Submitted.*

Oral presentations and poster presentations:

- Oral presentation at November 2007 DFG-Epigenetics meeting, Saarbrücken.
- Poster presentation at September 2006 and 2007 Max Delbrueck Center (MDC) and Forshungsinstitut für Molekulare Pharmacologie (FMP) PhD-retreat, Motzen and Joachimsthal respectively.
- Oral presentation at May 2006 MDC “Wollenberger Seminar”.